

Mario Fernando Jiménez Hernández

# Human-Robot-Environment Interaction Strategies for Walker-Assisted Gait

Vitoria - Brazil

December 2018





Mario Fernando Jiménez Hernández

# Human-Robot-Environment Interaction Strategies for Walker-Assisted Gait

Ph.D. Thesis submitted for the Postgraduate Program in Electrical Engineering (PPGEE), Federal University of Espirito Santo (UFES) as a preliminar requirement to obtain the Ph.D. degree in Electrical Engineering.

Federal University of Espirito Santo - UFES, Brazil

Postgraduate Program in Electrical Engineering

Supervisor: Dr. Anselmo Frizera Neto

Co-supervisor: Dr. Teodiano Freire Bastos Filho

Vitoria - Brazil

December 2018

Ficha catalográfica disponibilizada pelo Sistema Integrado de Bibliotecas - SIBI/UFES e elaborada pelo autor

---

J61h JIMENEZ HERNANDEZ, MARIO FERNANDO, 1981-  
Human-Robot-Environment Interaction Strategies for Walker-Assisted Gait : Human-Robot-Environment Interaction Strategies for Walker-Assisted Gait / MARIO FERNANDO JIMENEZ HERNANDEZ. - 2018.  
138 f. : il.

Orientador: Anselmo Frizera Neto.  
Coorientador: Teodiano Bastos Filho.  
Tese (Doutorado em Engenharia Elétrica) - Universidade Federal do Espírito Santo, Centro Tecnológico.

1. Robótica. 2. Controle. 3. Assistência. I. Frizera Neto, Anselmo. II. Bastos Filho, Teodiano. III. Universidade Federal do Espírito Santo. Centro Tecnológico. IV. Título.

CDU: 621.3

---

Mario Fernando Jiménez Hernández

## Human-Robot-Environment Interaction Strategies for Walker-Assisted Gait

Ph.D. Thesis submitted for the Postgraduate Program in Electrical Engineering (PPGEE), Federal University of Espirito Santo (UFES) as a preliminar requirement to obtain the Ph.D. degree in Electrical Engineering.

Examined by:



---

**Prof. Dr. Anselmo Frizera Neto**

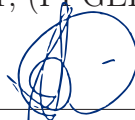
Supervisor, (PPGEE/UFES/Brazil)



---

**Prof. Dr. Teodiano Freire Bastos Filho**

Co-supervisor, (PPGEE/UFES/Brazil)



---

**Prof. Dr. Eduardo Rocon de Lima**

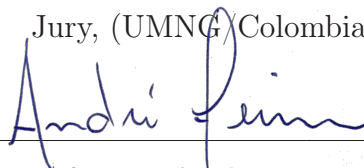
Jury, (CAR/CSIC/Spain)



---

**Prof. Dr. Mauricio Felipe Mauledoux Monroy**

Jury, (UMNG/Colombia)



---

**Prof. Dr. Andre Ferreira**

Jury, (PPGEE/UFES/Brazil)



---

**Prof. Dr. Eliete Maria de Oliveira Caldeira**

Jury, (PPGEE/UFES/Brazil)

Vitoria, Brazil

*“One, remember to look up at the stars and not  
down at your feet. Two, never give up work.  
Work gives you meaning and purpose, and life  
is empty without it. Three, if you are lucky  
enough to find love, remember it is there and  
don’t throw it away”.*

*Stephen Hawking*

*“Imagination will often carry us to worlds  
that never were, but without it we go nowhere”.*

*Carl Sagan*

I dedicate this doctoral thesis to all my family and friends, especially to people that supported me each day and contributed to my professional and personal development: my wonderful wife Rosa Milena Muñoz Villanueva, my parents Fernando Jiménez and Yolanda Hernández, my sister and brother Nataly Jiménez Hernández and Diego Leonardo Jiménez Hernández, and my niece Mariana.



## Acknowledgements

This thesis has been possible thanks to the support of different institutions and people.

- In the First place, I wish to express all my gratitude to my advisor Prof. Dr. Anselmo Frizzera Neto, who granted me the guidance and the freedom to make decisions during my research, and also for giving me the opportunity of being a part of this amazing team. Special thanks to my co-supervisor Prof. Dr. Teodiano Freire Bastos Filho, for his permanent availability, disposition and recommendations to improve my manuscripts. Together, provided me the possibility to work in this wonderful, and challenging project. In addition, they helped me to grow as a person and as a professional.
- I also want to thank Prof. Dr. Ricardo Carelli for advising me on the design and development of the control strategy that gave the beginning of this thesis.
- CAPES and CNPq that supported me these years to complete my PhD thesis successfully.
- To all my colleagues and classmates of the NTA group from UFES/Brazil, and IN-AUT/Argentina, who shared a lot of their experience with me in different ways.
- To all my family and friends, who are very important in my life, wishing me all the best always, as well as providing all the necessary support.

Now, I would like to thank specially to:

- All my family who provided me all support and attention, in order to help me during my living experience in Brazil. Especially thanks to my wonderful wife Rosa Milena Muñoz Villanueva for dedicating unconditionally to this life project, giving me her patience and confidence, as well as helping me when necessary. My mom Yolanda Hernández, who told me many years ago that I have to dream big. My dad Fernando Jiménez, who has provided me the support in my personal and professional life. My brother and sister, Diego Leonardo Jiménez Hernández and Nataly Jiménez Hernández, who always shared the family time. Besides, thanks to my niece Mariana Jiménez, who with her innocent voice gave me happy moments during my stay in Brazil. Finally, my grandmother Ligia, who always has a big hug for me.

- Furthermore, I would like to thank my partners at the NTA group, especially to Kevin, Nicolas, Laura, Alejandra, Cecilia, who provided me with all their support and attention as professionals and friends. Thanks for dedicating a lot of your time in meeting and tests related to my PhD project.
- Ricardo C. Mello, Franco Viera, and Wander Cleyson Scheidegger, my great SW team, who did substantial work on the development of the UFES Smart Walker. Thanks for their dedication and support during my stay in Brazil.
- Andrés Ramírez and his family, who provided me all support and attention as professional and friend as well. Thanks for dedicating your time to discuss our projects, and sharing me your amazing presence.
- Denis Delisle, whose dedication to discuss our projects was always enriching.
- Sergio Sierra and Jonathan Casas, who during their stay in Brazil shared time with me to build good memories.
- Juan Miguel Escobar, who gave his unconditional support during my stay in Brazil.
- My friends from my undergraduate degree, who always showed the interest in the topic of my PhD and provided me support when it was necessary.



## Abstract

Smart Walkers (SWs) are robotic devices that may be used to improve balance and locomotion stability of people with lower-limb weakness or poor balance. Such devices may also offer support for cognitive disabilities and for people that cannot safely use conventional walkers, as well as allow interaction with other individuals and with the environment. In this context, there is a significant need to involve the environment information into the SW's control strategies. In this Ph.D. thesis, the concept of Human-Robot-Environment Interaction (HREI) for human locomotion assistance with a smart walker developed at UFES/Brazil (turned UFES's Smart Walker - USW) is explored. Two control strategies and one social navigation strategy are presented. The first control strategy is an admittance controller that generates haptic signals to induce the tracking of a predetermined path. When deviating from such path, the proposed method varies the damping parameter of the admittance controller by means of a spatial modulation technique, resulting in a haptic feedback, that is perceived by the user as a hard locomotion towards the undesired direction. The second strategy also uses an admittance controller to generate haptic signals, which guide the user along a predetermined path. However, in this case, the angular velocity of the smart walker is implemented as a function of a virtual torque, which is defined using two virtual forces that depend on the angular orientation error between the walker and the desired path. Regarding the navigation strategy, it involves social conventions defined by proxemics, and haptic signals generated through the spatial modulation of the admittance controller for a safe navigation within confined spaces.

The USW uses a multimodal cognitive interaction composed of a haptic feedback and a visual interface with two LEDs to indicate the correct/desired direction when necessary. The proposed control strategies are suitable for a natural HREI as demonstrated in the experimental validation. Moreover, this Ph.D. thesis presents a strategy to obtain navigation commands for the USW based on multi-axial force sensors, in addition to a study of the admittance control parameters and its influence on the maneuverability of the USW, in order to improve its HREI.

**Keywords:** Admittance Control, Spatial Modulation, Cognitive Assistance, Social Interaction, Haptic, Smart Walker.

# Glossary

**cHRi** Cognitive Human-Robot Interface.

**FLC** Fourier Linear Combiner.

**FSR** Force Sensor Resistor.

**HREI** Human-Robot-Environment Interaction.

**HRI** Human-Robot Interaction.

**IMU** Inertial Measurement Unit.

**KTE** Linear Estimation Error.

**LRF** Laser Ranger Finder.

**MSE** Mean Square Error.

**NTA** Center for Assistive Technology.

**pHRi** Physical Human-Robot Interface.

**ROS** Robotic Operative System.

**SCI** Spinal Cord Injury.

**SFM** Social Force Model.

**SLAM** Simultaneous Localization and Mapping.

**SW** Smart Walker.

**USW** UFES Smart Walker.

**WFLC** Weighted-Frequency Fourier Linear Combiner.

**WHO** World Health Organization.



# List of Tables

4.1	Virtual mass values and user weight. . . . .	45
4.2	Values of constants used in the control strategy. . . . .	46
5.1	Constants values used in the control strategy. . . . .	74
6.1	Parameters values used in the control strategy. . . . .	94



# List of Figures

2.1	Examples of mobility assistive devices: a) Canes; b) Crutches; c) Wheeled knee walker; d) Manual wheelchair; e) Active orthoses. . . . .	11
2.2	Walkers frames: a) Standard; b) Front-wheeled; c) Rollator. . . . .	12
2.3	a) UFES's Smart Walker (USW); b) Interaction layers. . . . .	20
3.1	Physical Human-Robot interface based on force sensors. . . . .	23
3.2	Block diagram to eliminate the cadence from force signals. . . . .	25
3.3	Experiment 1, where the subjects were asked to follow a straight line. . . . .	27
3.4	Experiment 2, where the users were asked to follow a lemniscate curve indicated on the floor. . . . .	27
3.5	Adaptive filter behavior. . . . .	28
3.6	Tendency of user discharge force with respect to the mass $m_\nu$ . . . . .	29
3.7	a) Controller behavior with a good selection of admittance control parameters ( $m_\nu = 15 \text{ kg}$ , $d_\nu = 10.35 \text{ kg/s}$ ); b) Controller behavior with an erroneous $m_\nu$ value ( $m_\nu = 22 \text{ kg}$ , $d_\nu = 10.35 \text{ kg/s}$ ). . . . .	30
3.8	User discharge force with respect to $m_\omega$ . . . . .	31

3.9	a) Following the eight-shaped curve with a good selection of admittance control parameters ( $m_\omega = 0.26, d_\omega = 20$ ); b) Following the lemniscate curve with bad admittance control parameters ( $m_\omega = 0.35, d_\omega = 20$ ). . . . .	32
4.1	Block diagram of the controller with admittance modulation. . . . .	38
4.2	Predetermined path for following. . . . .	39
4.3	Block diagram of the admittance modulator. . . . .	39
4.4	Curve of damping force $d_\nu$ . . . . .	41
4.5	Criterion for orientation correction. . . . .	42
4.6	Curve of torque damping $d_\omega$ . . . . .	42
4.7	Obstacle detecting zone. . . . .	43
4.8	Position of LEDs on the <i>USW</i> . . . . .	44
4.9	Experiments with different paths. (a) Experiment 1. Following straight segments. (b) Experiment 2. Finding the circle path. . . . .	47
4.10	Following the straight path. (a) Path following considering cognitive interface information. (b) Path following with induced error. . . . .	48
4.11	Spatial modulation curve of $d_\nu$ and haptic force response of the straight path of Fig. 4.10b. Up to down: Control and SW linear velocities, user's force signal, $\tilde{\theta}$ signal and $d_\nu$ signal. . . . .	49
4.12	Spatial modulation curve of $d_\omega$ and haptic torque response of the predetermined path in Fig. 4.10b. Up to down: SW angular velocities, user's torque signal, $\tilde{\theta}$ and $d_\omega$ . . . . .	50



4.13	Errors in the following straight path. Group 1: Second part of the Experiment 1 (user 7 of Table 4.1). Group 2: Average data of path following by user in the first part of the Experiment 1. (a) Linear velocity. (b) Angular velocity. (c) Kinematic Estimation Error (KTE).	52
4.14	Finding the circle path. (a) Finding the path with the haptic feedback. (b) Finding the path with the multimodal cognitive interaction.	53
4.15	Kinematic estimation error ( <i>KTE</i> ). Group 1: with haptic feedback. Group 2: with multimodal cognitive interaction.	54
4.16	Qualitative evaluation for the guided experiments. Questions: a) “I felt that the SW was guiding me”; b) “I felt an intuitive interaction with the SW”.	55
4.17	Recommendation of turn by cognitive interface signals.	56
4.18	Safety parameters of supervisor.	58
5.1	Social interaction with a navigation companion within a confined space.	63
5.2	Social interaction strategy on a corridor for an SW. Social zones: Interpersonal-social zone (IPSz), Interpersonal-public zone (IPPz). Red points describing the virtual canal of navigation to each person.	64
5.3	Block diagram of the navigation strategy.	66
5.4	Zones to detect obstacles.	67
5.5	Blocks diagram of the social navigation.	70
5.6	a) IPSz ellipse strategy; b) IPPz ellipse strategy.	70
5.7	a) Ellipses distances design; b) Corridor distances, wide = 3 m, length = 28 m.	75

5.8	Situations within a corridor. Situation 1: navigation with accompanying person. Situation 2: person walking in front of the SW. Situation 3: person represents a fixed obstacle. Situation 4: person crosses in front of the SW. Situation 5: person walks in the opposite direction to the SW. . . . .	76
5.9	Natural situations within a corridor. . . . .	77
5.10	Controlled situations within a corridor. Corridor dimensions: $w = 3 m, l = 28 m$	77
5.11	Spatial modulation curve of $d_\nu$ and haptic force response of the social navigation. From top to bottom: a) Control and SW linear velocities; b) User's force signal; c) $\tilde{\theta}$ signal; and d) $d\nu$ signal. All the corridor situations are described in Sections 1 to 5. . . . .	79
5.12	Spatial modulation curve of $d_\omega$ and haptic force response of the social navigation. From top to bottom: a) Control and SW angular velocities; b) user's torque signal; c) $\tilde{\theta}$ signal; and d) $d\omega$ signal. All the corridor situations are described in sections 1 to 5. . . . .	80
5.13	Recommendation of turn by the multimodal cognitive interface using the LEDs channel. All the proposed at the corridor situations are described in sections 1 to 5. . . . .	81
5.14	Real environment within the corridor. . . . .	82
5.15	Real situations within a corridor. Corridor dimensions: $w = 3 m, l = 28 m$ . . .	82
6.1	Block diagram of the controller strategy to guide visually impaired people. . . .	88
6.2	Virtual force modulation. a) Left turn. b) Right turn. . . . .	89
6.3	Control strategy simulated for different paths designs. a) Path with a curve of $90^\circ$ ; b) Path with a curve of $120^\circ$ ; c) Path with a soft curve (radius= $1 m$ . . . .	92
6.4	The pre-established path to be followed by participants. . . . .	93

6.5 Scenery of the experiment. The participant starts from the building entrance (box 1) and is guided to a room (box 5). . . . . 94

6.6 Following the desired path. a) User wearing the blindfold. b) User without the blindfold. . . . . 95

6.7 Following the desired path using the blindfold. Up to down: user’s force signal  $F_H(t)$ , user’s torque signal  $\tau_H(t)$ , Control and SW linear velocities, Control and SW angular velocities,  $\tilde{\theta}$  signal. . . . . 96

6.8 Following the desired path without use of blindfold. Up to down: user’s force signal  $F_H(t)$ , user’s torque signal  $\tau_H(t)$ , Control and SW linear velocities, Control and SW angular velocities,  $\tilde{\theta}$  signal. . . . . 97

6.9 Qualitative evaluation for the guided experiments. Questions: a) “I felt safe handling the SW”. b) “I felt that I controlled the SW”. c) “I felt that the SW was guiding me”. d) “felt an intuitive interaction with the SW”. Group 1. Following the desired path using the blindfold. Group2. Following the desired path without use of blindfold. . . . . 98

6.10 Group 1: Average data from all runs of the first part of the experiment. Group 2: Average data from all participants without the use of the blindfold. (a) Statistic of linear velocity. (b) Statistic of the angular velocity. . . . . 99



# Contents

<b>Acknowledgements</b>	<b>v</b>
<b>Glossary</b>	<b>ix</b>
<b>List of Tables</b>	<b>xiii</b>
<b>List of Figures</b>	<b>xv</b>
<b>1 Introduction</b>	<b>1</b>
1.1 Motivation . . . . .	1
1.2 Objectives . . . . .	3
1.3 Justification . . . . .	4
1.4 Ph.D. Thesis Organization . . . . .	6
<b>2 Human Mobility Impairments and Smart Walkers as Assistive Devices</b>	<b>8</b>
2.1 Human Mobility and Disabilities . . . . .	8
2.2 Mobility Assistive Devices . . . . .	10
2.3 Technological Advances in Walkers . . . . .	13

2.3.1	Passive and Active Walkers . . . . .	14
2.4	Current Trend in Smart Walkers: From Human-Robot to Human-Robot-Environment and Social Interaction . . . . .	16
2.5	UFES's Smart Walker (USW) . . . . .	20
<b>3</b>	<b>Admittance Controller Applied to Walker-Assisted Gait</b>	<b>22</b>
3.1	Admittance Control Strategy . . . . .	23
3.2	Navigation Commands Recognition . . . . .	25
3.3	Experimental Study . . . . .	26
3.3.1	Experiment 1. Following a Straight Line . . . . .	26
3.3.2	Experiment 2. Following the Lemniscate Curve . . . . .	26
3.4	Experimental Results and Discussion . . . . .	28
3.4.1	Experiment 1: Following the Straight Line . . . . .	28
3.4.2	Experiment 2: Following the Lemniscate Curve . . . . .	31
<b>4</b>	<b>Human-Robot-Environment Interaction Based on Spatial Modulation of Ad- mittance Controller for Smart Walker Navigation</b>	<b>35</b>
4.1	Background . . . . .	36
4.2	Control Strategy for Smart Walker Navigation . . . . .	37
4.2.1	Admittance Spatial Modulator . . . . .	39
4.2.2	Safety Supervisor . . . . .	43
4.2.3	Visual Cognitive Interface . . . . .	44
4.3	Experimental Study . . . . .	45

4.3.1	Following Straight Segments . . . . .	45
4.3.2	Finding the Circle Path . . . . .	47
4.3.3	Supervisor Functionality . . . . .	47
4.4	Results and Discussions . . . . .	48
4.4.1	Following Straight Segments . . . . .	48
4.4.2	Finding the Circle Path . . . . .	53
4.4.3	Qualitative Evaluation . . . . .	55
4.4.4	Checking the Supervisor Functionality . . . . .	56

**5 Admittance Modulation Technique Based on Proxemics for Navigation in Confined Spaces 60**

5.1	Social Interaction in Walker-Assisted Gait . . . . .	61
5.2	Human-Robot-Environment Interaction (HREI) Within Confined Spaces . . . . .	65
5.2.1	Social Navigation for the USW . . . . .	69
5.3	Experimental Study . . . . .	73
5.3.1	Navigating Through a Controlled Scenario . . . . .	75
5.3.2	Navigating Through an Uncontrolled Scenario . . . . .	76
5.4	Results and Discussions . . . . .	77
5.4.1	Navigating Through a Controlled Scenario . . . . .	77
5.4.2	Navigating Through an Uncontrolled Scenario . . . . .	81

<b>6</b>	<b>Haptic Feedback to Guide Visually Impaired People Across Complex Environments</b>	<b>84</b>
6.1	Related Works . . . . .	85
6.2	Guidance Control Strategy . . . . .	87
6.3	Controller Simulation and Path Design . . . . .	91
6.4	Experimental Setup . . . . .	92
6.5	Results and Discussions . . . . .	95
<b>7</b>	<b>Conclusions and Future Works</b>	<b>100</b>
7.1	Contributions . . . . .	103
7.2	Acknowledgements . . . . .	104
7.3	Publications . . . . .	104
	<b>References</b>	<b>106</b>



# Chapter 1

## Introduction

This work focuses on a Human-Robot-Environment Interaction (HREI) strategy for human mobility assistance using a smart walker developed by UFES/Brazil (USW). The integration of Human-Robot Interaction (HRI) concepts into the USW allows establishing natural channels of communication between the walker and the human. This Ph.D. thesis also presents a multimodal cognitive interface that provides a guidance system for the user during navigation. Thus, the USW not only works to allow a gait assistance but also offers a cognitive assistance. Additionally, the USW involves social conventions and human behavior within its HREI to allow a suitable interaction with the environment and other people. This chapter presents some remarks regarding the motivation of this research, the goals, and the justification.

### 1.1 Motivation

Functional mobility is fundamental to the independence and daily living of people, as it is an essential skill to ensure satisfactory quality of life and wellbeing [1]. Mobility difficulties can often be linked to the elderly population and, which, according to the World Health Organization, between 2017 and 2050 the number of people aged over 60 years is projected to grow more than twofold, from 652 million to 2.1 billion. Especially, in Latin America and the Caribbean, the older population is projected to increase from 76 to 198 million. By 2050, the elderly pop-

ulation that lives in developing regions is projected to grow 79 percent more, reaching nearly 2.1 billion individuals [2].

Elderly are the main population to suffer from impaired and cognitive disabilities that affect the locomotion [3]. However, independent locomotion may be also affected by injuries, neurological diseases or surgical interventions, which affect not only the autonomy of individuals but may also cause social isolation and premature psychological and cognitive degradation [4]. Diseases are the most common reason of locomotion impairments in people aged from 65 to 84 years old [5]. Stroke, Parkinson's disease, Alzheimer's dementia, degenerative joint disease, acquired musculoskeletal deformities, intermittent claudication, and impairments after an orthopedic surgery may also result in locomotion problems [3].

Due to mobility impairments, several studies have been conducted to develop assistive devices that aid people with gait disabilities to allow them to improve balance and increase independence during locomotion [6]. Conventional assistive devices for mobility, such as walkers, crutches, and canes have been used to improve balance and body weight support in these people [7].

Conventional walkers may be prescribed to people with lower extremity weakness or poor balance to improve stability, and to facilitate mobility by increasing their partial body weight support [8]. Walkers may also be used to decrease the risk of falling, with positive reflexes in the quality of life. However, conventional walkers can be difficult to maneuver [7] and, as a result, hard to navigate. Moreover, users may also require active support for guidance, orientation and localization as they may suffer from cognitive disorders [9]. In these cases, a higher level of assistance can be required to promote independent locomotion than the one found on conventional walkers.

Robotic concepts have been integrated with conventional walkers to allow the development of SWs, which can offer a whole new range of functionalities, contributing to health support, gait assistance, and increased autonomy in daily life [10]. SWs are devices that can provide physical support, sensorial and cognitive assistance, health monitoring and advanced human-robot interaction [11]. These devices are often able to provide extended features, such as gait

and navigation assistance, sit-to-stand transfer, obstacle avoidance and fall prevention [6], which can be used in control strategies for mobility assistance, providing comfort, safety, and easy maneuverability of the walker [8].

This Ph.D. thesis is based on previous researches that were developed either inside of our research group called on Center for Assistive Technology (NTA) or within the execution of collaboration projects. One of the main works developed by NTA was [12], which focuses on Human-Robot Interaction (HRI) strategy for human mobility assistance using an SW.

Until now, innovative (HRIs) have been developed with the aim to generate a natural relation between user and walker [12, 13]. However, this kind of strategies still does not integrate the capacity to generate a natural interaction with the environment, due to the use of sensors on the user or environment [10]. Therefore, it is necessary to develop strategies with a natural Human-Robot-Environment interaction (HREI) for the SW, without use of external sensors on the user or environment. Such new strategies for the SW have also to involve physical assistance, cognitive assistance, sensorial assistance and social interaction, providing the user with an active role during navigation.

## 1.2 Objectives

The main objective of this research is to propose, develop and implement novel strategies for a natural Human-Robot-Environment Interaction that allow assisting the SW's users, in order to provide them a safe navigation. The following specific objectives are proposed to reach such strategy.

1. Perform a literature study regarding smart walkers.
2. Implement a strategy to detect the human motion intentions during walker-assisted gait using force sensors for a natural Human-Robot Interaction.
3. Design multimodal cognitive interaction strategies that allow guiding the user during navigation with the smart walker.

4. Develop Human–Robot–Environment control strategies for a walker-assisted gait that promote a natural interaction between user and SW.
5. Develop a navigation strategy that provides the user with social interaction possibility with other people around.
6. Design and implement a Human–Robot–Environment control strategy to guide visually impairment people using the smart walker.

### 1.3 Justification

There is a growing interest in developing robotic assistive devices for elderly and people with physical and cognitive disabilities [14]. Similar to conventional walkers, SWs are used to provide mobility assistance to people with disabilities that present lower motor function and low balance, by improving their autonomy, and, more generally, by improving their quality of life [11].

Through sensorial information, an SW can guide people with mobility impairments to navigate within semi-structured or structured environments, and, when providing guidance, it is expected that its navigation strategies produce a natural and intuitive HRI. In this context, it is necessary to develop interaction strategies and interfaces to detect the human motion intention in order to obtain a natural and safety HRI. By doing so, the user can interact at physical and cognitive levels with the device during navigation, which must respond in natural ways to the human motion intention while guaranteeing safety for the often frail user.

According to the literature [12, 15, 16], the human motion intention in robotic walker can be measured or estimated through the use of force sensor and/or laser sensor. For example, through force sensors installed under the SWs forearm or hand supports, motion intention can relate with linear and angular velocity [10, 15, 16]. On the other hand, laser sensor have been used in order to obtain human-robot formation [12, 13], in which the human is the leader of the formation with the SW.

Regarding the controllers used to generate an HRI in SWs, one of the strategies commonly

used to develop a natural interaction between the human and the SW is the admittance control [15,16]. This control strategy emulates a dynamic system and provides the user with a sensation of interaction with the SW. The admittance controller depends on the users' force/torque sensing, and allows detecting the user's motion intention in a natural way, without the need of external sensors in either the user or the environment. However, this kind of controller only has impact on the HRI.

Many technological solutions to enable natural channels of communication between the walker and the user have been developed. It is inevitable to involve physical assistance, and sensorial assistance within the gait assistance. The first two kinds of assistance are integrated in a natural way on the HRI of the SW [12,13,16–18]. Regarding sensorial assistance, most of the HREI needs either wearable sensors and actuators on the user, or sensors at the environment [15,19,20], which might be unnatural and be uncomfortable for the user. Also, the HREI strategies normally include the definition of predetermined paths [15,16,21], restricting the process of decision-making by the user during navigation, putting him/her to a secondary role.

Therefore, it is necessary to develop a strategy with natural HREI that stimulates the cognitive system, for example, through decisions making, giving an active role to the user at navigation. Furthermore, it is necessary to take into account that the user shares the same space of the robot. For this reason, the navigation strategies not only must be in the capacity to offer navigation assistance, sit-to-stand transfer, obstacle avoidance, and fall prevention [6], but also have concepts of social interaction.

Whenever SWs are employed to assist human navigation, these devices must not only empower locomotion, but also allow social interaction. In addition, as a user makes use of an SW, the control algorithms responsible for navigation must take into consideration social conventions and human behavior to allow for proper interaction with the environment and other people [22,23]. Therefore, it is important also to integrate some cognitive capabilities to the device when used in shared spaces.

Literature regarding SWs has overlooked social concepts, and navigation systems have been implemented in similar ways to traditional robotics [6,24,25], not including user requirements

related to social interaction. In this context, it is necessary to guarantee a natural incorporation of SW into social spaces by implementing navigation strategies that allow a suitable interaction between the user and other humans that are present in the environment. This way, it is possible to avoid social isolation and premature psychological and cognitive problems due to the absence of social interaction of the SW's user, especially when the user is an elderly [4].

In summary, one of the most important challenges for the SWs is to provide control strategies that allow a natural Human-Robot-Environment Interaction (HREI), as well as an intuitive and easy way to transmitting the human motion intention to the SW. Thus, multimodal interfaces to allow easy communication between the user and the SW are required. Also, in spite of many studies involving social aspects within the robots navigation strategies, this requirement has not been taken account in SW's navigation strategies. For this reason, the novel HREI strategies proposed here includes social interaction concepts in order to obtain a better user experience during navigation with the SW.

## 1.4 Ph.D. Thesis Organization

This document is composed of seven chapters. Chapter 1 introduces the motivation, the research goals, and the justification of this Ph.D. thesis.

Chapter 2 presents the description of the population most likely to have mobility impairments, and a short description of the common devices used by gait assisted. Furthermore, state of the art around SWs is described, as well as the current trend in SWs, from HRI to HREI.

Chapter 3 explains the method used in the UFES's Smart Walker (USW) to detect the human motion intention in a natural way, which is based in an admittance control strategy. Also presents the behavior of the admittance control and the influence on the maneuverability of the USW, as a consequence of the values assigned to the parameters in this control strategy can influence the user experience, due to the USW maneuvering can be hardest or easily.

Chapter 4 exposes a new proposal of controller that continuously modifies dynamic parameters

of the admittance controller to induce the user to follow a predetermined path in a natural and intuitive way. In addition, taking advantage of the physical contact between the user and the USW, a haptic feedback is generated to induce the user to follow such predetermined path.

Chapter 5 describes a new strategy to navigate with the USW in confined spaces. Also, the social interaction into the USW navigation is introduced, and the definition of social zones allows a safe navigation for the user.

Chapter 6 presents a study of the haptic feedback signals that are present when an user is guided by the USW. In this case, in order to keep the user along the path, the human intention to turn does not affect the guidance, hence minimizing the errors and providing feedback over the correct direction to follow.

Finally, Conclusions, Future Works, and Contributions are presented in Chapter 7.

## Chapter 2

# Human Mobility Impairments and Smart Walkers as Assistive Devices

Human gait depends on a complex interaction of the nervous, musculoskeletal and cardiorespiratory systems [26]. The gait can be affected by age and neurological diseases, which may produce the loss of personal independence, and affect the quality of life [1]. Neurological diseases can impact the human mobility at different levels, causing partial or total loss of the locomotion capacity, especially, when the person is an elderly [3]. Depending on the impairment level, there are specific assistive devices to improve balance in order to offer support during the gait, such as crutches, walkers and canes [27, 28]. However, when the user requires active support for guidance orientation, and localization, such devices may not be ideal. In these cases, more assistance can be required to promote the independent locomotion than the one found on the conventional assistive devices. In this context, SWs gain a great interest in the assistance for people with mobility impairments.

### 2.1 Human Mobility and Disabilities

Mobility is one of the fundamental human faculties and can be defined as the ability of an individual to move his or her body within an environment or between environments, and the



ability to manipulate objects [29], in order to perform daily activities easily.

Such dysfunctions are common among the elderly and can be associated with the loss of independence [3] and cognitive problems [30], resulting in a degradation in their quality of life and wellbeing [1]. Besides, the elderly population has increased worldwide in recent years [2].

According to the World Health Organization (WHO), the global population aged 60 years overpass 652 million in 2017, more than twice as large as in 1980, when there were 382 million older persons worldwide [2]. Furthermore, it is expected that in the developing regions, people aged over 60 years will be 2.1 billion for 2050 [2]. Specifically, in Latin America, the number of people aged over 60 years is projected to grow 160.7 percent by 2050 [2]. This increment of the elderly part of the population is also observed in the other areas of the world [2].

Also, WHO reports that the proportion of older people living alone has increased in recent years [2]. It is essential to take into account this tendency due to the increasing of many health disorders with age [31]. Moreover, many of physical impairments linked with aging are associated with neurological conditions, orthopedic problems and medical conditions [26] and, within these, neurological diseases are the most common reason for locomotion impairment in people aged over 65 [7].

Stroke has been considered the leading cause of neuromuscular damages worldwide [32] and one of the most common causes of walking disabilities, with approximately 60 percent of the individuals suffering from persistent problems in walking [33]. As a consequence of stroke, the individual also presents abnormal muscle activation and impaired postural control [33,34]. On the other hand multiple Sclerosis is a disease that can produce disturbances of balance and motor coordination [26]. It is important to consider that cerebral diseases may also reduce the individual's quality of life through visual dysfunction [35], which may also be supported with assistance devices. Cerebral palsy affects the gait too, due to the permanent disorders of movement and the non-progressive disturbances that occur in the infant's brain [36]. In this case, children and young adults need to make a higher effort to maintain the coordination between muscles and motor control [37]. It is estimated that the 11.3 percent of the children with cerebral palsy used a hand-held mobility device to improve efficiency, stability, and posture [36].

Cardiopulmonary and musculoskeletal diseases are other factors that generate a slow gait speed in elderly and may also cause reductions in vision, standing balance, and physical activity [3].

Dementia diseases (e.g., Alzheimer) produce a concurrent and progressive cognitive impairment, but can also be considered as one of the diseases that affect the gait [3]. Such disease may produce a fear of falling, and as a consequence, generate a gait disorder [3]. Spinal Cord Injury (SCI) is another condition that affects the human mobility. People with SCI are exposed to fall while walking because of the loss of balance, affecting the patient independence and their quality of life [38]. In this context, almost all rehabilitation therapies are related to recovering independence and mobility [39]. In addition, declining gait speed is a frequent condition that affects the cognitive system, independence, and quality of life [40]. For this reason, developing assisted-gait devices that also stimulate the cognitive system in a positive way is an interesting topic, especially for the elderly.

## 2.2 Mobility Assistive Devices

The ability to move freely enables the individual with the capacity of doing typical life activities. However, these tasks might be compromised when mobility impairments are presented. According to the WHO, there are more than 1 billion people with any kind of disability worldwide [41], and this population may benefit from assistive technologies, such as mobility assistive devices [42].

Such as aforementioned, several mobility assistive devices can be used in gait rehabilitation and assistance scenarios. Among these devices, canes (see Fig. 2.1a), crutches (see Fig. 2.1b), wheeled knee walkers (see Fig. 2.1c) and walkers (see Fig. 2.2a) are commonly found. Furthermore, wheelchairs (e.g. manual or powered) (see Fig. 2.1d), tricycles and scooters are also used. Likewise, as shown in Fig. 2.1e, orthoses (e.g. callipers, braces, and splints), as well as, prostheses (i.e. artificial lower limbs) have been developed [42].

In this context, assistive devices are appropriate for people who exhibit gait impairments as well as for elderly with mobility difficulties. These devices are designed to enhance people's

quality of life and to provide critical functional benefits: independence, user's weight support, and safety [7]. This kind of devices may also have an impact on the prevention of injuries, falls and premature death [42]. This way, mobility assistive devices are frequently involved in users' daily living, assisting their activities and facilitating their social connectedness.



Figure 2.1: Examples of mobility assistive devices: a) Canes; b) Crutches; c) Wheeled knee walker; d) Manual wheelchair; e) Active orthoses.

The selection of a suitable device depends on the patient's weight bearing restriction, daily ambulation requirements, fitness level, cognitive function, and balance [43]. For instance, canes are used to increase gait stability by improving the base of support, by they also provide tactile information about the ground. However, as canes support only a single weak lower limb, gait symmetry is compromised [7]. Moreover, the effort of hand holding the cane might produce carpal tunnel syndrome [44], and, additionally, cane-assisted gait decreases the step length [45].

Another frequently prescribed assistive devices are the auxiliary crutches. Crutches are helpful for patients with lower-limb injury, who need to use their arms, not only for balance but weight bearing and propulsion [7]. One crutch can support 80 percent of weight body, and two crutches provide 100 percent weight support [7]. Even though auxiliary crutches are familiar and readily available, they are often described by patients as awkward, difficult to use and have demonstrated to demand a substantial energy cost [43]. In order to address such issue, wheeled knee walkers (see Fig. 2.1c) have been developed, which, compared with crutches, are used to improve the comfort, stability, and mobility [43].

Walkers appear as other important option within the assistive devices, as they are characterized by their structural simplicity, low cost, and rehabilitation potential [12]. In addition, they

provide support during locomotion while empowering the individual's gait capacity as well as improving his/her stability for those with lower limb weakness or poor balance. Therefore, walkers are used for facilitating and improving mobility by increasing the patient's base of support and supporting the patient's weight [7]. In addition, there is evidence pointing that walker-assisted gait is related to psychological benefits as they increase confidence and safety perception during ambulation [46].



Figure 2.2: Walkers frames: a) Standard; b) Front-wheeled; c) Rollator.

There are many types of established walkers in the market. The standard frame is the most stable one (see Fig. 2.2a), which is based on a four-legged rigid metal frame with rubber tips on the end of each leg. The standard walker generates a slower gait since the patient must completely lift the walker off the ground at each step. This may be challenging for frail older people with decreased upper body strength [7]. The extra level of force required to maneuver such devices constrains its use for those who also present severe levels of metabolic, cardiac or respiratory dysfunctions [47].

A front-wheeled walker (see Fig. 2.2b), also known as two-wheeled walker, is a variation of the standard one, which is characterized by the presence of two wheels on the front legs, affecting ground contact [12]. This walker is less stable than a standard walker, but maintains a more normal gait pattern and is better for those who are unable to lift a standard walker [7], as the energy cost is lower compared with the conventional walker [48].

Four-wheeled walker, commonly called rollators, are useful for higher functioning patients who do not need walkers as a base of weight support. This kind of walker presents wheels attached

to its four legs and brakes on its handlers. The use of rollators allows faster locomotion and more natural gait patterns. Often, these devices include a seat, being particularly useful for those with respiratory diseases or congestive heart failures, who often need to stop ambulating and sit down to rest [7]. Despite the four-wheeled walker easiness to propel, it is not appropriate for patients with significant balance problems or cognitive impairments, as it can roll forward unexpectedly, ending up in falls [7].

Walkers have a positive influence in health and wellbeing of users and their families, however, conventional walkers can present difficulties for maneuvering [7], resulting in greater attentional demands to navigate. In this context, some degree of cognitive abilities is required to maneuver the walker. In fact, active support for guidance, orientation and localization are needed, since physical assistance is not enough.

## 2.3 Technological Advances in Walkers

Robotic concepts have been integrated to conventional assistive devices to allow the development of smart devices, with the aim of offering a whole new range of functionalities, contributing to health support, gait assistance, and the increase of autonomy in daily activities [12]. The so-called SWs [10] are devices that can provide physical support, sensorial assistance, cognitive assistance, health monitoring, in addition to advanced human-robot interaction. By leveraging the intrinsic physical assistance provided by those devices, sensorial information, for example, may be used to guide people with mobility impairments. By doing so, the user interacts at a physical and at a cognitive level with the device, which must respond in natural ways to the human motion intention while guaranteeing safety for the often frail user. These devices are used for extended features, such as gait and navigation assistance, sit-to-stand transfer, obstacle avoidance, and fall prevention [6].

### 2.3.1 Passive and Active Walkers

Many research groups have worked over the last few decades on SWs, which usually are inspired by rollator frames. According to the literature evidence, SWs can be classified into two groups: passive and active walkers.

The first one corresponds to *passive walkers*, as they allow the user to be in full control over the locomotion. This kind of walkers may use sensors to obtain the orientation, localization, and to avoid obstacles [9]. Usually, these devices contain mechanical actuators to stop the locomotion, but not to insert energy. The *COOL Aide* [49] is a passive walker built on a commercial three-wheeled walker frame, with two force sensors on the handles and two encoders used to estimate the walker's velocity, position, and heading, and a Laser Ranger Finder (LRF) sensor used to provide a map of the environment surrounding. The MARC [50] passive version is a three-wheeled walker that lacks propulsion and rely on their user to provide forward motion. This walker is equipped with sonar, infrared sensors and wheel encoders to determine its localization in a local environment. In [9], a standard rollator walker with externally mounting sensors is used, which is equipped with laser scanners and vibration motors attached to each handle for tactile feedback about the environment.

The second group is composed of *active walkers*, which have a propulsion system based on motors to assist and propel the user locomotion. Likewise, as passive walkers, these devices are equipped with sensors to help the navigation and to guide the user through a free path within an environment.

Guido [51] is a SW developed by Haptica (Dublin, Ireland), which has sonar sensors to avoid short-range obstacles and to detect transparent objects, table edges and overhangs that the laser sensor would miss. The laser sensor is used to detect down drops, and a PC104 300 MHz is the onboard processor for motors control and processing task. The XR4000 [52] is a robot mobile platform with an omnidirectional drive. The robot is equipped with two ultrasonic transducers, two infrared near-range sensors, and a LRF sensor, in order to perceive obstacles at various heights. The LRF sensor is used for navigation (mapping, localization and path

planning).

The ABSGo++ [53] is a 4-wheeled motorized walker equipped with a LRF sensor to measure the distance between the walker and the user. Cameras are used for leg/foot tracking and upper body monitoring. Also, there are autonomous localization and navigation functions. The JARoW [54] is a walker with three motorized omnidirectional wheels, which are used to allow moving forward and backward, slide sideways, and rotate on the same spot. It also contains proximity sensors to detect the user's lower limb localization. The NeoASAS [55] uses a sensor system for the characterization of the HRI during assistive gait and force sensors integrated into the upper base support to detect the human motion intention. The SW of the PAMM system [15] has a force-torque sensor mounted under the user's handle to detect the human motion intention, and onboard sensors monitor the user's basic vital signs. The system also uses wireless communication with a central computer in order to receive updated planning information and to provide information on the health and user localization.

Another SW is the i-Walker [18], which is a standard rollator modified with sensors and actuators to promote upright control and walking for people with mild/moderate stroke. Two hub motors are the actuators integrated into the rear wheels, which are used to brake and help the user gait. This walker also has two modified handlebars with brake handles and force sensors to determine and adjust the amount of help that each motor should be giving to the user gait. The MARs [16] is the mobility assistance platform of MOBOT project [56]. This SW is a rollator-type equipped with supportive handlebars and a range of sensors to measure environment (LRF sensor) and human gait (LRF sensor and Kinect), and an Inertial Measurement Unit (IMU) used to estimate the robot angular acceleration. The CAIROW [21] is an SW with sensors to determine its localization in an indoor environment and to detect the user gait. Force sensors on the handles are used to perform human-interactive functions. The Devices for Assisted Living (DALi) uses a walking assistant called c-Walker [57], which has an Intel Barebone mini desktop to do processing tasks, such as image processing, situation assessment, trajectory planning, and guidance. The SW orientation is composed of encoders mounted on wheels and an IMU. Furthermore, it uses a Kinect in front of it to detect obstacles in the environment and to track people moving close to it.

Hence, through sensors, a SW may obtain information to improve both the HRI and the HREI. Nevertheless, it is also necessary to use HRI and HREI for strategies that facilitate the user experience with the SW, which is the subject of the next topic.

## 2.4 Current Trend in Smart Walkers: From Human-Robot to Human-Robot-Environment and Social Interaction

When SWs are employed to assist the human locomotion, the cognitive and physical processes of the user are involved [12]. Both are necessary, as the SW may use this information to learn, adapt and/or optimize its functions and interact with the user and the environment in a natural way.

As the user and walker share the same space, the user should have an active role in the HRI and HREI to promote the user safety, planning ability, reasoning capacity, execution of locomotion and finally, social interaction. Furthermore, the walker needs specific functions, such as the identification of the user's motion intention, health monitoring, gait monitoring, mapping, localization, path planning, and obstacle detection and avoidance, and thus, to have autonomous capabilities for cooperating directly with humans on the working space. Also, these functions generally are necessary to improve the HRI and the HREI.

Research works have focused on HRI, which is usually supplied through sensors to detect the motion intention. In Guido [51], force sensors at the handlebars are used to detect the user intention. JAIST [54] and CAIROW [21] use a laser sensor to detect the user's leg position and generate velocity control commands for the SW.

In [12], the human movement intention is captured by force sensors on the arm support whereas an LRF sensor detects the legs' pose in relation to the walker. The user interacts in this case on a physical and cognitive level with the walker, as the SW follows the user velocity, and his/her motion intention, resulting in a natural channel of communication.

In [13], a controller for a human-robot formation is introduced, in which the human is the leader



of the formation. LRF and ultrasound sensors are used to detect the user location and motion intention. In this context, SWs can offer support for people with physical disabilities and those that cannot operate conventional walkers, reinforcing personal autonomy and improving their daily living. However, when users also presents cognitive impairments, it may be necessary to assist them at a different level. In this context, guidance and navigation functionalities may be an interesting approach to assist them to reach the desired objective directly.

Despite the intense scientific and technological development around the SWs, little attention has been paid to HREI. In [16], a shared control is proposed, whose control architecture integrates cognitive, sensorial and physical assistance. A path following technique is also used to support the cognitive assistance and, a LRF sensor is used for obstacle avoidance. CAIROW [21] has functions for path following, localization and obstacle avoidance. All these SWs can guide people, however, none of them allow the user to make decisions about navigation.

In PAMM [15], an adaptive controller is implemented to guide the user back to a predetermined trajectory when the user deviates from it. It also detects its localization at the environment and, based on a performance evaluation, its controller generates a virtual force input based on the environment information to guide the user. The shared control included in PAMM allows that the user makes decisions about the SW, but, when the user deviates from the predetermined trajectory, the controller guides the user back to it, although the authors understand that additional forces generate by the walker control strategy must be avoided, as external perturbations may compromise the user's balance [15].

The i-Walker [18] promotes cognitive assistance, helping the user's guidance in everyday situations like moving uphill, downhill, turning left/right, and/or standing still, standing up, among others. Force sensors placed at the handlebars are used to detect the user's motion intention, whereas sensors installed on the environment helps navigation and promotes cognitive assistance. Nevertheless, the use of external sensors requires an extra investment to offer cognitive aid focused on memory reinforcements and activities of daily living support, also requiring known or predetermined environments for navigation, which could limit the user's independence.

In [9] and [20], the SWs provide sensorial assistance for blind people navigation. In these walkers, haptic feedback signals are provided through both the vibration of a belt and the walker handles to indicate the spatial information and navigation commands. In both cases [9,20], a laser sensor provides information for obstacle detection. The interpretation of the navigation commands requires a user's cognitive process, which introduces natural delays and may induce fatigue in the user [58].

There are research works involving new sensors and control strategies to improve the SWs capabilities in different contexts [12,15,18,59]. However, most of the HREI strategies found in the literature needs either wearable sensors and actuators on the individual, or sensors at the environment. Also, when the user is an elderly and he/she is navigating with help from such devices, in some cases, a travel path can be programmed for an easy displacement, and the user does not make any decision about the SW, relieving the user from greater efforts and cognitive process. In this case, the user is just being guided by the SW, with a secondary role in the HREI [9,15,60]. Therefore, it is necessary to develop strategies with natural HREI, and thus, stimulate the cognitive system through decisions making, giving an active role to the user at navigation.

On the other hand, when SWs are employed to assist human navigation, such devices must not only empower locomotion but also provide tools for allowing social interaction and improve the HREI. As a user makes use of an SW, the control algorithms responsible for navigation should take into consideration social conventions and human behavior to allow for proper interaction with the environment and other people [61]. Therefore, it is essential to integrate some cognitive capabilities to the device when used in shared spaces. Inspired by the proxemics studies developed by Hall [62], some social conventions have been established in robot navigation to avoid or interact within the different social spaces of human depending on the task.

However, literature regarding SWs has traditionally overlooked this kind of social behaviors, and navigation systems [6,24,25] have been implemented in similar ways to traditional robotics, not including the interaction with objects of the environment. For example, in [63] the Robot Operating System (ROS) navigation stack and SLAM (Simultaneous Localization and Mapping)

Gmapping library were adopted, which are used for autonomous robots navigation in mobile robotics. These algorithms do not permit the user to interact with another person during navigation, as detected objects are considerate obstacles that should be avoided. In [15,50,64], path following and obstacle avoidance techniques are used to guide the user to the final destination. As people are perceived as obstacles, social interaction is also not permitted. Others SWs uses haptic [19] or acoustic [65] signals to guide navigation. In both cases [19,65], the interpretation of the navigation commands requires an user's cognitive process, and introduces natural delays that may induce fatigue in the user [58]. Furthermore, in both studies [19,65], all obstacles in the environment are seen as objects to avoid.

SWs are typically employed in environments such as hospitals, clinics and nursing homes, and, in such indoor environments, the ability to move through confined spaces (i.e., corridors) is necessary. However, works in the literature that address such kind of navigation are focused on robotic wheelchairs [66,67] and traditional mobile robots [68,69]. As regards to SWs, the project DALi developed the c-Walker to offer assisted navigation in complex indoor environments [57], and to guide older adults across complex public spaces [23]. The c-Walker can detect and interpret human behavior in the environment in order to plan the route of navigation, and through haptic bracelets and audio signals, the user receives feedback for trajectory correction. Also, people on the surrounding environment are seen as dynamical obstacles, and their trajectory is calculated using the social force model (SFM) [70], to avoid collisions. Nevertheless, such strategy does not foresee the SW's user engaging in a conversation with other people during navigation.

If the SW's user cannot interact with another people during navigation, the distress, depression and emotional problems may appear and affect his/her health, especially when the user is an elderly [14]. In this context, it is necessary to integrate social interaction concepts into the SW control strategy. According to the literature, social navigation depends on the environment and of socio-cultural rules [71]. Specifically, through proxemics [62], spatial distances can be defined to avoid obstacles using social rules and/or to allow a companion during locomotion with the SW, to finally have social concepts into the SW navigation and improve the HREI.

## 2.5 UFES's Smart Walker (USW)

The robotic platform used in this work is shown in Fig. 2.3a. An embedded computer PC/104-Plus standard is used to control and perform processing tasks, which consists of a 1.67 GHz Atom N450 with 2 GB of flash memory (hard disk) and 2 GB of RAM memory. This computer is integrated into a real-time architecture based on Matlab-Simulink Real-Time xPC Target Toolbox. A laptop is additionally used to program the embedded computer and to store experimental data when necessary. It is connected to the PC/104-Plus by Ethernet using the User Datagram Protocol (UDP).

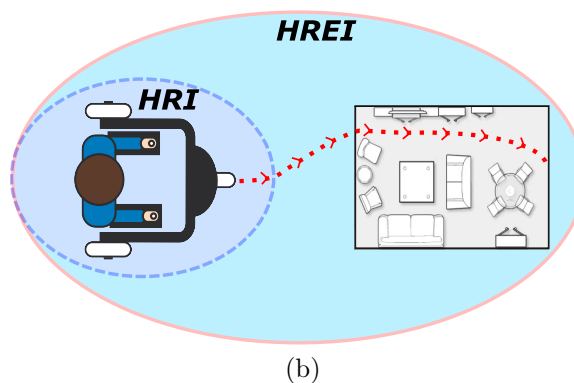
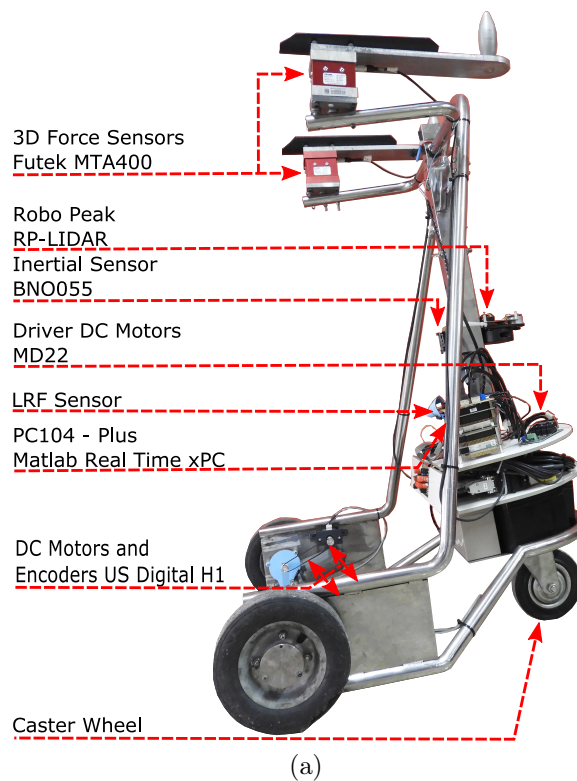


Figure 2.3: a) UFES's Smart Walker (USW); b) Interaction layers.

The USW integrates two interaction layers; one for *HRI* and another one for *HREI* (see Fig. 2.3b). The implemented HRI strategy is performed relying on both physical and cognitive interfaces [10, 12] based on two kinds of sensors: a pair of 3D force sensors (model MTA400 - Futek, US), installed under the forearm supporting platforms, and a LRF sensor (model Hokuyo URG-04LX) to obtain the distance between the user's legs and the walker [12].

The HREI strategy is based on the environmental and displacement information, which is defined by the following sensors: odometry, determined through a 9 DOF inertial sensor BNO055, and an optical shaft encoders H1 (US Digital, US), which measures the wheels velocities. Both sensors are used to provide the robot's pose (position and orientation) in real-time. Another LRF sensor, a RP-LIDAR (Robo Peak, China), is located in front of the SW, which is used as sensory assistant, recovering environment information to detect walls, obstacles and people.

As a conclusion of this chapter, the HRI and HREI implemented have improved the SWs capabilities in different contexts. However, some strategies have unnatural interaction between user and walker, as they need external sensors on the user and/or environment to offer safe navigation. Furthermore, many strategies leave the user in a secondary role during navigation. In this context, it is necessary to develop control strategies that allow a natural HREI, thus avoiding taking away the user control of the robot, giving to him/her the main role during navigation, and contributing in a positive way to the cognitive system of the user. In addition, to facilitate the HREI, it is necessary to include social concepts within the SW's control to promote social-aware navigation, and as a result, to improve the social acceptance of the SW and promote the user social interaction.

## Chapter 3

# Admittance Controller Applied to Walker-Assisted Gait

Such as aforementioned in Chapter 2 (see Section 2.3), SWs provide users with physical, sensorial and cognitive support as well as assistance for guidance, orientation and localization [8].

According to the literature, the human motion intention in robotic walker can be measured or estimated through the use of force and/or laser sensors. For example, PAMM [15], MARs [16], ISR-AIWALKER [17] and i-Walker [18] employ force/torque sensors mounted under the walker's handle to serve as the main Physical Human-Robot Interface (pHRi) and Cognitive Human-Robot Interface (cHRi), which are used to develop the HRI strategy. Force-sensing resistors (FSR) and LRF sensor are used in a multi-sensor fusion method to detect the human walking intention [72]. In [12], the human movement intention is captured by force sensors installed under the forearm supporting platforms. Regarding the SW control, a control strategy commonly used to develop a natural interaction between the human and the SW is the admittance control [10, 15, 16].

Admittance control can be used to develop a natural interaction between the human and the SW, and also to generate signals to indicate the path to be followed in a real environment through haptic feedback. The admittance control emulates a dynamic system and provides the user with a sensation of interaction with the SW. This chapter presents the development

of a strategy to detect the human motion intention to command a SW, based on previous studies of [12,73,74]. The user’s cadence oscillation and other noises present in the force signals are filtered by the combination of Fourier Linear Combiner (FLC) and Weighted-Frequency Fourier Linear Combiner (WFLC) filters [12]. This way, taking advantage of the physical contact between the user and the SW, an interface to detect the human motion intention in a natural and intuitive way is also presented. In addition, this chapter presents a study of the influence of the admittance control parameters on the linear and angular velocities of the SW, as this can affect the HRI, and, as a consequence, the user experience.

This chapter is organized as follows. First, it describes the pHRi and cHRi, presenting also the admittance control strategy and the adaptive filters. Second, it describes the experimental setup and the strategy of interaction. Finally, it shows the discussion of the experimental results and the respective conclusions.

### 3.1 Admittance Control Strategy

The USW employs an impedance controller [10, 16] to relate linear and angular velocities with the force signals that are produced naturally on the forearms when the user is assisted by the SW, thus establishing a comfortable speed for locomotion. This way, it leverages the physical interaction between the SW and the user to generate the navigation commands (see Fig. 3.1).

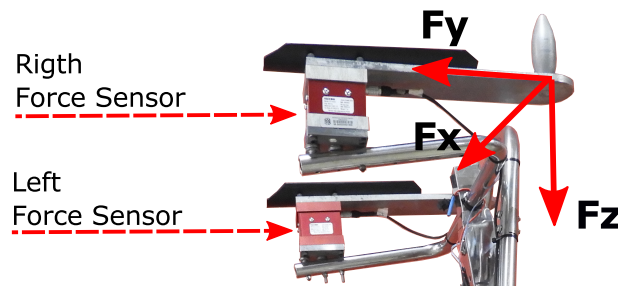


Figure 3.1: Physical Human-Robot interface based on force sensors.

The signal on the  $F_y$  axis captured by each sensor is processed to infer the user’s motion intention, and the signal on the  $F_z$  axis is used as one of the safety parameters to assure adequate partial body weight support. The force ( $F(t)$ ) and torque ( $\tau(t)$ ) signals are calculate

according to 3.1 and 3.2:

$$F(t) = -\frac{F_{LY}(t) + F_{RY}(t)}{2} \quad (3.1)$$

$$\tau(t) = -\frac{F_{LY}(t) - F_{RY}(t)}{2} \times d, \quad (3.2)$$

where  $F_{LY}$  is the left arm forward force,  $F_{RY}$  is the right arm forward force, and  $d$  is the horizontal distance between the sensors.

$F(t)$  and  $\tau(t)$  signals are used by the admittance controller to generate the desired linear  $\nu_c(t)$  and angular  $\omega_c(t)$  velocities for the walker, defined as:

$$\nu_c(t) = \frac{F(t) - m_\nu \dot{\nu}(t)}{d_\nu} \quad (3.3)$$

$$\omega_c(t) = \frac{\tau(t) - m_\omega \dot{\omega}(t)}{d_\omega}, \quad (3.4)$$

where the masses  $m_\nu$  and  $m_\omega$ , and the damping  $d_\nu$  and  $d_\omega$  are parameters that have to be adjusted, as they have a direct influence on the HRI. Section 3.3 shows the experiment used to assign the value of the admittance control parameters.

Both velocities are also used to impose not only the start and end of the locomotion with the SW, but also a comfortable gait speed. Furthermore, these velocities are sent to each motor of the SW using the Eq. 3.5 and 3.6 [75].

$$Motor_{Left} = \nu_c(t) - \omega_c(t) \frac{D}{2}, \quad (3.5)$$

$$Motor_{Right} = \nu_c(t) + \omega_c(t) \frac{D}{2}, \quad (3.6)$$

where  $D$  is the distance between the SW wheels.



## 3.2 Navigation Commands Recognition

When the user is walking supported by the SW, natural trunk oscillations during gait are converted into force interaction signals. Additional mechanical vibrations caused by floor irregularities were also observed on force interaction signals in [76].

As shown in previous works [76, 77], it is necessary to apply an adaptive filtering strategy to obtain a more suitable force signal to be used with the proposed control strategy.

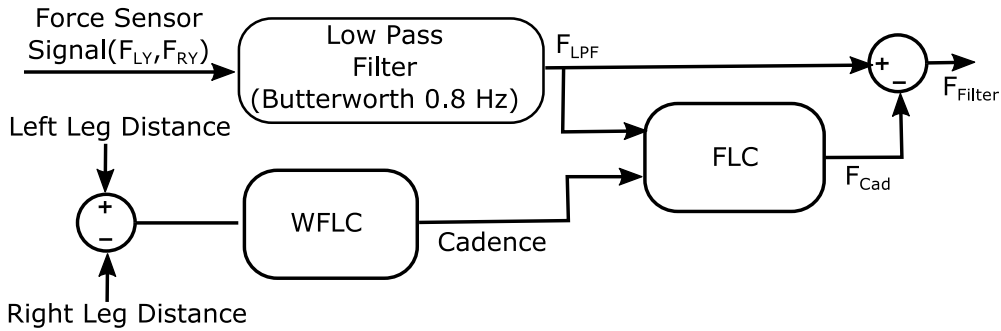


Figure 3.2: Block diagram to eliminate the cadence from force signals.

Relying on past developments of the research group [12], the author also applies the combination of the Fourier Linear Combiner (FLC) [78] algorithm to estimate and cancel cadence components of each input signal ( $F_{LY}$  and  $F_{RY}$ ), and a Weighted-Frequency Fourier Linear Combiner (WFLC) [12] for the estimation of the cadence signals obtained from the signals acquired by the LRF sensor (see Fig. 3.2).

Other mechanical vibrations caused by floor or wheels irregularities are filtered by traditional low pass filtering topologies, as such components are more easily separable from the force components related to the motion intention. In this work, we applied a second order Butterworth low-pass filter (cutoff frequency of 0.8 Hz) to reject high frequency components that are not associated with the gait cadence.

### 3.3 Experimental Study

Twenty subjects without previous training with the SW participated in the experiments. A computer was used to record both the SW velocities and user data, such as discharged force on the SW, force, and torque. The masses of the participants are  $66.72 \pm 13.63$  kg, and their heights are  $1.66 \pm 0.075$  m. Two different experiments were proposed to validate the filter behaviour and to establish the value of the admittance control parameters.

#### 3.3.1 Experiment 1. Following a Straight Line

The first experiment focused on the linear velocity parameters. For this, the protocol 4-Meter Walk Test (4MWT) presented in [6] was used, which is enough to the controller reach the steady-state conditions. The user was asked to walk a straight line with the SW (see Fig. 3.3). The special interest of this experiment was at the start and the end of the locomotion with the SW, due the fact that the movement needs to be natural and the SW must not have any inertia that makes its locomotion difficult, i.e., the user has not to do an additional force to start or stop his/her displacement. In this experiment, the mass  $m_v$  was decreased 2 kg, starting at the value equivalent to 50 % of the user's weight (which was an empirical criterion), until finding a parameter value where the user could have an easy locomotion with the SW. Once the user started feeling comfortable maneuvering of the SW, these parameters were fine-tuned in steps of 0.5 kg until finding the suitable value, thus, the user had to walk the straight line n-times. The damping  $d_v$  parameter, on the other hand, was adjusted in order to have a comfortable gait. Wrong values of these parameters make hard breaking the inertia moment at the beginning of the locomotion and difficult to stop the SW.

#### 3.3.2 Experiment 2. Following the Lemniscate Curve

At the second experiment, the mass  $m_w$  decreased each 1 kg, starting at the value equivalent to 20 % of the subject's weight (which was an empirical criterion). Once the user could do the

movement without feeling any effort on the lower limbs or on the hip, the mass was fine-tuned in steps of 0.05 kg until finding the suitable value, this way, the user had to follow the path n-times until finding the correct value. In order to determine the damping value, a path performing a lemniscate curve (see Fig 3.4) was used. This kind of path was chosen due to it is possible to analyze the performance of the controller in straight and in curve-shaped trajectories exciting its dynamics. Each participant was asked to do one and a half eight-shaped curve, starting from the middle of the path indicated on the floor. The damping  $d_\omega$  value was then adjusted for each user, such that a movement without any effort was achieved. Both the dynamics of the SW and the user have an influence on the maneuverability of the SW. Furthermore, it was necessary to do another adjust to  $m_\omega$ , as the inertia introduced for this mass affected the USW's maneuverability, which occurred at the exit and entry of the curve.

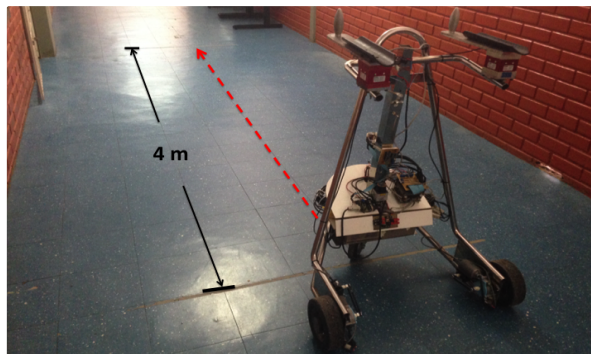


Figure 3.3: Experiment 1, where the subjects were asked to follow a straight line.



Figure 3.4: Experiment 2, where the users were asked to follow a lemniscate curve indicated on the floor.

In both experiments, bigger parameter values of mass and damping that lead to an easy SW's maneuverability were determined. This criterion was defined just in the point when the user

began to do the locomotion in a natural way and without any force/torque that reflected an effort on the legs or hip. For smaller values, the user could drive the SW without any difficulty.

### 3.4 Experimental Results and Discussion

First, it was necessary to verify the behavior of the algorithm established to eliminate the cadence-related component, which was filtered from the force signal ( $y$  - axis). For this, data recorded of one participant following the lemniscate curve was used. Figure 3.5 shows the behavior of the adaptive filter. It can be observed that the oscillations detected by the force sensors, caused by the user's cadence, which was 0.5 step/seg, and mechanical vibrations of the SW, were eliminated.

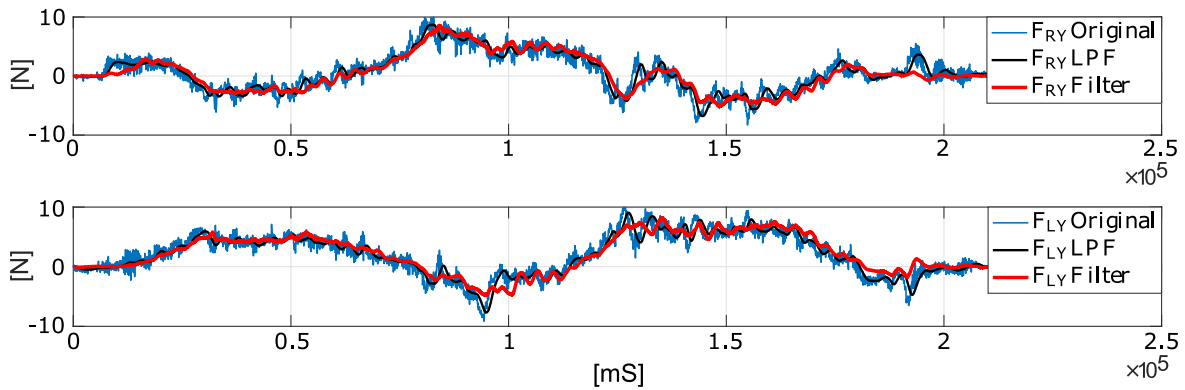


Figure 3.5: Adaptive filter behavior.

Regarding the study of the admittance control parameters and its influence on the user experience, the results are presented below.

#### 3.4.1 Experiment 1: Following the Straight Line

The quantitative variables like the users' height and weight do not seem to have any relation to the linear velocity of the admittance control parameters. However, after analyzing the recorded data, a proportional relation between the user's discharge force on the SW and  $m_\nu$  was found with an exponential trend (see Fig. 3.6). Such as it can be seen from the figure, for users with small discharge force, the mass value was also small.

A damping  $d_\nu$ , with a mean of  $10.35 \pm 1.38$ , was found, which only influenced the comfort gait speed. Nevertheless, it is necessary to limit the control signal of the linear velocity to 0.5 m/s, due to the DC motors limitation. This limit is close to the gait speed estimate for usual pace in elderly people with mean age equal to 70 years old and without any gait disorder [79].

The relationship between the user's discharge force on the SW and the mass  $m_\nu$  of the linear velocity (see Eq. 3.3) can be defined by the following mathematical model:

$$m_\nu(t) = A.r^{(Discharge\ force)}, \quad (3.7)$$

where  $A = 8.47$  and  $r = 1.05$ . This model can be implemented in the embedded computer of the USW in order to automatically compute the value of  $m_\nu$ . By fixing the value of  $d_\nu$  to 10.35 kg/s, the linear velocity parameters of the admittance controller can be computed on-line.

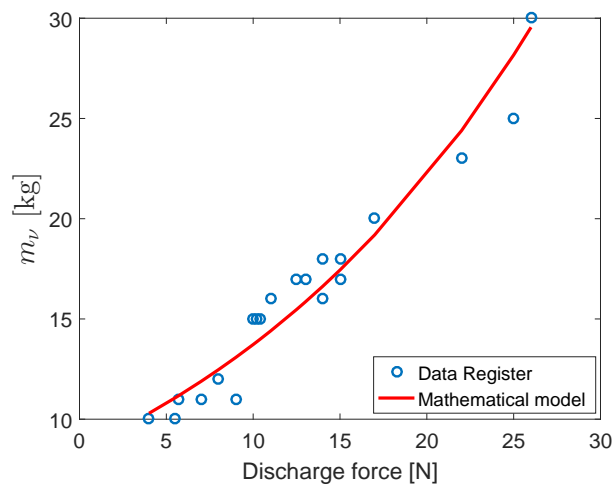
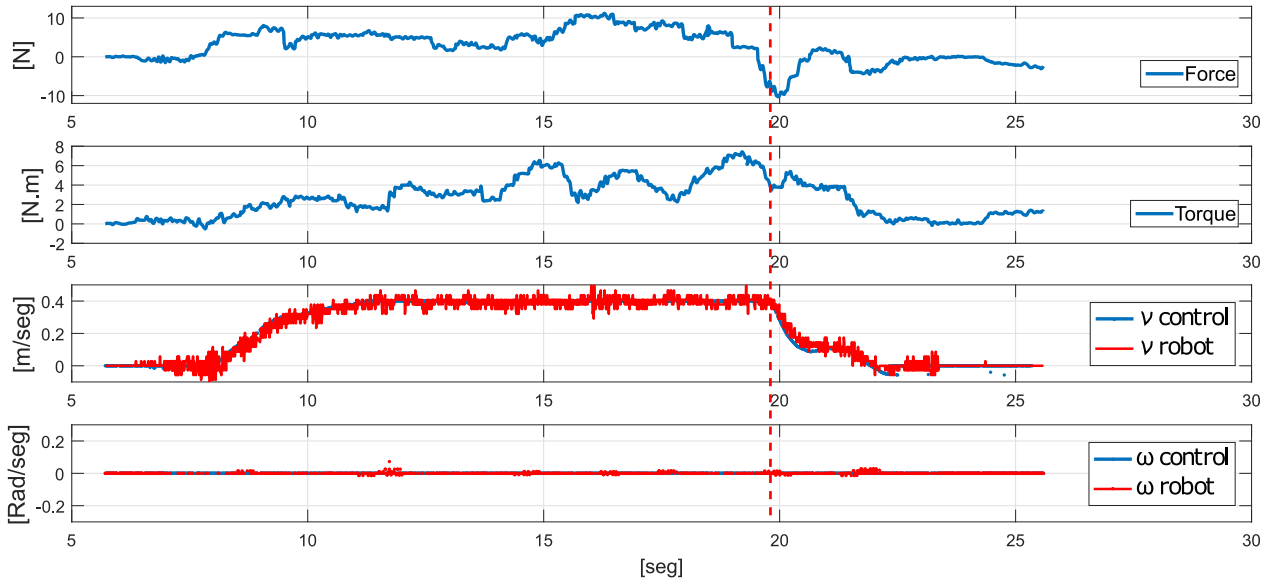


Figure 3.6: Tendency of user discharge force with respect to the mass  $m_\nu$ .

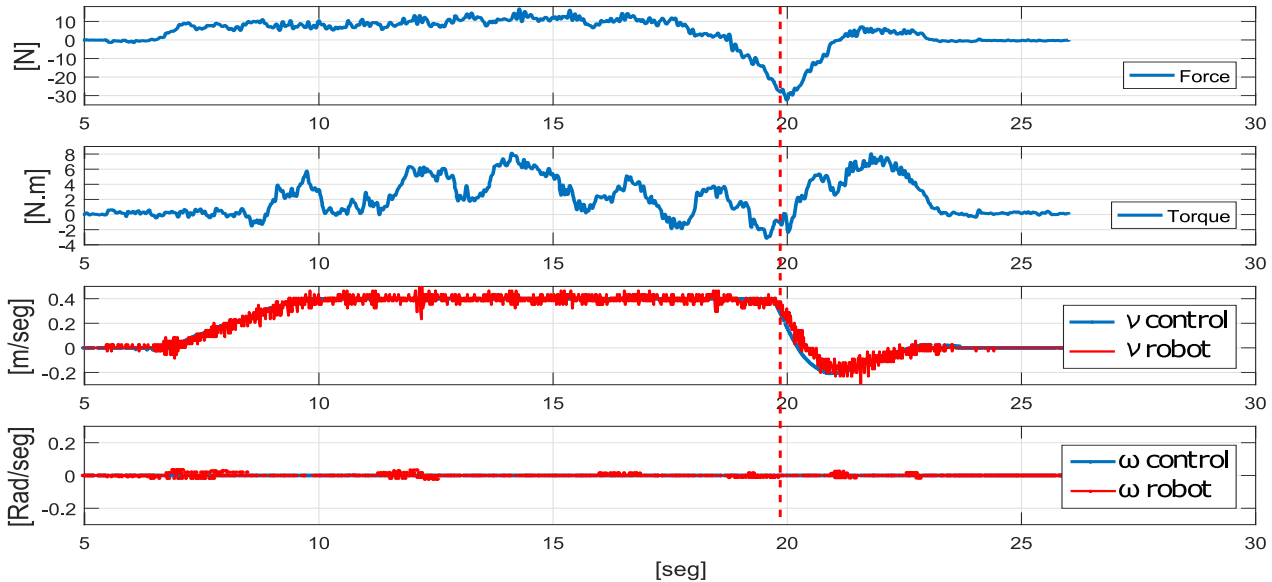
From Experiment 1, it was observed that mass is the parameter that has the highest influence on the SW maneuverability. An erroneous value of this parameter makes the start and the end points of the SW locomotion very difficult.

Figure 3.7a shows the behavior of the main variables of the controller for an easy locomotion. For this case, the controller data were: mass  $m_\nu = 15$  kg, damping  $d_\nu = 10.35$  kg/s and *discharge force* = 10N. The user parameters were: height = 1.67 m and weight = 72 kg. With the same user, the results depicted in Figure 3.7b were obtained using a mass value of  $m_\nu = 22$

*kg*. This last value lead to a very difficult locomotion with the USW.



(a)



(b)

Figure 3.7: a) Controller behavior with a good selection of admittance control parameters ( $m_\nu = 15 \text{ kg}$ ,  $d_\nu = 10.35 \text{ kg/s}$ ); b) Controller behavior with an erroneous  $m_\nu$  value ( $m_\nu = 22 \text{ kg}$ ,  $d_\nu = 10.35 \text{ kg/s}$ ).

In Figure 3.7a, it is possible to see that the linear velocity slowly decreases around 20 s, where a natural stop of the user locomotion occurs. However, when the controller has a wrong mass value, the user has to do additional movements to manipulate the SW and stop it (see second 20 of Fig 3.7b). It is also possible to observe that force and torque are higher in Figure 3.7b, compared to Figure 3.7a. This is the result of setting the controller parameters according to

the user discharge force. Moreover, when the linear velocity equation has an erroneous mass value, the user has to do a high compensating force to stop the SW (see after the dotted line of Fig 3.7a and 3.7b). This action can generate torque signals on the user and affect his/her balance as well as produce a collision between the user and the SW, if the SW does not have a restriction for negative linear velocities. In addition, the Mean Square Error (MSE) of the linear velocity oscillates between  $0.11 \text{ m/s}$  and  $0.13 \text{ m/s}$ , and the angular velocity oscillates between  $0.015 \text{ rad/s}$  and  $0.016 \text{ rad/s}$ .

### 3.4.2 Experiment 2: Following the Lemniscate Curve

Once the linear velocity parameters were established, the angular velocity parameters were adjusted. In this experiment, no relationship, neither linear nor non-linear, was found between the height, weight or discharge force of the user and the  $m_\omega$  parameter. Figure 3.8 shows the distribution of user discharge force with respect to  $m_\omega$ .

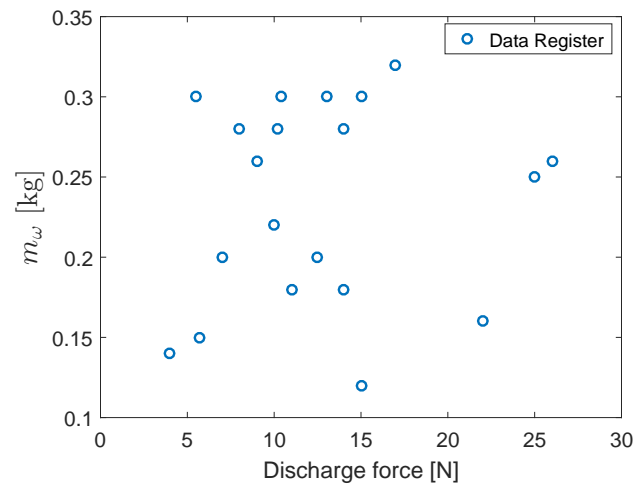
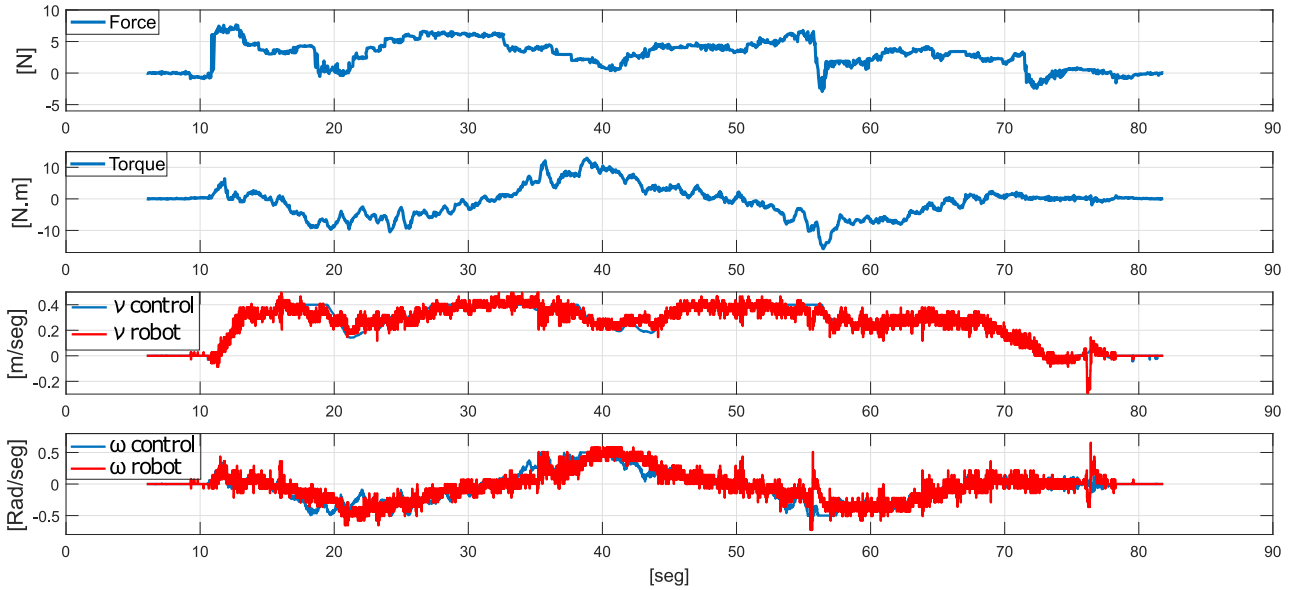


Figure 3.8: User discharge force with respect to  $m_\omega$ .

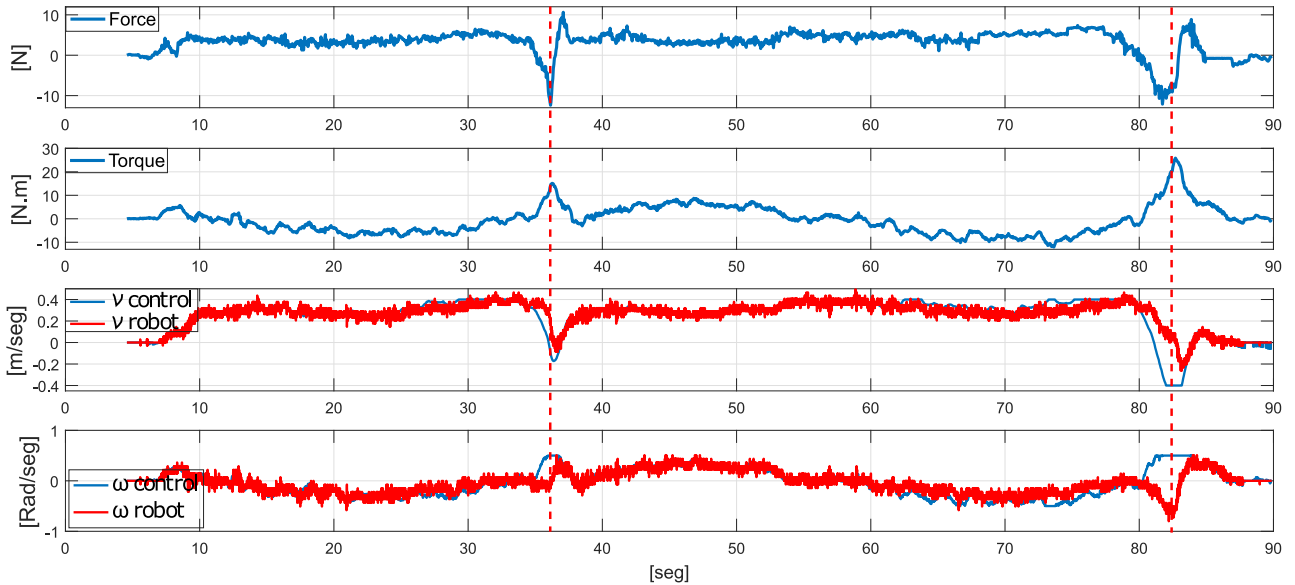
The results of this second experiment suggest that the parameter  $m_\omega$  depends on the dynamics of the SW and the user. Furthermore, the linear velocity value of the SW, when entering the curve, strongly influences the SW maneuverability during the execution of the curve. According to the data registered during the experiment, it is recommended to set this value to 0.01% of  $m_\nu$ , if an online calculation is required, as this criterion allows move the SW without any effort.

The selection of this value can be supported by the fact that it was typically lower than the upper limit accepted by each participant during the experiment. Moreover, with this value, the user does not put any additional effort on the lower limbs or on the hip.

Concerning the damping parameter  $d_\omega$ , the recorded mean value was  $20 \pm 0.5 \text{ m/kg}$ . In addition, the results suggest that its value affects the user angular locomotion speed. Hence, for a comfortable steering velocity during the curves,  $d_\omega$  could be set to  $20 \text{ m/kg}$ .



(a)



(b)

Figure 3.9: a) Following the eight-shaped curve with a good selection of admittance control parameters ( $m_\omega = 0.26, d_\omega = 20$ ); b) Following the lemniscate curve with bad admittance control parameters ( $m_\omega = 0.35, d_\omega = 20$ ).



Figure 3.9a shows the controller behavior used to follow the path shown in Figure 3.4. The parameter values for the linear velocity were the same as those defined for Figure 3.7a. The controller behavior for a good parameter selection is shown in Figure 3.9a, whereas Figure 3.9b shows the controller curves for a bad selection of  $m_\omega$ . From Figure 3.9a, it can be observed that the user had to apply a lower force to drive the SW compared to the one depicted in Figure 3.9b. Furthermore, when the  $m_\omega$  is wrongly defined, the user has to apply additional force and torque in order to control the SW when exiting the curve (see red dotted line in Fig 3.9b). This can affect the balance of the user and increase the risk to fall. In addition, the MSE of the linear velocity oscillates between  $0.2 \text{ m/s}$  and  $0.23 \text{ m/s}$ , and the angular velocity oscillates between  $0.1 \text{ rad/s}$  and  $0.15 \text{ rad/s}$ .

The data and the results produced during this study confirm that the interaction between the user and the SW can be affected by the admittance control parameters. Thus, a good selection of these variables results in a natural locomotion of the SW. On the other hand, the locomotion during the curve can be made more comfortable if the linear velocity is limited.

As the conclusions of this chapter, the admittance control strategy proposed here allows a natural locomotion with the USW. Also, it was shown that with this control strategy the user can regulate a comfortable gait speed. In addition, the use of only force sensors to define a natural HRI is reflected on the computational efficiency and low processing of the control algorithm in real time. This experimental study allowed obtaining good results in terms of user's locomotion performance, according to his/her motion intention. This way, the interface developed here allowed a natural interaction between the user and the SW without the need of external sensors on either the user and/or the environment.

A good set of filter parameters allowed correctly detecting the human motion intention, and through the use of an admittance control strategy, the SW attended such motion intention. Once established the suitable filter, this chapter showed that the motion intention was executed in real time, and the signal oscillations and noise were canceled.

According to the study of the influence of the admittance control parameter within the HRI, it was noticed that the damping parameters influenced the comfortable gait speed in the navi-

gation with the USW. Conversely, the inertia added by the mass parameters affected the start and stop locomotion movements, as well as the start and end of the curve. From these results, it is clear that a good selection of parameters might prevent possible falls and collisions of the user, and, on its turn, avoid compromising the user's health during navigation.

The model established in this chapter to calculate the admittance control parameters will be used in an offline way in the next chapters. However, a mathematical model to compute the different admittance control parameters, in an online way, will be investigated in a future work. Apart from this, the next chapter describes new control strategies to improve the HRI with a real environment using haptic feedback to guide the user navigation. This way, novel strategies to allow a natural and intuitive HRI will be developed.

## Chapter 4

# Human-Robot-Environment Interaction

## Based on Spatial Modulation of

## Admittance Controller for Smart Walker

## Navigation

This chapter presents the proposal, implementation and validation of a new strategy for continuously modifying the dynamic parameters of the admittance controller to induce the user to follow a predetermined path in a natural and intuitive way. The proposed method generates a spatial modulation of the damping parameter, simulating a virtual canal for locomotion through variable friction, and inducing a sensation of hard navigation whenever the user deviates from the right path or is outside of such virtual canal. The user perceives such sensation through the physical contact between his/her forearms and the SW structure. Furthermore, the user receives a haptic feedback as an increment in the difficulty of locomotion also when he/she is steering in the wrong direction. This way, the user needs to search the right direction and intuitively find the easy maneuver. The proposed controller uses a multimodal cognitive interaction with the user through two channels. The first one is composed of a cHRi and a pHRi, which uses a haptic feedback that results from the physical interaction between user and SW.

The second channel is a cHRI, which uses a visual interface through two LEDs that indicate the direction that the SW should take to follow the correct path. This control strategy induces the user to follow the path in a natural and intuitive way, providing a “feeling” of command over the SW. Also, the user’s cognitive system is stimulated through decision making when direction correction is needed.

## 4.1 Background

Few works consider the variation of the admittance controller parameters for the user interact with the environment. In [15], the author proposes a shared control with a cost function for the force signal, which combines the proximity to obstacles, the deviation from the planned trajectory and human stability criteria. The shared control varies the force gains to provide more authority to the human or the robot. This way, the force signal of the admittance controller is varied. However, the user’s motion intention may be affected because the user’s force/torque signals do not command the smart walker. This change of robot control authority may produce a confusion sensation in the user and affects his/her cognitive system. With the control strategy presented in this chapter, the SW maneuverability is affected based on the damping parameter variation, but the user’s motion intention is maintained. Nevertheless, the user needs to make decisions about keeping effort to drive the SW or correcting the locomotion direction and have an easier navigation. In [16], a shared control is proposed in order to on-line adapt the damping parameter of the admittance controller using the drift diffusion (DD) model proposed by [80]. That model describes the decision-making in humans as a process in which decisions are based on past decisions, and the decision criteria are continuously adjusted in order to maximize the reward obtained throughout task execution [16]. Based on the DD model, decision maker blocks for sensorial, cognitive and physical assistance decide the level of robot assistance. As the user moves far away from the main task (desired path, obstacle avoidance), the controller assigns a higher decision making power to the robot, which makes the user lose maneuverability control on the robot. The strategy proposed in this chapter never takes away the user control of the robot. Furthermore, it allows varying, in real-time the

damping parameter of the admittance controller based on its spatial information, and gives the user a main role in the HREI through a haptic sensation to discern the best path to follow.

This chapter is organized as follows. First, it describes the control strategy for the HREI and how the admittance parameters are modulated. Second, it describes the experimental setup, showing the way the user is guided along the path. Then, it shows the experimental results, as well as the discussion about them. Finally, conclusions about the controller strategy are presented.

## 4.2 Control Strategy for Smart Walker Navigation

A novel control strategy, shown in Figure 4.1, is introduced here, which relies on the admittance controller proposed in [16] to obtain the user's motion intention. The admittance controller emulates a dynamic system and gives the user a feeling as if he/she is interacting with the system specified by the admittance model [16]. A path following controller [75] is used to guide the user through a predetermined path. The objective of the path following controller is to provide a desired orientation to the SW. The admittance modulator takes the orientation error and the user's torque intention to change, in real-time, damping parameters of the admittance controller. A supervisor is used to establish safe parameters for the user. Each block in Figure 4.1 is explained in the following sections.

The user's motion intention is determined, such as described in Chapter 3. Using the pHRi composed of the force sensors localized under user forearms platforms (see Fig. 3.1), the signals from the  $y$  axes of each sensor are used to obtain force and torque measurements (box 1 Fig. 4.1), depending on the arm motion, as shown in 3.1 and 3.2. For the linear control velocity  $\nu_c(t)$  and angular control velocity  $\omega_c(t)$ , (box 2 Fig. 4.1), the procedure described in Chapter 3 is used, which is calculated as shown in 3.3 and 3.4, respectively.

To guide the user through a predetermined path, a path following controller is used (box 3 Fig. 4.1), which uses the kinematic model of an unicycle-like mobile robot [81]. The use of the kinematic model for controlling the movement of the SW is based on the fact that the assistance

device moves with slow velocities and accelerations. In that sense, it is not necessary to apply a dynamic model, as the dynamic imposed by the admittance control is slow when compared with the robot dynamics.

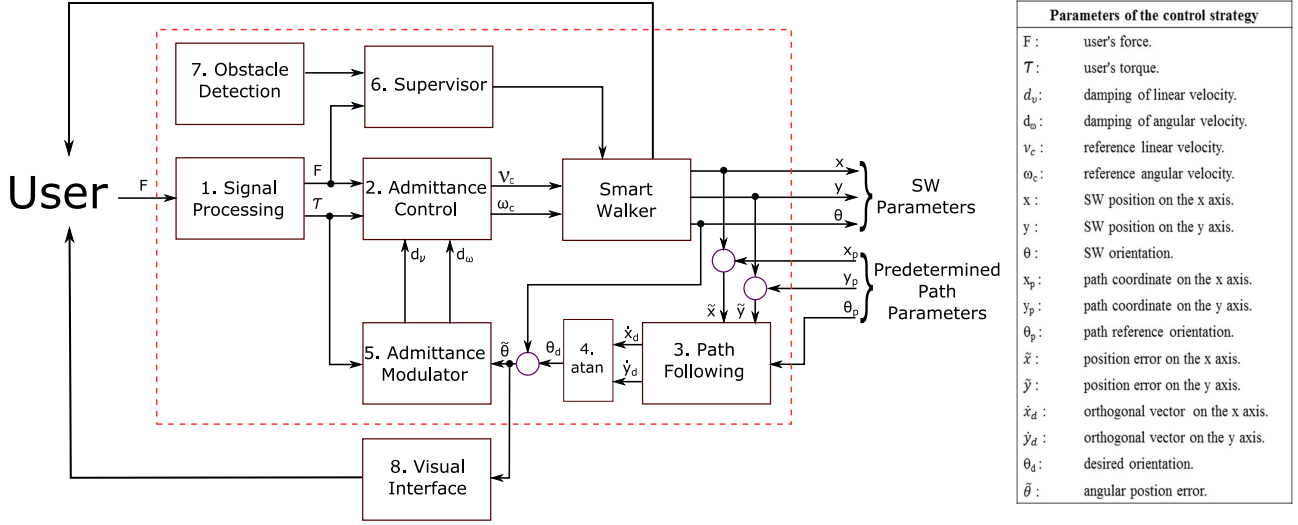


Figure 4.1: Block diagram of the controller with admittance modulation.

As the user has the domain of the walker, the path following controller provides the reference orientation. Such desired orientation is calculated through the control structure for path following developed by Andaluz et al. [75]. The reference point is placed in the middle of rear wheels axis, at the initial user's feet position. In closed loop, the equation is defined in the following way:

$$\begin{bmatrix} \dot{x}_d \\ \dot{y}_d \end{bmatrix} = \nu_p + \nu_a, \quad (4.1)$$

where  $\nu_p$  is the path velocity vector and  $\nu_a$  is the path attraction velocity vector. Hence, the full equation is represented by:

$$\begin{bmatrix} \dot{x}_d \\ \dot{y}_d \end{bmatrix} = \begin{bmatrix} \nu_r \cos \theta_p + l_x \tanh\left(\frac{k_x}{l_x} \tilde{x}\right) \\ \nu_r \sin \theta_p + l_y \tanh\left(\frac{k_y}{l_y} \tilde{y}\right) \end{bmatrix}, \quad (4.2)$$

where  $\nu_r$  is the path desired velocity;  $\theta_p$  is the path reference orientation, defined by the tangent of the nearest point to the path;  $l_x$  and  $l_y$  establish the saturation limits of position error;  $k_x$  and  $k_y$  are constant gains that determine the slope of the  $\tanh$ ;  $\tilde{x}$  and  $\tilde{y}$  are the position errors of the robot with respect to the path; and  $\nu_r$  is a reference velocity (see Fig 4.2).

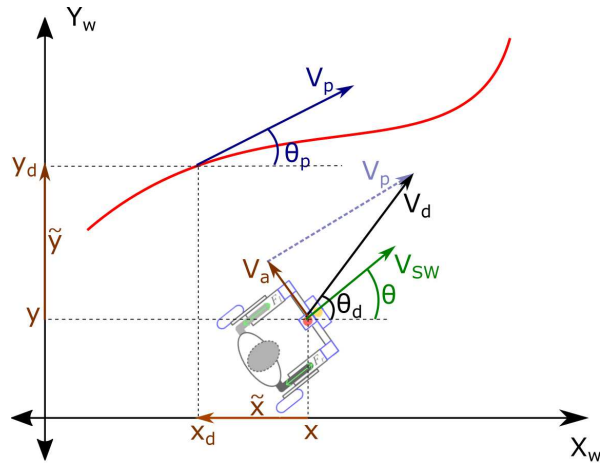


Figure 4.2: Predetermined path for following.

The function in closed loop (Eq. 4.2) is used to calculate the desired orientation  $\theta_d$  (box 4 Fig. 4.1) shown in 4.3 (see Fig. 4.2), which is generated from the orthogonal vectors  $\dot{x}_d$  and  $\dot{y}_d$ , and is the strategy proposed to relate the path following controller with the HREI.

$$\theta_d = \text{atan} \left( \frac{\dot{y}_d}{\dot{x}_d} \right) \quad (4.3)$$

### 4.2.1 Admittance Spatial Modulator

The key difference from the controller used here compared to the classical admittance controller, is that it allows the variation of its dynamic parameters according to sensors input signals. The admittance modulator (box 5 Fig. 4.1) is in charge to generate the signals that produce the haptic sensation of the control strategy proposed here.

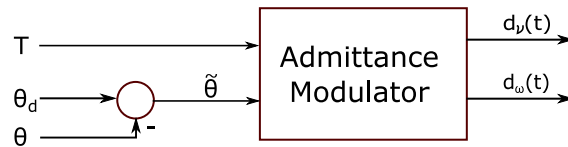


Figure 4.3: Block diagram of the admittance modulator.

The new strategy of the *admittance spatial modulator* is used to change the damping parameter of Equations 3.3 and 3.4 as a function of information collected from the environment. Hence,

the reference velocities are defined as:

$$\nu_c(t) = \frac{F(t) - m_\nu \dot{\nu}(t)}{d_\nu(t)} \quad (4.4)$$

$$\omega_c(t) = \frac{\tau(t) - m_\omega \dot{\omega}(t)}{d_\omega(t)} \quad (4.5)$$

The damping  $d_\nu(t)$  and  $d_\omega(t)$  are the dynamic parameters of the admittance control, which allows the desired HREI, and can increase or decrease the linear velocity  $\nu_c(t)$  and angular velocity  $\omega_c(t)$ .

The admittance modulator is in charge of establishing a dynamic signal that modifies the damping parameter in the admittance controller, thus generating the haptic feedback through the pHRi. This modulator has as input variables the desired orientation  $\theta_d$  and the SW orientation  $\theta$  (see Fig. 4.3). The angular position error ( $\tilde{\theta}$ ), shown in Eq. 4.6, is calculated with respect to the actual orientation  $\theta$  of the SW. Such errors occur when the robot has diverted from its path.

$$\tilde{\theta} = \theta_d - \theta \quad (4.6)$$

Now, it is necessary to establish the function that modifies in real-time, the parameters of the admittance control, and, in this way, guides the user along the predetermined path. The damping parameter implicitly hints the correct direction of the path following, decreasing when the device is on the correct path.

From Eq. 4.4, the parameter  $m_\nu$  remains constant, and  $d_\nu$  has an inverted Gauss behavior (see Fig. 4.4), as this function offers changes with soft transitions, which are reflected in the user experience. The function describing the curve in Figure 4.4 is shown in Eq. 4.7.

$$d_\nu(t) = d_{\nu max} - d_{dmax} e^{\left(-\frac{\tilde{\theta}}{\delta_{d\nu}}\right)^2}, \quad (4.7)$$

where,  $d_{\nu max}$  is the maximum limit of  $d_\nu(t)$ ;  $d_{dmax}$  is the maximum decrease of velocity damping (see Eq. 4.4); and  $\delta_{d\nu}$  is the parameter that determines the width of  $d_\nu(t)$  function (see Eq. 4.4).



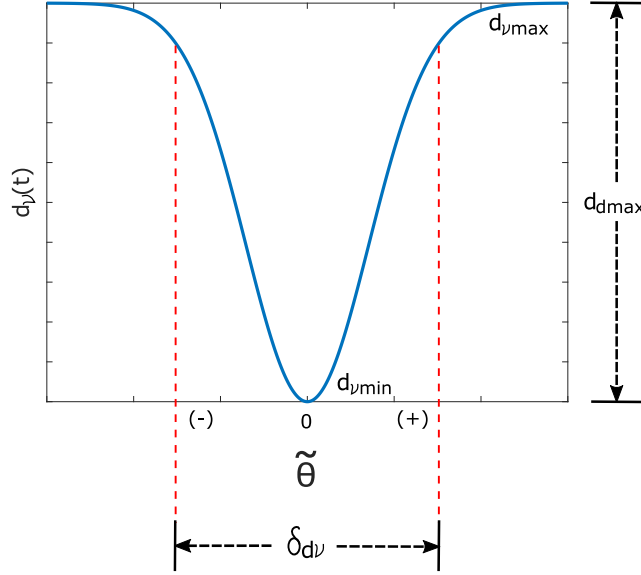


Figure 4.4: Curve of damping force  $d_\nu$ .

This way, when  $\tilde{\theta}$  is zero, the damping is minimum, allowing the SW to move with great facility. The bigger the orientation error, the bigger is the locomotion difficulty with the SW. Also, the linear velocity  $\nu_c(t)$  decreases.

To define  $d_\nu$ , it is necessary to take into account (see Fig. 4.4):

$d_{\nu max}$ : maximum damping wished for linear velocity (see Eq 4.4)

$d_{dmax}$ : maximum variation of  $d_\nu(t)$  function. ( $d_{\nu max} - d_{\nu min}$ ).

$\delta_{d\nu}$ :  $\tilde{\theta}$  for maximum damping.

For  $\omega_c$ , the same restriction as in  $\nu_c$  is taken, i.e.,  $m_\omega$  remains constant. In Eq. 4.5, the definition of  $d_\omega$  is given by:

$$d_\omega(t) = d_{i\omega} + G_{d\omega} \tanh\left(\frac{1}{P_{d\omega}} \tau \tilde{\theta}\right), \quad (4.8)$$

where  $d_{i\omega}$  is the initial damping value in the angular velocity  $\omega_c(t)$ ;  $G_{d\omega}$  is the gain variation of the torque damping (see Ec. 4.5), and  $P_{d\omega}$  is the variation slope of curve of  $d_\omega$ .

It is necessary to take into account the restriction presented in Eq. 4.9 to avoid having negative values in  $d_\omega(t)$

$$d_{i\omega} > G_{d\omega} \quad (4.9)$$

When  $\tilde{\theta}$  is positive and the user's torque  $\tau$  induces a negative  $\omega_c$ , and vice versa, it implies that the walker's user intends to correct the angular position error (see Fig 4.5). In this context, when  $\tilde{\theta}$  becomes smaller,  $d_\omega$  tends to decrease. On the contrary, the user has to apply more effort to turn the SW.

To define  $d_\omega$ , it is necessary to take into account (see Fig. 4.6):

$d_{i\omega}$ : (maximum damping desired ( $d_{\omega max}$ ) + minimum damping desired ( $d_{\omega min}$ ))/2.

$G_{d\omega}$ : (maximum damping desired ( $d_{\omega max}$ ) - minimum damping desired ( $d_{\omega min}$ ))/2.

$P_{d\omega}$ : defined by empirical criterion in function of haptic feedback.

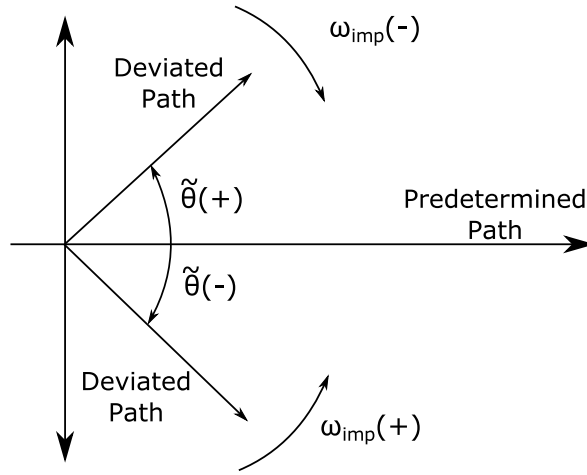


Figure 4.5: Criterion for orientation correction.

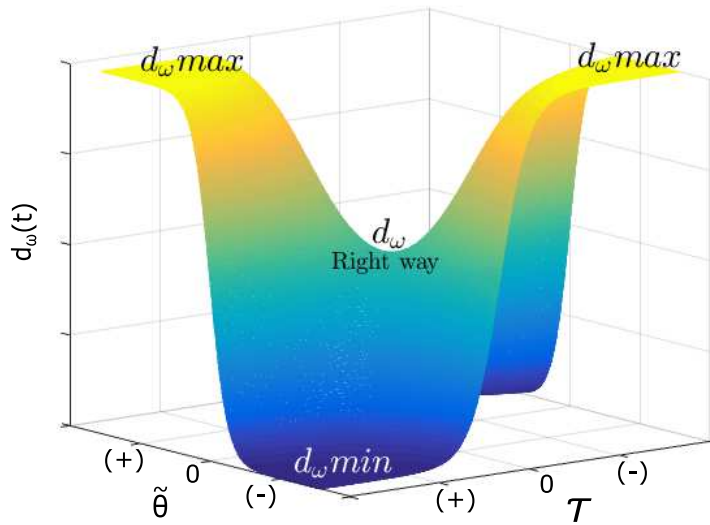


Figure 4.6: Curve of torque damping  $d_\omega$ .

The spatial modulation of  $d_\nu$  and  $d_\omega$  can be adjusted on the limits where the user starts to feel the haptic feedback (i.e. mobility difficulty when the walker does not follow a predetermined path). The user interprets the SW movement within the limits as a virtual mobility canal that allows easier locomotion. Furthermore, the cognitive interface provided by the haptic feedback interacts with the user through a process of decision-making about the path to follow, keeping the brain active.

### 4.2.2 Safety Supervisor

Although the USW offers a stable assistance for walking, it is necessary to establish safety parameters for the user through a sensory assistant and a cognitive interface, in order to have a safe HREI. In this case, a supervisor (box 6 Fig. 4.1) with three safety layers was implemented. The first safety rule regards the user's partial body weight support on the SW platform, which has a threshold of  $0.6 \text{ kgf}$  in the  $z$  axis of each force sensor. If a threshold is not surpassed, no motor/control command is sent to the drivers. In this manner, a suitable posture or body weight support is necessary for the system to operate. Otherwise, the robot remains blocked to allow the user to position himself/herself. Once the controller detects that the threshold was reached in each sensor,  $\nu_c(t)$  and  $\omega_c(t)$  assume the values defined by the control strategy.

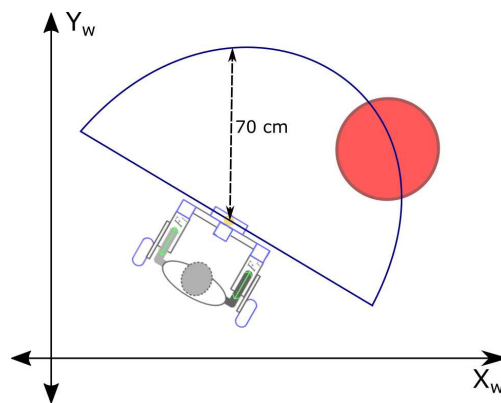


Figure 4.7: Obstacle detecting zone.

In the second safety rule, a protection zone with  $70 \text{ cm}$  of radius around the RP-LIDAR laser sensor is defined (see Fig. 4.7), therefore, if the laser sensor detects an obstacle within the interest zone (box 7 Fig. 4.1),  $\nu_c(t)$  and  $\omega_c(t)$  become zero to avoid a possible collision; if the

contrary happens, they acquire the values of velocity provided by the controller. As obstacle avoidance is not the object of this study, this simple solution was implemented to guarantee user's safety when navigating with the robotic device.

The third safety rule defines a lower limit of 20 *cm* and an upper limit of 50 *cm* of distance between the user and the SW. This way, when the user drives the SW backwards and the LRF sensor measures a distance smaller than the established lower limit,  $\nu_c(t)$  and  $\omega_c(t)$  become zero to avoid collisions between the user's legs and the SW. Furthermore, when the LRF sensor measures a distance higher than the upper limit,  $\nu_c$  and  $\omega_c$  also become zero to avoid user falls. Otherwise, the SW is driven by the velocities obtained from the proposed controller.

### 4.2.3 Visual Cognitive Interface

Two LEDs are used as cHRi with the user (Fig. 4.8). Such visual interface (box 8 Fig. 4.1) indicates to the user the correct orientation when the walker is outside the predetermined path. As the controller establishes a virtual mobility canal for easier locomotion, a limit of  $\pm 25^\circ$  for  $\tilde{\theta}$  was defined, because, under this limit,  $d_v$  takes a value that allows an easier maneuverability with the SW.

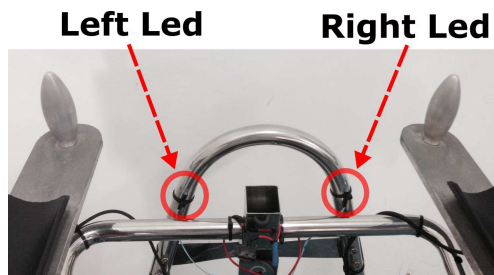


Figure 4.8: Position of LEDs on the *USW*.

Also, the limit in  $\tilde{\theta}$  allows that the visual channel of the multimodal cognitive interface does not saturate the user's vision. Once  $\tilde{\theta}$  surpasses the error limit, this cHRi indicates the turn intention that the user should make, and, this way correcting the error in  $\tilde{\theta}$ . Then, LEDs light on according to the turn recommendation. When the user achieves the correct direction, the two LEDs turn off. The visual interface assists cognitively the user to achieve the correct direction to come back to the predetermined path, complementing the haptic feedback.

## 4.3 Experimental Study

Eight people ( $28.5 \pm 5.42$  years old) without any history of gait dysfunctions and with no previous training with the SW participated of the experiments. During the experiments, the following data was recorded: 1. The control signals ( $\omega_c, \nu_c, d_\nu, d_\omega, \tilde{\theta}$ ); 2. SW position ( $x, y$ ); 3. Linear and angular velocities of the SW; 4. LEDs signals; User-walker interaction parameters ( $F$  and  $\tau$ ); 5. User legs distance to SW (using LRF sensor).

Table 4.1: Virtual mass values and user weight.

User No.	Weight [kg]	$m_\nu$ [kg]	$m_\omega$ [kg]
1.	53.6	1.8	1.3
2.	57.4	1.3	1
3.	58	1.3	1
4.	60.4	1.8	1.4
5.	61.4	2	1.5
6.	65.4	3.8	3.5
7.	71.7	3.3	3
8.	101.6	3.8	3.5

Two different paths unknown by the participants were proposed, which were used to evaluate the controller performance and the cognitive interaction. In order to improve the HREI, the user weight was taken into account. It was found an empirical relation between the discharge force of the user on the SW and the values to be assigned to the constants  $m_\nu$  and  $m_\omega$  in Equations 4.4 and 4.5, respectively. The weight range of participants was  $53.6 \text{ kg}$  to  $101.6 \text{ kg}$  (see Table 4.1). Once the constants of virtual mass were known, it was verified that the user could move the SW comfortably through a short path in straight line. The other constants values used in the controller were determined empirically from the experiments with the control strategy, which are described in Table 4.2.

### 4.3.1 Following Straight Segments

The aim of this experiment was to observe the controller behavior using the multimodal cognitive interface and the haptic feedback. Here, the user voluntarily went outside the predeter-

mined path. The start point of the experiment was at  $x = 0$  and  $y = 0$ . A path made of three segments linked with angles of  $90^\circ$  was used (see Fig. 4.9a). This path has a first segment of  $2.6\text{ m}$  in a straight line, then a left turn of  $90^\circ$ , followed of a straight segment of  $1.5\text{ m}$ , and at last, a right turn of  $90^\circ$  for a final segment of  $10.4\text{ m}$  in a straight line. The points of the path were set every  $0.2\text{ m}$ . On the first part of the experiment, the user was asked to follow LED indications of the SW until reaching the end point, which was  $5.2\text{ m}$  from the start point. On the second part, in the first turn, the user was asked to ignore the controller recommendations and try to maintain it in the straight direction, in such a way that the user could feel the controller action through the haptic feedback. When the SW became difficult to maneuver, the user was asked to follow the visual interface by LEDs and re-direct the walker in the right direction.

Table 4.2: Values of constants used in the control strategy.

<i>Path following</i>	
Constant	Value
$k_x$	0.7
$k_y$	0.7
$l_x$	3
$l_y$	3
$\nu_r$	$0.3\text{ m/s}$
<i>Spatial modulator of <math>d_\nu</math></i>	
Constant	Value
$d_{\nu_{max}}$	30
$d_{d_{max}}$	29.5
$\delta_{d_\nu}$	0.8
$m_\nu$	see Table 4.1
<i>Spatial modulator of <math>d_\omega</math></i>	
Constant	Value
$d_{i_\omega}$	4
$G_{d_\omega}$	3.5
$P_{d_\omega}$	2
$m_\omega$	see Table 4.1

### 4.3.2 Finding the Circle Path

This experiment was conducted to validate the path following controller, and to observe the controller guiding action when the user was outside of the path. In this experiment, as a hypothetical case, the user starts the locomotion outside the predetermined path (see Fig. 4.9b). A circle was used as predetermined path, with radius of 2 m and center at  $x = 3$  and  $y = 0$ . The start point of the experiment was at  $x = 0$  and  $y = 0$ . At this experiment, the user had greater interaction with the haptic feedback compared to the experiment No. 1. In this case, the user had to feel the changes of locomotion difficulty of the SW to find the path. In the first experiment, the user had to find the circle path using the haptic feedback only. In the second experiment, the user had to use the multimodal cognitive interface to find the circle path.

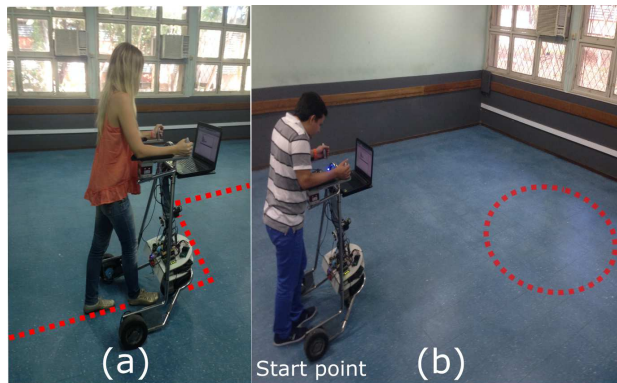


Figure 4.9: Experiments with different paths. (a) Experiment 1. Following straight segments. (b) Experiment 2. Finding the circle path.

### 4.3.3 Supervisor Functionality

This experiment was conducted to verify the supervisor functionality. A straight line path of 15 m was used, and it was checked if the linear and angular velocities became zero when the SW was very close to obstacles, or when the threshold in the  $z$  axis for the two sensors was not exceeded. The obstacles were located at coordinates  $(6, 0)$  and  $(9, 0)$ . The bad user's posture was simulated at the beginning and the end of the predetermined path in this experiment.

## 4.4 Results and Discussions

### 4.4.1 Following Straight Segments

In the first experiment, users were asked to follow a predetermined path while complying with recommendations from the multimodal cognitive interaction. Figure 4.10a shows the results from one participant for the first part of the experiment. It can be seen that the LEDs indications were useful to provide hints about the predetermined path, allowing the user to stay on the path most of the time.

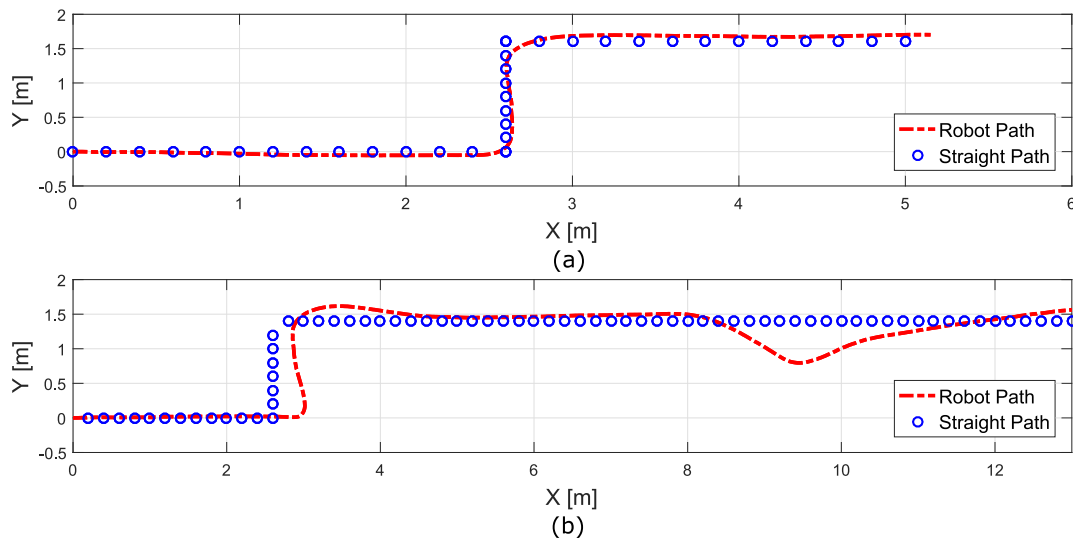


Figure 4.10: Following the straight path. (a) Path following considering cognitive interface information. (b) Path following with induced error.

A representative result of the second part of the experiment related to the path of straight segments is shown in Fig. 4.10b. In this case, the data collected from user 7 (see Table 4.1) was used. In such case, the user was asked to go ahead at the straight path and to ignore the turn recommendation given by the visual cognitive interface. By doing so, when deviating from the predetermined path, the user felt the haptic feedback provided by the controller. As a consequence, physical interaction forces between the user and the walker increased while the user attempted to keep going forward (see Fig. 4.11). Once the user started to feel the controller action, the user was asked to follow the visual recommendation of the LEDs and to do a turn movement to the correct orientation. After following the controller recommendations



through the multimodal cognitive interface for a while, the user was once again asked to deviate from the predetermined path intentionally to force a reaction of the control strategy (see Fig 4.10b at 8 m of distance in  $x$  axis, approximately). Once the user could not keep going forward with the SW, the user was asked to follow the LEDs recommendations, rotating in the correct orientation and returning in the direction to the predetermined path.

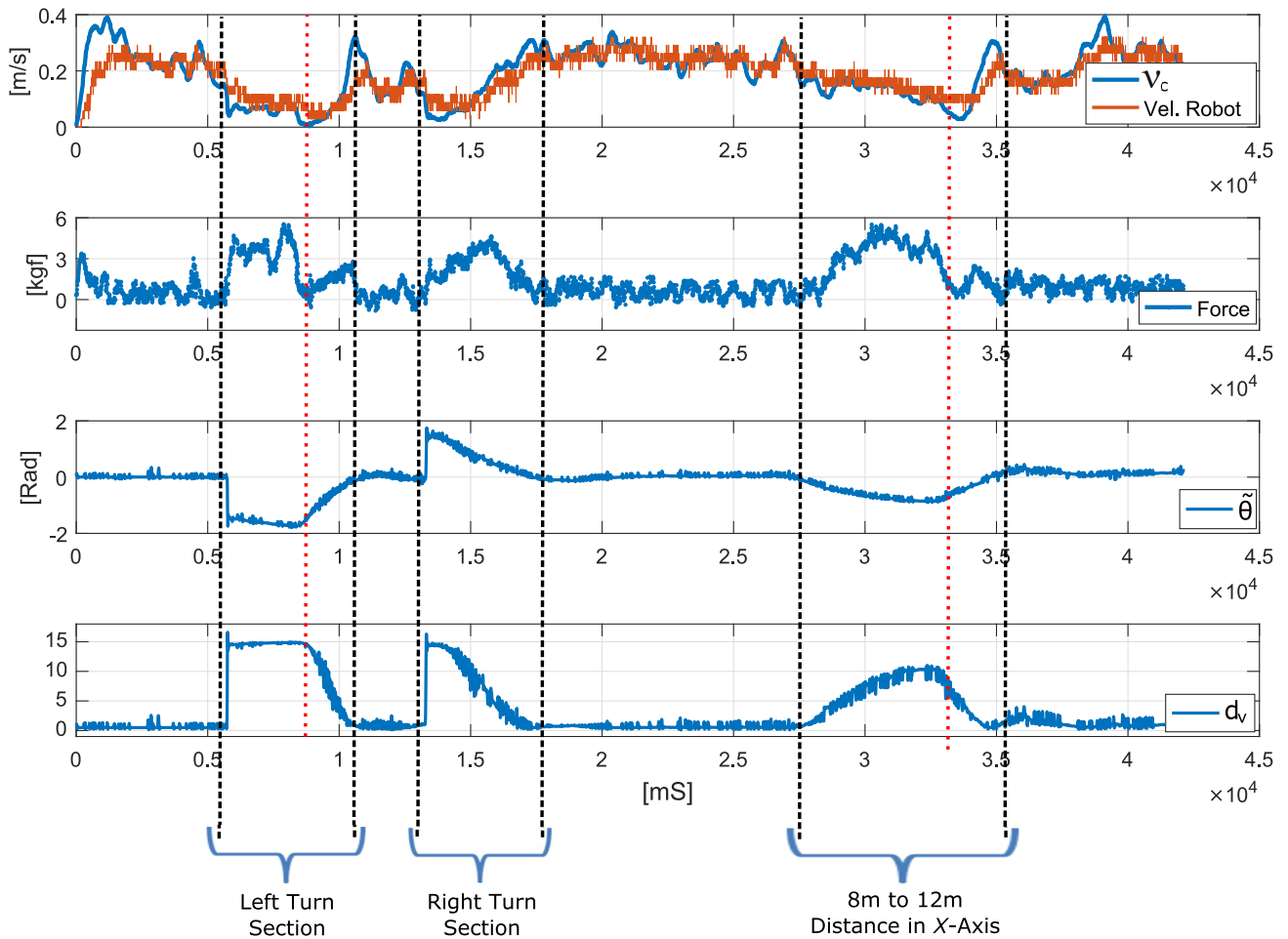


Figure 4.11: Spatial modulation curve of  $d_v$  and haptic force response of the straight path of Fig. 4.10b. Up to down: Control and SW linear velocities, user's force signal,  $\tilde{\theta}$  signal and  $d_v$  signal.

A smaller guiding force is produced when the SW is on the predetermined path (see Fig. 4.11). In that situation, the parameter  $d_v$  assumes its minimum value, but, once  $d_v$  increases, it is observed that the user has to make more force to keep the locomotion (see black line spacing sections Fig. 4.11). While the walker is on the predetermined path, the force applied in the  $y$  axis of the sensors is between 0.2 kgf and 1 kgf, and the linear velocity of the device is higher (0.3 m/s approximately). When the spatial modulation acts, the linear velocity of the

SW decreases to  $0.05 \text{ m/s}$ , and the user needs to apply higher forces in order to move the SW. In this case, the SW is out of the predetermined path and the applied force is around or higher than  $5 \text{ kg}$  (see Fig. 4.11 -Force). At the strong curves of the predetermined path, i.e., on  $90^\circ$  curves, the spatial modulator of  $d_v$  becomes saturated (see Fig. 4.11, left and right turn sections). The user interprets this as an uncomfortable effort that does not allow keeping going ahead. When the exit from the predetermined path is gradual, the user feels as the effort to move the SW goes increasing progressively. Thus, the user has to increase the force applied on the SW in order to move ahead (see Fig. 4.11, between  $8 \text{ m}$  and  $12 \text{ m}$  of distance in  $x$  axis section). In this case, the haptic feedback of the controller has a natural and intuitive interaction, generating a comfortable user' experience, as he/she does not make an effort to maneuvering the SW.

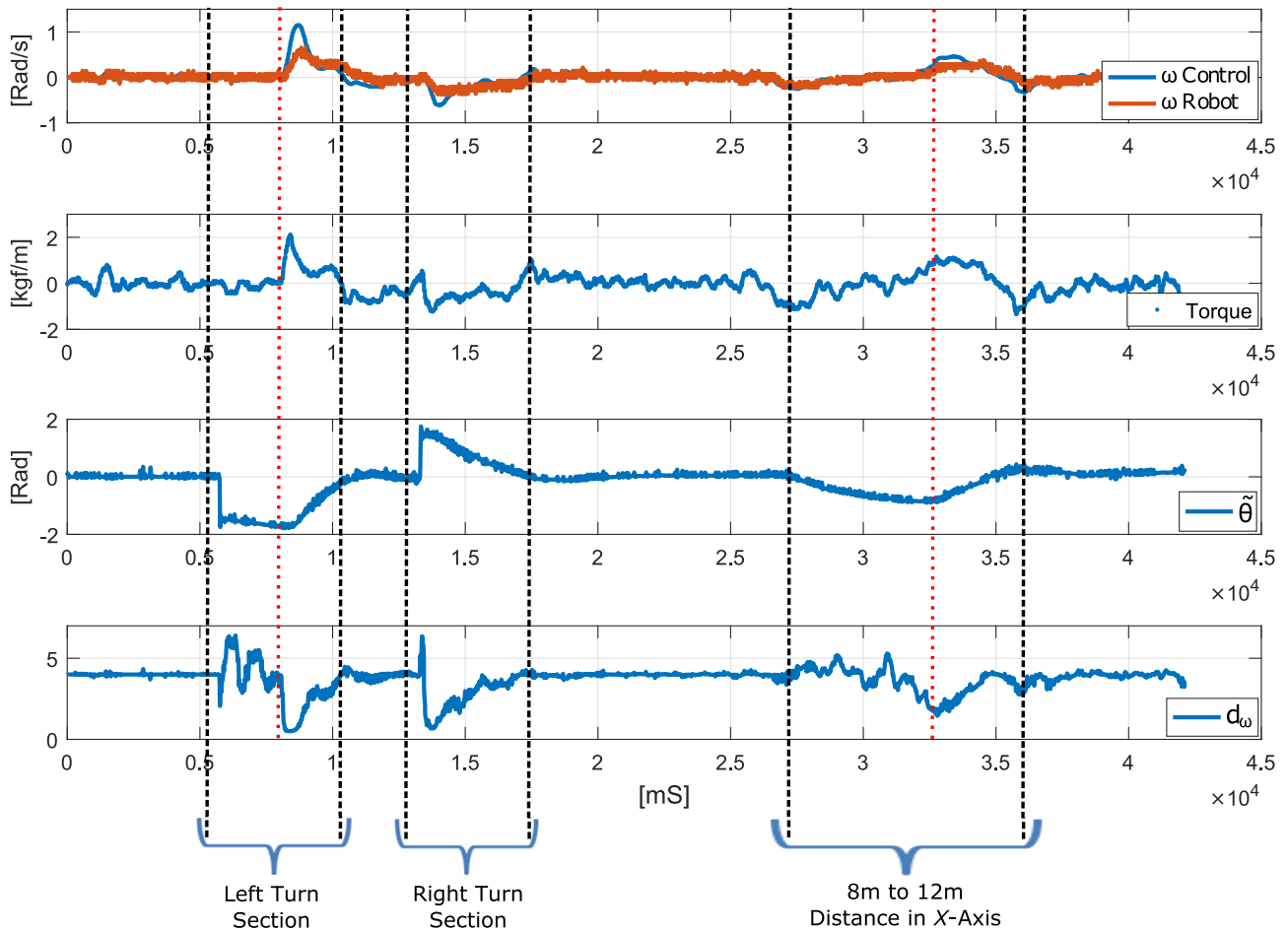


Figure 4.12: Spatial modulation curve of  $d_\omega$  and haptic torque response of the predetermined path in Fig. 4.10b. Up to down: SW angular velocities, user's torque signal,  $\tilde{\theta}$  and  $d_\omega$ .

Figure 4.12 shows the control signals related to the torque. In this case, when an error in  $\tilde{\theta}$  is

present, it can be observed that the signal of  $d\omega$  begins to increase. The user feels the haptic feedback when performing a change towards the wrong orientation on its own axis (see Fig 4.12 -Torque). In this context, when the user rotates around its own axis with the intention of correcting the angular position error  $\tilde{\theta}$ , the torque needs to decrease (see red dotted line on Fig. 4.11 and Fig. 4.12, at the left turn section). Therefore, the linear velocity of the SW begins to increase. Once it is found in the correct direction, it is not necessary to apply torque anymore, hence, the angular velocity decreases to  $0 \text{ rad/s}$  approximately. The section between  $8 \text{ m}$  to  $12 \text{ m}$  of distance in the  $x$  axis of Fig. 4.11 and Fig. 4.12 shows that the SW goes out of the predetermined path intentionally. It can be observed that when the user begins to rotate towards the predetermined path, the torque applied by the user to manipulate the SW begins to decrease. When the correct orientation is reached, the linear velocity increases and the angular velocity decreases to become  $0 \text{ rad/s}$  (see Fig. 4.12 -Torque).

Additionally, Fig. 4.12 shows that when the user applies a torque in a wrong direction (see Fig 4.12), the value of the  $d_\omega$  increases and the angular velocity of the SW decreases. This leads the user to apply more torque to keep rotating. Nevertheless, when the user wants to correct the angular position error  $\tilde{\theta}$  or follow the visual cognitive interface, the value of  $d\omega$  becomes minimum. In such case, the torque and  $\tilde{\theta}$  have contrary signs. This is reflected to the user as a soft turn movement, easing the SW maneuverability.

Through the signals of Fig. 4.11 and 4.12, it can be observed the feedback form that the admittance spatial modulation controller has on the user. This haptic feedback becomes a signal for the HREI and, consequently, a natural and intuitive way to guide the user on a predetermined path.

At the experiment 1, the absolute error of linear and angular velocities of the controller was analyzed. A metric termed the Kinematic Estimation Error (KTE) is shown in Eq. 4.10 [76], which compares the path traveled to the predetermined path:

$$KTE = \sqrt{|\bar{\varepsilon}|^2 + \sigma^2}, \quad (4.10)$$

where  $|\bar{\epsilon}|^2$  is the mean square of the errors between the predetermined path and the path followed by the SW, and  $\sigma^2$  is the variance of this data. Thus, KTE also increases with the increase of variance.

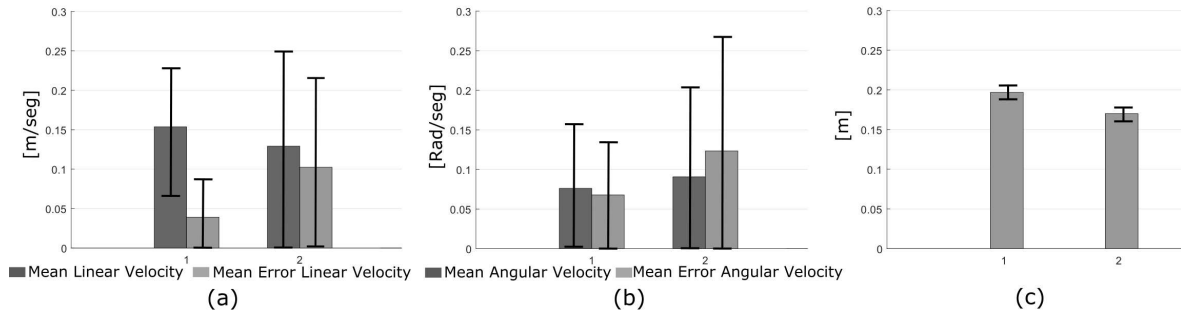


Figure 4.13: Errors in the following straight path. Group 1: Second part of the Experiment 1 (user 7 of Table 4.1). Group 2: Average data of path following by user in the first part of the Experiment 1. (a) Linear velocity. (b) Angular velocity. (c) Kinematic Estimation Error (KTE).

In Fig. 4.13, the bars of Group 1 refer to the data collected from the user 7 (see Table 4.1) in the second part of the Experiment 1. The travel along the predetermined path shown in Fig. 4.10b is also performed by user 7. The data that correspond to the Group 2 are referred to the 8 users of the experiment. In addition, it can be observed that the linear velocity error oscillates between  $0.12 \text{ m/s}$  and  $0.15 \text{ m/s}$  (see Fig. 4.13a), and the angular velocity error oscillates between  $0.075 \text{ rad/s}$  and  $0.08 \text{ rad/s}$  (see Fig. 4.13b). This is because no participant had any training with the SW, and, hence, some of them were cautious at the moment of manipulating the walker. For some users, it was not easy to keep the motion close to the predetermined path, because they did not know the path and could not see it. Therefore, they had to apply torques mainly guided by the LEDs. This is evidenced in the absolute error average calculated for the angular velocity (see Fig 4.13). Regarding the path following, it is shown that the user 7 had a higher KTE error, as this user was intentionally asked to induce errors during the travel along the predetermined path on the second part of the experiment. Nevertheless, the KTE with variance  $\pm 0.019$  to Group 1 and  $\pm 0.017$  to Group 2 never went over  $0.2 \text{ m}$  in both cases (see Fig. 4.13c), which seems to be adequate to comply the purpose of guiding the user.

## 4.4.2 Finding the Circle Path

In relation to Experiment 2, once the users learned how to handle the SW, this experiment was aimed at finding the predetermined path, whose start point was away from them. Here, the users were guided by the multimodal cognitive interaction, and by pHRi through the haptic feedback which is given by the physical contact between the user and the SW. Two representative results can be observed in Figure 4.14. Figure 4.14a shows how the user was guided by the haptic feedback until finding the circle, and Figure 4.14b shows how the user was able to find the path aided by the multimodal cognitive interaction. When the haptic feedback is used, the path followed by the user presents oscillations, due to the virtual limits of the canal for easier locomotion defined by  $d_\nu$  and  $d_\omega$  through the spatial modulation. Once this limits are overpassed, the controller begins to change  $d_\nu$  and  $d_\omega$ , and the user begins to feel the difficulty for locomotion, establishing the zone where he/she can move.

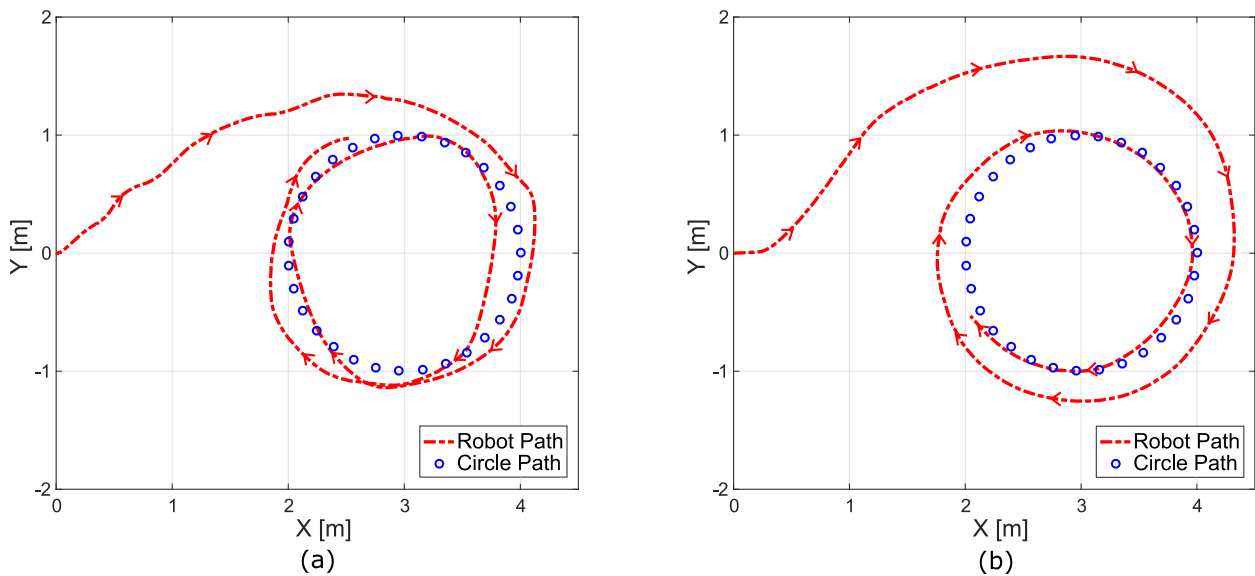


Figure 4.14: Finding the circle path. (a) Finding the path with the haptic feedback. (b) Finding the path with the multimodal cognitive interaction.

If the visual interface is used, the SW's handling becomes softer and, consequently, it is easier to maintain on the predetermined path, once this is found (see Fig. 4.14a). When the movement is based on the LEDs recommendation and the haptic feedback, the virtual limits of the channel, for easier locomotion, are determined a little bit after the LEDs begin to turn on in an intermittent way. This way, the user knows that he/she has to do a soft turn in the direction

provided by the LEDs, either right or left. On the contrary, if the LED is on always, but, not in an intermittent way, the mobility with the SW is the hardest, as a consequence of the admittance spatial modulation strategy. Also, it is observed that the user takes more time to find the circle path when using the multimodal cognitive interaction, as he/she needs to process more information. The LEDs signals and haptic feedback together imply a more complex cognitive process. Such process introduces natural delays due to the information processing by the user [58]. However, the path travel time may be reduced by training with the SW. The effect of such training process is an ongoing study.

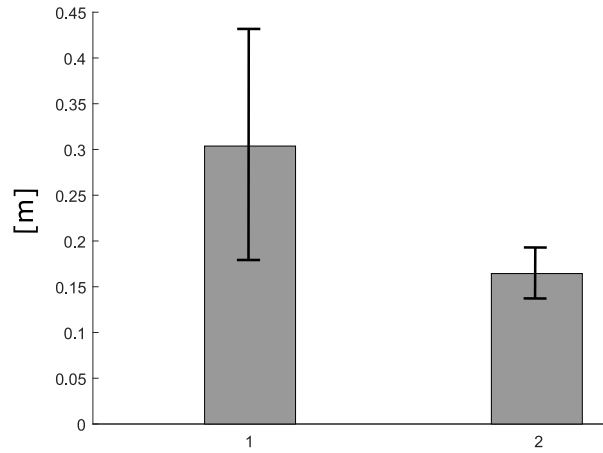


Figure 4.15: Kinematic estimation error ( $KTE$ ). Group 1: with haptic feedback. Group 2: with multimodal cognitive interaction.

Figure 4.15 shows the statistic error calculated once the SW is on the predetermined path. When the haptic feedback is used, the maximum position error is  $0.3\text{ m}$ , once the user is on the path (as shown in Fig. 4.14b). The position error value is due to the hard torque movement that has to do the user to correct the SW direction. This error can decrease once the user has more training with the handling of the SW, or by doing an adjustment of the virtual masses assigned for  $m_v$  and  $m_\omega$  (see Table 4.1), because, depending on these values, the SW maneuverability becomes easier or harder. The KTE calculated when the user is guided through the multimodal cognitive interaction is  $0.1617 \pm 0.0295\text{ m}$  (see Fig. 4.15). This value is lower compared with the following error when the person is guided by the haptic feedback ( $0.3 \pm 0.1337\text{ m}$ ).

The user does not keep all the time on the predetermined path when using only the haptic feedback, which is a consequence of the movement within the limits established by the virtual

mobility canal for easier locomotion. Furthermore, with this experiment, it was verified that the two channels of the multimodal cognitive interaction are complementary when guiding the user along the predetermined path. The control strategy proposed in this work makes the user feel comfortable when him/her is maneuvering the SW. The user has enough freedom in controlling the SW movement, within limits established by the spatial admittance modulator.

### 4.4.3 Qualitative Evaluation

To evaluate the acceptance of the proposed control strategy, qualitative questionnaires were applied after the participants had finished the two experiments. Figure 4.16 shows the results of two main questions, which report the perception of the participants about the control strategy. In general, the participants accepted the proposed control strategy and the multimodal cognitive interaction. Although the average ratings were relatively high, Figure 4.16a shows a trouble related to the way of guiding the user. We believe that the  $\delta_{d\nu}$  value influenced the results, as this parameter modify the width of  $d_\nu(t)$  function. Hence, the virtual limits of the canal for easier locomotion may be lower. Once determined the mass values, the participants agreed that the handling of the SW was intuitive (see Fig. 4.16b). Also, comments on “safe-driving the SW”, “ease of control”, “natural interaction”, “good velocity of locomotion” and “ease of learning” were registered after the experiments.

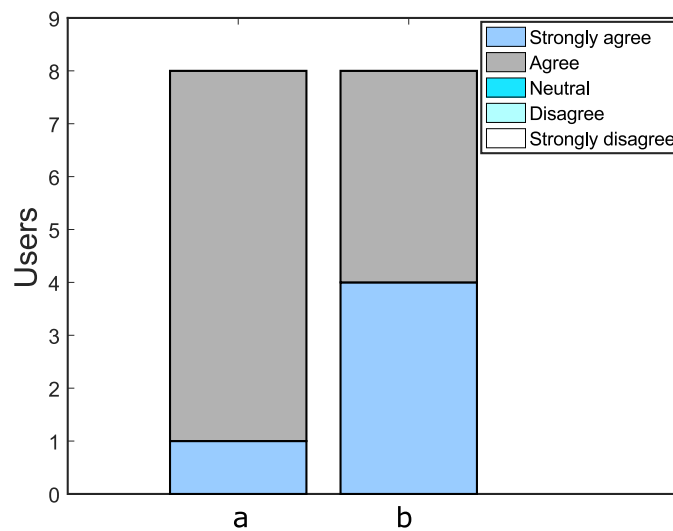


Figure 4.16: Qualitative evaluation for the guided experiments. Questions: a) “I felt that the SW was guiding me”; b) “I felt an intuitive interaction with the SW”.

#### 4.4.4 Checking the Supervisor Functionality

Regarding the supervisor functionality, its performance was verified in two different experiments. In the first one, the predetermined path of Experiment 1 (see Fig 4.10b) was used to validate the visual interface. In the second experiment a straight line is used as predetermined path to verify the two safety factors established for the controller supervisor. The initial position was at  $x = 0$  and  $y = 0$ . During this straight path, a bad position of the user in the SW was simulated through the force sensors. Furthermore, the supervisor answer was checked when the sensor RP-LIDAR detected an obstacle within the protection zone (see Fig. 4.7).

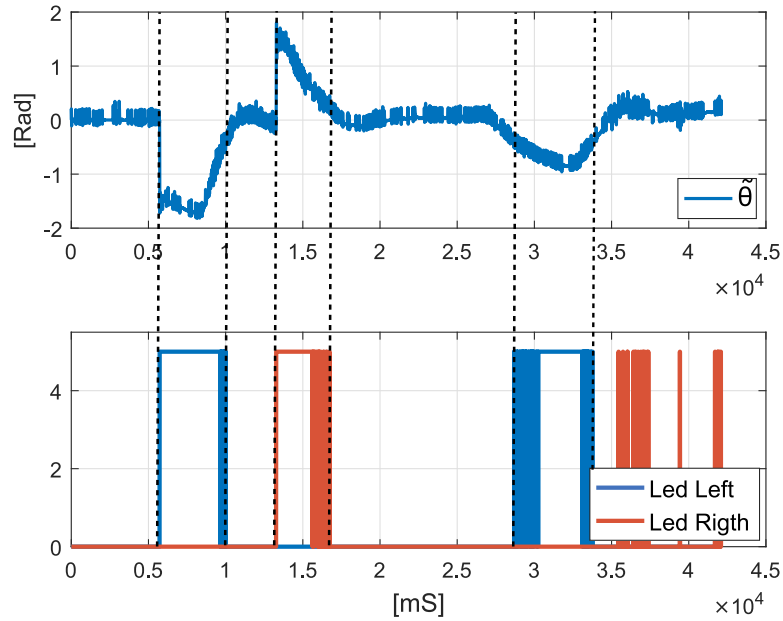


Figure 4.17: Recommendation of turn by cognitive interface signals.

Figure 4.17 shows the LEDs activation every time that an error in  $\tilde{\theta}$  higher than  $\pm 0.43 \text{ rad}$  or  $\pm 25^\circ$  occurred. According to the predetermined path of Figure 4.10b, the LEDs recommended a turn in the direction to correct the angular position error  $\tilde{\theta}$  (see dashed line section zones of Fig 4.17). This way, it is easier to the user interpret the turn direction that he/she should undertake in order to correct the orientation error and, consequently, to get into the zone where the SW is easier to maneuver.

The performance of the safety supervisor parameters is shown in Figure 4.18. The different situations where the linear and angular velocities of the SW became zero are represented in the



framed zones through red segmented lines. In zone (1), it can be observed that the controller detects the force signal as an indicator of starting the mobility, however, the supervisor does not detect force on the  $z$  axis in each sensor, therefore, the velocities of the SW become zero. In zone (2), a bad user's position on the SW is simulated, showing that the velocities continue being zero, as long as the supervisor does not detect the signal of  $z$  axis in both sensors. In zone (3), the RP-LIDAR sensor detects an object that enters into the protected region defined in front of the SW, generating a flag for the supervisor. Then, the linear and angular velocities of the SW become zero and the collision is avoided. Once there is no obstacle anymore, the SW can take the velocity values provided by the control strategy. In zone (4), the LRF sensor detects that the distances established for this safety rule were exceeded, generating a flag for the supervisor. Then, the linear and angular velocities of the SW become zero. This way, the risk of falls or collisions between the user and the SW are avoided. Moreover, it is evidenced that when the supervisor detects a force in the  $z$  axis of both sensors that surpasses the threshold established, and the controller has a force signal as a command of mobility, the SW achieves the velocities calculated by the proposed control strategy.

It is worth mention that the controller proposed here not only can assist people with gait disabilities, but also assist blind people [9]. This is another interesting topic of research around the SWs with this spatial modulation controller.

As a conclusion, this chapter presented a new implementation and validation of a control strategy that contributes for a natural interaction between Human–Robot–Environment using a new criterion for admittance control, as it takes advantage of the generation of a haptic feedback while the user navigates with the SW. In addition to the visual interface, the multimodal cognitive interaction presented here makes more intuitive for the user the way to know which is the correct path by where he/she should make locomotion. On the other hand, the spatial modulation concept allows to establish virtual limits for an easier locomotion zone with the SW. This contributes in a positive way for the cognitive system of the user, as it promotes the interaction between the user and the environment through the user's decisions.

One of the advantages of this controller is the use of only one sensor to define the natural

interaction *Human-Robot-Environment*, which is reflected in the computational efficiency and in the processing of the control algorithm in real time. In this case, the experimental study allowed obtaining quite good results in terms of performance, at the moment of following or finding a predetermined path for the locomotion with the walker. This was verified through real experiments where the user, by means of the control strategy, could maintain himself/herself within the path using the controller recommendations through multimodal cognitive interaction with results of the pHRi and the cHRi used for the strategy proposed in this chapter.

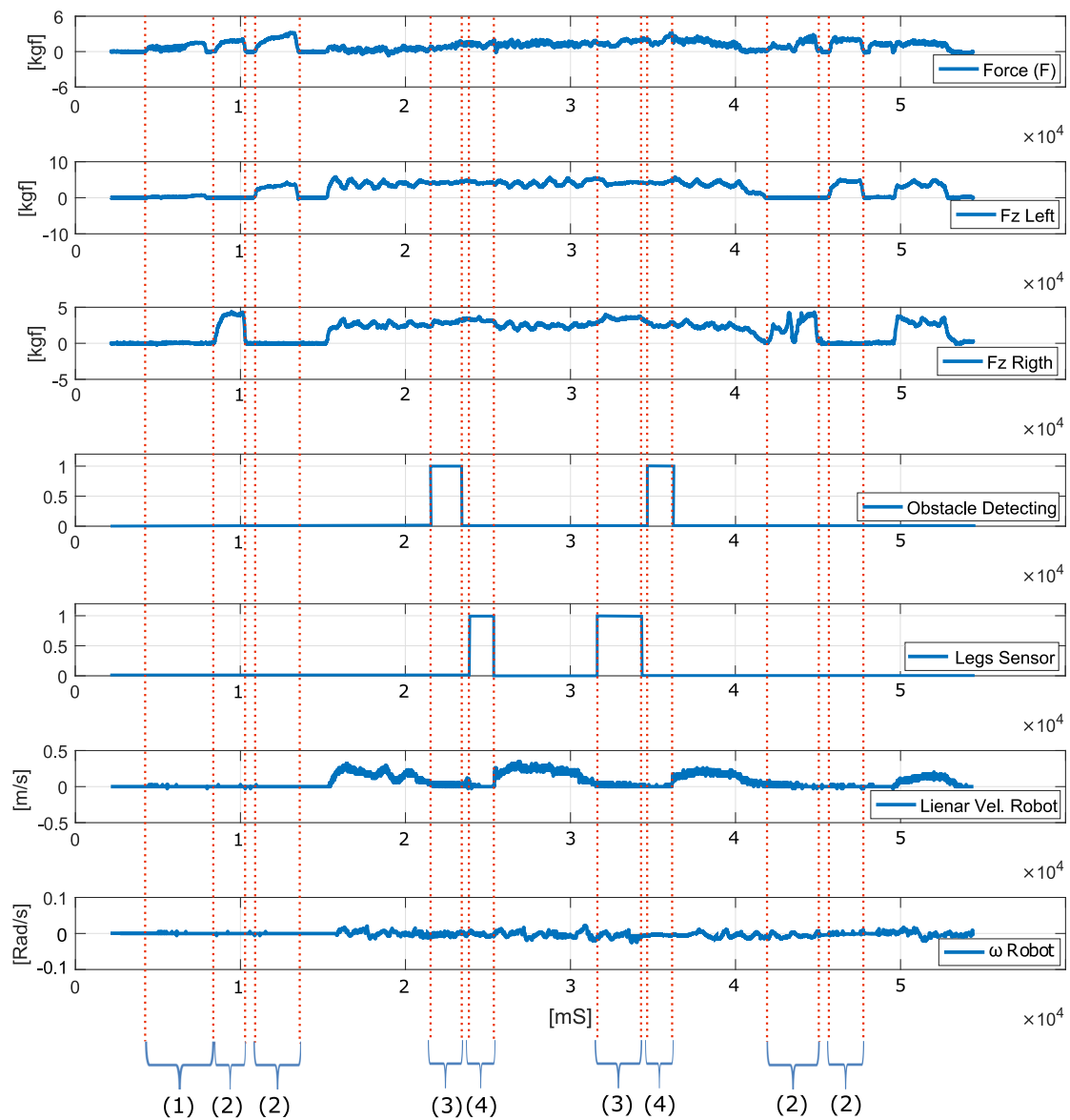


Figure 4.18: Safety parameters of supervisor.

The use of a haptic feedback as a result from the physical interaction between user and SW has contributed to the research area related to assistance tools for people's mobility. Through

a sensation that is not visual or auditive, the user of the SW can obtain information that is related to his/her environment, thanks to the physical interaction of the arms with the SW.

In the next chapters, new control strategy will be described, which will promote the haptic feedback for the user of the SW. Additionally, algorithms for obstacle avoidance with concepts of social interaction to complete the navigation system of the USW will be introduced.

## Chapter 5

# Admittance Modulation Technique Based on Proxemics for Navigation in Confined Spaces

The task of finding an adequate path to navigate across real environments is effortless to individuals with no disabilities, but can become complex to people with cognitive or mobility impairments [19], as the perception of the environment and the ability to navigate may be compromised [23].

In this chapter, a new strategy to navigate with the USW in confined spaces, such as corridors, is proposed. Using the admittance controller with spatial modulation proposed in the Chapter 4, the commands to navigate are given by the user. Such control strategy induces a sensation of hard navigation whenever the SW detects the presence of obstacles, people coming towards the SW, and walls, which are detected using a classifier based on unsupervised learning. The direction that the SW takes for an easy navigation is recommended by a multimodal cognitive interaction composed of a set of two LEDs and a haptic feedback that result from the physical contact between the user's forearms and the SW. Taking advantage of such contact, an appropriate HRI based on a haptic feedback and a non-verbal communication is generated, which is recommended for assistive robotics [69].

The proposed strategy aims at providing a natural and intuitive interaction with the SW while stimulating the cognitive capabilities through decision making when direction correction is necessary. Proxemics zones [62] are brought within the SW for a safe navigation within corridors, giving to the user the possibility of interacting with other people within the corridor. The strategy proposed in here never takes away the user control of the robot and gives the user the main role in the HREI.

This chapter is organized as follows. First, it describes the concepts of social interaction. Second, it describes the navigation strategy used to confined spaces. Then, the experimental setup is described, showing the way the user is assisted during navigation along the corridor. Finally, it shows the experimental results, as well as the discussion about them, and the respective conclusions.

## 5.1 Social Interaction in Walker-Assisted Gait

While navigating in indoor environments, the SW's user may come across other people, which may be considered either as obstacles to be avoided or people with whom to interact with (e.g., engage in a conversation) [82]. In this context, it is important to guarantee the natural incorporation of the SW into social spaces by implementing navigation algorithms that allow the user to interact with other humans in a safe manner. Thus, the use of proxemics [83] can guide such social spaces and, therefore, ease the communication and understanding of human behavior by the SW.

Proxemics is the study of the distances (or spatial zones) that human unconsciously maintains in various social and interpersonal situations [62, 83]. These distance depend on the human behavior, environment configuration, and cultural factors. In this context, the way in which people use the environment to socially interact with others defines those spatial zones. The proxemics theory, as established by Hall [62], involves four spatial zones that regulate social interactions: intimate distance, personal distance, social distance and public distance [84]. These kind of social zones have been applied to generate social rules in robotics and HRI

literature. The main proxemics factors considered in robotics are speed [83], appearance [83], direction of approach [83], and obstacle avoidance [23, 85].

In the robotics literature, proxemics is mainly applied to mobile robotics, being used to establish social navigation strategies. In [83], four kind of spaces for a socially-aware robot navigation were included: the ones related to a single person, to groups of people interacting, to human-object interaction, and to human-robot interaction. Such spaces are used to establish a collision avoidance method with social cues. In [86], the robot takes measures in front of itself to determine zones with the lowest human-presence. Those zones are modeled as elliptical potential fields, and the best elliptical zone (i.e., the one with the lowest human presence) is defined as the cognitive zone in which the robot can travel and avoid pedestrian collision. Another example of proxemics applied to mobile robotics is addressed in [87], in which the robot estimates the proxemics goal state according to a computational framework, based on probabilistic models of social signals, such as speech and gesture produced by a human. All those strategies aim at improving HREI through the inclusion of social interaction rules in navigation techniques.

Traditionally, HREI has been implemented in SWs in the same way as in mobile robots, by using semicircle zones defined by a minimum distance [10, 16, 88] to interact with obstacles and/or to calculate the travel safe path. These strategies have a good performance for detecting and avoiding obstacles. However, when the SW navigates within confined spaces such as corridors, the semicircles can be too restrictive. Such strategy often leads to perceiving the walls as obstacles to avoid, inducing the SW to navigate on the middle of the corridor, which may be a problem in human-shared spaces. Additionally, SWs usually present nonholonomic constraints, which impact on obstacle avoidance. In addition, the possible presence of a companion person walking together the SW, may be perceived as an obstacle to avoid.

Due to these particularities, traditional navigational algorithms may not be suitable to such devices. An SW interacts in a physical level with its user, which shares the same space of the robot, therefore, human-like navigation strategies must be developed for such devices. For this reason, the search for different ways to model social zones to guide HREI can be seen as an interesting approach, especially when navigating in confined human-shared spaces (see Fig.

5.1).



Figure 5.1: Social interaction with a navigation companion within a confined space.

Few works involving SW research have included social interaction strategies to improve the HREI. The main work in this field is the c-Walker [23, 57], which makes use of Social Force Model (SFM) to represent people as 2D circles with attractive and repulsive forces. In such strategy, it is possible to model the force that attracts the SW's user and other people towards the same interest point, as well as the repulsive force that naturally prevents the user from colliding with walls or other individuals. Regarding other assistive robots, a wheelchair that navigates while sharing space with outsiders pedestrians is presented in [85]. In such work, the user indirectly interacts with other people, as they share the same space passing by each other, and the wheelchair computes a safe travel path to avoid disturbing other people.

When navigating in corridors, people normally walk in a straight line [89] and the social zone projected to interact with other pedestrians can be modeled as an elliptical zone [86]. The social model that introduces the ellipse shape to describe such social zone is the SFM [70, 83]. SFM defines a decreasing exponential function to generate repulsive forces to and from other pedestrians with equipotential lines having the form of an ellipse that is directed into the direction of motion. Thus, the SFM and the interpersonal distances proposed by proxemics are two models that can be directly applied into SWs to generate new guidelines to detect obstacles and to interact with other people within a corridor.

Figure 5.2 shows our proposal of social interactions zones to guide the implementation of navigation algorithms in SWs. The two ellipses projected on the front of the SW are determined to

allow a social interaction and improve the HREI when the SW is navigating within a corridor.

These two zones are described below:

- *Interpersonal-social zone* (IPSz) is established taking as bases the distances of the personal and social spatial zones described by proxemics [84]. The personal zone (considered the range from 0.46 m to 1.2 m) [84] is used to define the ellipse small axis, and the distance of the social zone (from 1.2 m to 3.7 m) [84] defines the ellipse big axis. In this case, the personal zone allows the contact between people, from relatively intimate to more formal [84], avoiding the stress produced when the personal space is invaded by others [90]. The social zone allows avoiding obstacles within the corridor to a comfortable distance for the SW's user, while also allowing for more lateral space between the obstacle and wall to navigate within the corridor.

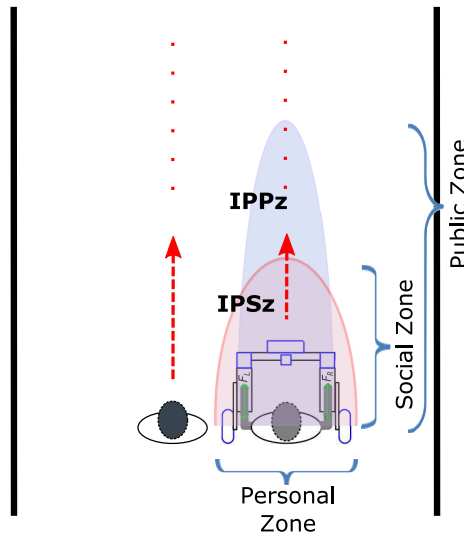


Figure 5.2: Social interaction strategy on a corridor for an SW. Social zones: Interpersonal-social zone (IPSz), Interpersonal-public zone (IPPz). Red points describing the virtual canal of navigation to each person

- *Interpersonal-public zone* (IPPz) is defined from personal and public spatial zones described by proxemics [84]. The personal zone is used in the same way that in IPSz, but in this case, the small axis is smaller compared with the axis of the first ellipse. This criterion was established to avoid conflicts between the two elliptical shapes, and to leave the IPSz as the main zone of contact with other people. The distance of the public zone (from 3.7 m to 7.6 m) [84] is used to define the ellipses big axis. The public zone is used



to avoid collisions with people that walk in opposite direction to the SW, and are in the same virtual zone of navigation.

## 5.2 Human-Robot-Environment Interaction (HREI) Within Confined Spaces

As depicted in Fig. 5.3, the strategy to navigate in confined spaces relies on an admittance controller with spatial modulation, as proposed in Chapter 4, to obtain the user's motion intention and to command the navigation. The admittance controller emulates a dynamic system, providing the user with a feeling of direct interaction with the system specified by the admittance model [16]. The desired orientation of the SW is calculated using zones for the social interaction, based on an obstacle avoidance strategy proposed in [91], and a classifier that identifies the elements within the corridor, such as people and walls. The admittance modulator takes the orientation error and the user's torque intention to dynamically tune the admittance controller damping parameters [10]. On top of those systems, a supervisor is implemented to establish safe parameters for the user. Each one of the blocks depicted in Fig. 5.3 is described below.

The control strategy allows the user to establish a comfortable speed for locomotion, as motion intention is determined through the two force sensors localized under the forearms supporting platforms (see Fig. 3.1). This way, it leverages the physical interaction between the SW and the user to generate the navigation commands. The signal on the  $F_y$  axis captured by each sensor is processed to infer the user's motion intention, and the signal on the  $F_z$  axis is used as one of the safety parameters to assure adequate partial body weight support. The force ( $F(t)$ ) and torque ( $\tau(t)$ ) signals (output of box 1, in Fig. 5.3) are calculate according to Eq. 3.1 and 3.2.

To detect the user's motion intention, the method described in Chapter 3, which was inspired in [12], was used here once the data were recorded, applying the FLC and WFLC algorithm to

estimate and cancel cadence component of each input signal  $F_{L_Y}(t)$  and  $F_{R_Y}(t)$ . Thus, signals of force  $F(t)$  and torque  $\tau(t)$  more stable are obtained.

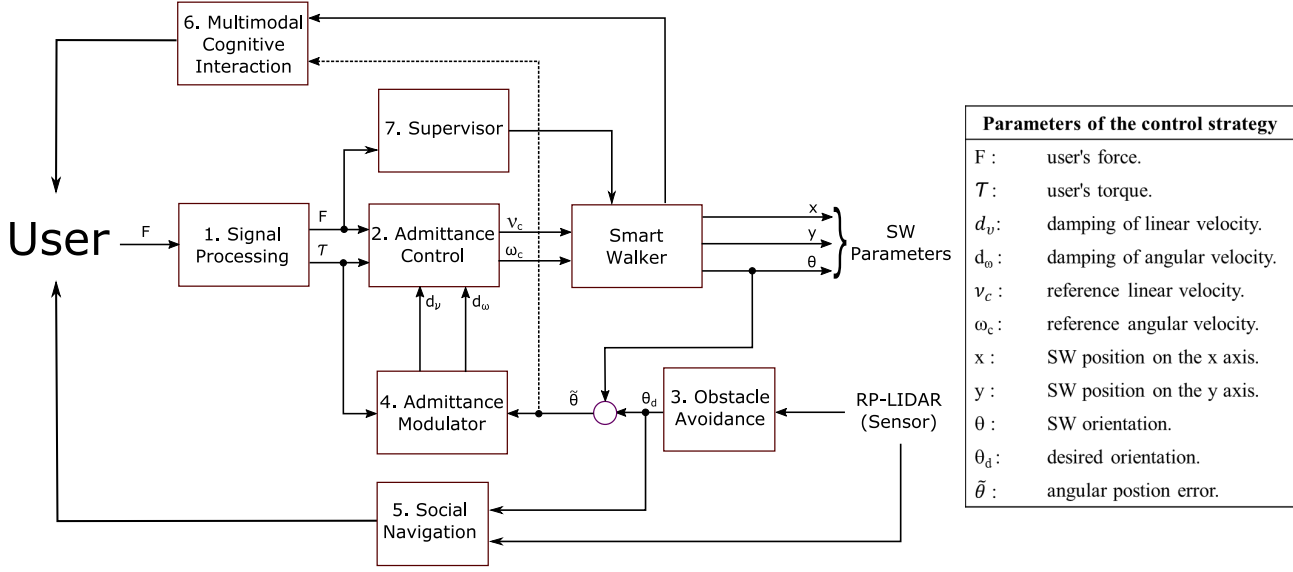


Figure 5.3: Block diagram of the navigation strategy.

The signals  $F(t)$  and  $\tau(t)$  are, then, used by the *admittance controller* (box 2 Fig. 5.3) to generate the desired linear  $v_c(t)$  and angular  $\omega_c(t)$  velocities for the walker, defined by Eq. 4.4 and 4.5.

$v_c$  and  $\omega_c$  are also used to impose not only the start and end of the locomotion with the SW, but also a comfortable gait speed. Moreover, the HREI dynamics is modified through the masses ( $m_v$  and  $m_\omega$ ) and damping ( $d_v$ ,  $d_\omega$ ) parameters.

The user can move freely within the corridor. However, when the user has mobility and/or cognitive impairments, it is important to implement an *obstacle avoidance* strategy to assist his/her navigation (box 3 Fig. 5.3). The obstacle avoidance is based on [91], which relates the obstacle position relative to the SW for calculating the desired orientation ( $\theta_d$ ), and thus avoiding obstacle. The proposed strategy generates an ellipsoidal repulsion zone around the SW for collision avoidance with static people, and walls (see Fig. 5.4). Consider the equation of each ellipse in the SW framework, expressed in polar coordinates by:

$$\frac{\cos^2 \beta}{a^2} + \frac{\sin^2 \beta}{b^2} = \frac{1}{r^2}, \quad (5.1)$$

where  $r > 0$  is the ellipse radial coordinate, and  $\beta \in [-\pi/2, \pi/2]$  the angular coordinate.  $a, b > 0$  are the lengths of the big and smaller axis of the ellipse, respectively.

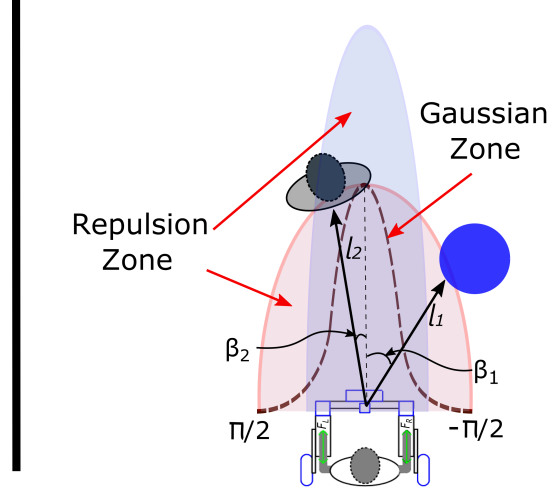


Figure 5.4: Zones to detect obstacles.

The RP-LIDAR sensor is used to measure the distances  $l_i$ ,  $i = 1, \dots, n_t$  and orientations  $\beta_i$ ,  $\beta_i \in [-\pi/2, \pi/2]$  related to the SW to the objects in the corridor (see Fig. 5.4);  $n_t$  is the number of measurements detected for each object found in each sensor turn.

The procedure to calculate the desired orientation to avoid an obstacle is described below. Note that such procedure is the same for both ellipses.

For each laser detection event, the distances  $l_i$  and the orientations  $\beta_i$  are captured. These measures are organized into two vectors respectively, and each sample (i.e., every 200 ms) of the RP-LIDAR sensor is updated. Then, Equation 5.1 and  $\beta_i$  are used to calculate the radials coordinates  $r_i$  of the ellipse. Once calculated the  $r_i$  vector, it is necessary to calculate the distance  $d_i$  (see Eq. 5.2), which determines the obstacle distances within the ellipse zone.

$$\tilde{d}_i = r_i - l_i \quad (5.2)$$

Vector  $\tilde{d}_i$  is used to generate an  $\alpha$  parameter, which discerns about the obstacle that has the higher collision influence. The function to determine the obstacle influence factor is shown in Eq. 5.3.

$$\alpha_i = C_1 e^{-\left(\frac{d_i}{\sigma}\right)^2}, \quad (5.3)$$

where  $C_1$  is a gain that modifies the influence factor of  $\alpha$ , and  $\sigma$  is the standard deviation of the Gaussian distribution to calibrate the width of the Gaussian area. It is important to note that  $\sigma$  is selected by considering the physical dimension of the SW, and it is set as the smallest value that allows the robot to pass through two close obstacles safely. The influence factor  $\alpha_i$  is used to calculate the obstacle orientation ( $\theta_o$ ), which is defined as:

$$\theta_o = C_2 \tanh \left( \frac{1}{n_t} \sum_{i=1}^{n_t} \beta_i \cdot \alpha_i \right), \quad (5.4)$$

where  $C_2$  is a second gain that can increment  $\theta_o$ , which increment is reflected in the obstacle avoidance way.

When the obstacle enters the repulsion zone, the influence factor  $\alpha_i$  on  $\theta_o$  increases. Finally, to establish the desired orientation  $\theta_d$  (box 3 Fig. 5.3) to avoid the obstacle, it is necessary to calculate the complementary angle of  $\theta_o$ , shown in Eq. 5.5.

$$\theta_d = \begin{cases} -\theta_o - \frac{\pi}{2} & \text{if } \theta_o < 0 \\ -\theta_o + \frac{\pi}{2} & \text{if } \theta_o > 0 \\ 0 & \text{if } \theta_o = 0 \end{cases} \quad (5.5)$$

The admittance modulator (box 4, in Fig. 5.3) works in the same way as was described in Chapter 4 (see Section 4.2.1), and in [10]. Such modulator is in charge of establishing a dynamic signal that modifies the damping parameter in the admittance controller, thus generating the haptic feedback. This modulator has as input variables the torque  $\tau(t)$  and the angular position error ( $\tilde{\theta}$ ) (see Fig. 5.3).  $\tilde{\theta}$  is calculated with respect to the SW orientation  $\theta$  and the desired orientation  $\theta_d$  (see Eq. 5.6). Such orientation errors only occur when the avoidance strategy detects an obstacle within the elliptical zones.

$$\tilde{\theta} = \theta_d - \theta \quad (5.6)$$

The haptic feedback implicitly guides the user to an obstacle-free zone by modifying, in real-time, the admittance control damping parameters. The modulation of the damping parameters of the admittance controller was previously presented in the Chapter 4 and is briefly described below.

From Eq. 4.4 the parameter  $m_\nu$  is constant, and  $d_\nu(t)$  has an inverted Gauss behavior. The Gauss function offers changes with soft transitions, which reflect directly into user's quality of experience. The user feels that moving forward with the SW is harder when the obstacle is closer. The function is shown in Eq. 4.7. Regarding Eq. 4.7, when  $\tilde{\theta}$  is zero, the damping is minimum, allowing the SW to move with the smallest restriction.

For  $\omega_c$ , the same restriction as in  $\nu_c$  is taken (i.e.,  $m_\omega$  remains constant). In Eq. 4.5, the definition of  $d_\omega(t)$  is given by Eq. 4.8. When  $\tilde{\theta}$  is positive and the user's torque  $\tau(t)$  induces a negative  $\omega_c$ , and vice versa, it implies that the SW's user intends to correct  $\tilde{\theta}$ . In this context, when  $\tilde{\theta}$  becomes smaller,  $d_\omega$  tends to decrease. In this manner, the user has to apply more effort to turn the SW.

The spatial modulation of  $d_\nu(t)$  and  $d_\omega(t)$  can be adjusted according to the user experience. This way, the haptic feedback can produce a higher or lower sensation of mobility difficulty with the walker in presence of people or walls. Furthermore, the haptic feedback never takes off the user's control over the SW, encouraging the user on the decision-making regarding the path to follow.

### 5.2.1 Social Navigation for the USW

The *social navigation* (box 5 Fig. 5.3) strategy developed for the USW navigation involves social conventions, which are established through a classifier and two ellipsoidal shapes, according to Section 5.1 (see Fig. 5.5). The first ellipse (IPSz) is used to avoid static obstacles and allows

side-by-side company of caretakers, doctors or visitors during navigation with the SW (see Fig. 5.6a). The second ellipse (IPPz) is used to avoid possible collisions with people that are walking in the same virtual path of the SW navigation, but on the contrary direction of the SW (see Fig 5.6b), no matter whether the person has a higher or lower speed compared with the SW velocity. In this context, it takes into account the premise that people walk in straight lines within corridors, and only change their virtual path of navigation to overpass other people or to avoid an obstacle.

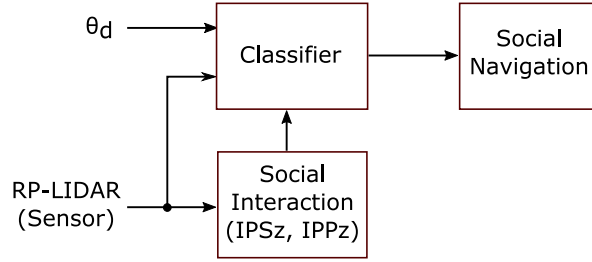


Figure 5.5: Blocks diagram of the social navigation.

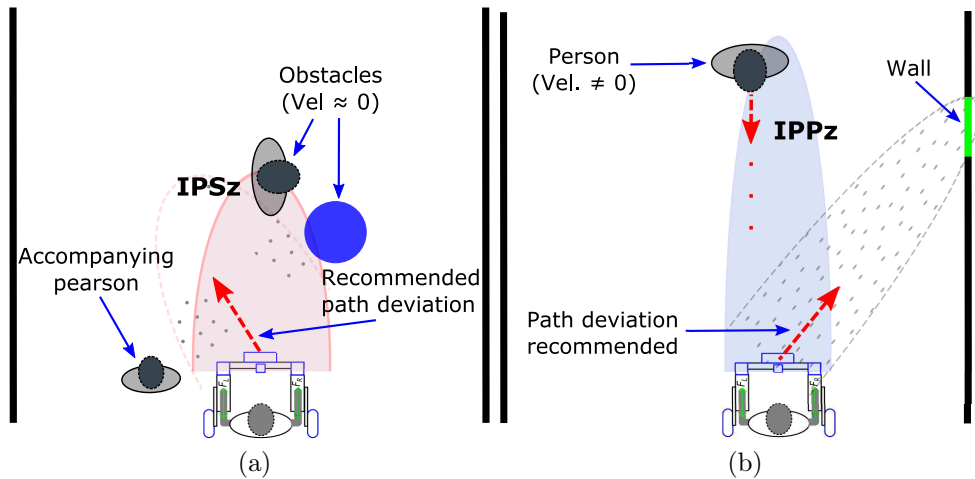


Figure 5.6: a) IPSz ellipse strategy; b) IPPz ellipse strategy.

When the SW's user is navigating within a corridor, he/she deviates from walls, fixed obstacles and mobile obstacles (such as people). In this context, the social interaction strategy proposed here is complemented by a classifier based on unsupervised learning to identify these obstacles (fixed and mobile) and walls. From the RP-LIDAR measurements, the algorithm performs the clustering of the possible obstacles using the density-based spatial clustering of applications with noise (DBSCAN) technique [92]. The algorithm requires two parameters: the first one is the minimum distance to clustering two point; the second is the minimum quantity of points

included in a cluster. Furthermore, the algorithm has a clustering based on cluster density planned to discover clusters in an arbitrary way [92].

In addition, the classifier not only separates the objects that are within the ellipse zones, but also eliminates individual points that are considered as noise. After clustering the obstacles and filtering the single points, a linear regression is performed for each group of points classified as objects, and determines if the obstacle is fixed or mobile, or whether it is a wall.

Once applying the linear regression, the Pearson correlation coefficient ( $R^2$ ) is used to determine the difference between a wall and an obstacle. Such coefficient is an adjustment measure of the linear model and varies between 0 and 1, explaining the dependence degree of the observed values [93]. The higher is  $R^2$ , more representative is the model, which is adjusted to the sample, indicating that the samples group is close to a straight line. This way, the classifier proposed here defines that values above a threshold of  $R^2 = 0.96$  identifies the clustering as a wall, whereas the values below such threshold are considered obstacles.

To differentiate between fixed and mobile obstacles, the obstacle relative velocity is calculated, with the SW velocity subtracted from the obstacle velocity. Thus, for relative velocity different from zero, the obstacle is considered mobile (see Fig. 5.6b).

Once the obstacle and its kind are identified, it is necessary to define the obstacle avoidance strategy using social interaction conventions. This task is accomplished through the algorithm shown below (see Algorithm 1).

Depending on each ellipse, Algorithm 1 is complemented with other conditions. For the IPSz ellipse, the classifier only detects noise, walls and/or fixed obstacles. When a wall is detected, it is recommended a  $\theta_d = \pi/4$ , which is enough to produce a hardest maneuverability on the SW when it moves in the direction of a wall. When the classifier detects an obstacle, the orientation value is given by the obstacle avoidance strategy.

The IPPz ellipse is in charge of preventing a collision with another person that navigates along the same virtual path of the SW within the corridor, but in the opposite direction. In this case,  $\theta_d$  takes the value assigned by the obstacle avoidance strategy. As a consequence, through the

multimodal cognitive interaction, the SW is recommended to change its navigation direction, however, the user is who takes the decision. After that, the classifier may detect a wall within the IPPz ellipse (see Fig. 5.6b). In this situation, the  $\theta_d$  value is ignored and the SW's user has more space to navigate within the corridor. However, if the user keeps going forward and the wall is detected within the IPSz ellipse,  $\theta_d$  is considered as the orientation to avoid the wall. Another condition where the  $\theta_d$  value is ignored is when the classifier detects a person walking in the same navigation direction of the SW. Thus, when  $\theta_d$  is ignored, the SW has an easier navigation.

---

**Algorithm 1** Obstacle = measures(RP-LIDAR)
 

---

```

if Obstacle > 0 then
  e = 0.3           ;minimum distance between two points.
  MinPts = 3       ;minimum number of points for a cluster.
  IDX = DBSCAN(Data, e, MinPts)
  k = max(IDX)     ;index that defines the cluster quantity.
  for j = 0 : k do
    Object = Data(IDX == j)
    if isempty(Object) then
      if size(Object) >= MinPts then
        do linear regression
        do calculate of R2
        if R2 >= threshold then
          wall
        else if R2 = 0 then
          noise
        else
          if VelObject ≈ 0 then
            Fixed obstacle
          else
            Person
  
```

---

Once the obstacle avoidance strategy is established, the *multimodal cognitive interaction* (box 6 Fig. 5.3) is in charge of recommending an orientation towards an obstacle-free zone. As presented in Chapter 4, the first cognitive channel or cHRi is a visual interface, which makes use of two LEDs (Fig. 4.8). In this case, the visual interface indicates to the user the correct orientation that the walker has to take to avoid the obstacle. A limit of  $\pm 25^\circ$  for  $\tilde{\theta}$  was defined, as under this limit, the control strategy allows an easier maneuverability with the SW [10]. Once  $\tilde{\theta}$  surpasses the error limit, the LEDs indicate the turn the user should make to correct the error in  $\tilde{\theta}$ . The LEDs light according to the direction of the turn recommendation. When the



user achieves the correct direction, both LEDs turn off.

The second cognitive channel uses both cHRi and pHRi to generate the haptic feedback, as the spatial modulator of the admittance control can increase or decrease the linear velocity  $\nu_c(t)$  and angular velocity  $\omega_c(t)$  of the SW. This way, this channel of the multimodal interaction is used to increment the difficulty of locomotion with the SW when the user is steering towards the wrong direction.

Regarding the *Supervisor* (box 7 Fig. 5.3), such as was defined in Chapter 4 (see Section 4.2.2), this strategy uses three of the safety rules. The first safety rule regards the user's partial body weight support on the SW platform, as the user has to overpass a minimum threshold established in the  $z$  axis of each force sensor. The second safety rule relates to the proxemics zones, in which, an intimate social zone [62,84] with 45 *cm* of radio around the RP-LIDAR laser sensor is defined. This way, if the laser sensor detects an obstacle within the intimate zone, the walker velocities  $(\nu_c, \omega_c)$  become zero to avoid a possible collision; otherwise, they acquire the values of velocity provided by the controller. Another safety rule defines a lower limit of 20 *cm* and an upper limit of 50 *cm* of distance between the user and the SW. This way, when the LRF sensor measures a distance smaller than the established lower limit or above the upper limit,  $\nu_c$  and  $\omega_c$  become zero to avoid collisions between the user and the SW. Otherwise, the SW acquires the velocities obtained from the admittance controller.

### 5.3 Experimental Study

Nine people ( $30.55 \pm 4.58$  years old) without any gait impairments and any previous training with the SW participated of the experiments. These people without mobility impairments were chosen to participate in the experiments as the main purpose of this work is to validate the social navigation strategy in confined spaces. Pathological gait will be the focus of future investigation. A computer was used to record the experiment data and to program the control strategy implemented in the SW's embedded hardware. The data recorded comprise: HRI parameters as  $F$ ,  $\tau$  and user legs distance to SW, control signals  $(\omega_c, \nu_c, d_\nu, d_\omega, \theta_d)$ , SW's linear

and angular velocities, and visual signals from the LED. In addition to the HREI information obtained with the RP-LIDAR sensor, the SW position  $(x, y, \theta)$  is also stored.

Table 5.1: Constants values used in the control strategy.

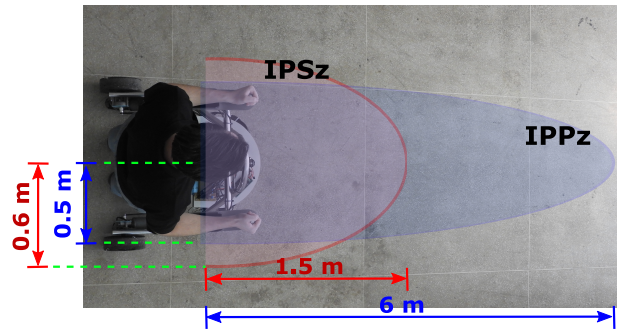
<i>Obstacle avoidance</i>				
Constant	$C_1$	$C_2$		
Value	20	20		
<i>Social Navigation Ellipses</i>				
Constant	$a_{IPSz}$	$b_{IPSz}$	$a_{IPPz}$	$b_{IPPz}$
Value	1.5	0.6	6	0.5
<i>Spatial modulator of <math>d_\nu</math></i>				
Constant	$d_{\nu_{max}}$	$d_{d_{max}}$	$\delta_{d_\nu}$	$m_\nu$
Value	100	90	0.3	1
<i>Spatial modulator of <math>d_\omega</math></i>				
Constant	$d_{i_\omega}$	$G_{d_\omega}$	$P_{d_\omega}$	$m_\omega$
Value	60	59	1	1
<i>Spatial modulator of <math>d_\omega</math></i>				
Constant	$d_{i_\omega}$	$G_{d_\omega}$		
Value	60	59		

As it was empirically found in Chapter 4,  $m_\nu$  and  $m_\omega$  are related to the discharge force of the user on the SW. The selected participants all had almost the same weight ( $68.66 \text{ kg} \pm 3.89$ ). The values assigned to the masses were  $m_\nu = 1 \text{ kg}$  and  $m_\omega = 1 \text{ kg}$ . Such values of the control parameters were determined for all participants, in order to they got a comfortable use of the SW. Then, it was verified that the user could move with the SW comfortably through a straight line of  $4 \text{ m}$  and also avoid obstacles. Such constants are described in Table 5.1. Regarding the safety rule, it was established in an empirical way with a minimum threshold of  $6 \text{ N}$  for the  $z$  axis of each force sensor.

Figure 5.7a shows the axis and distances in each elliptical shape. Considering that the corridor in which the SW is navigating is  $3 \text{ m}$  wide, the big axis of the IPSz ellipse was defined as  $1.5 \text{ m}$  long to allow sufficient maneuvering space. The big axis of the IPPz ellipse was defined according to the maximum RP-LIDAR distance range ( $6 \text{ m}$ ), which should give sufficient time for the user to react and avoid collision with people coming towards the SW (see Fig. 5.7b).

Two experiments were proposed to evaluate the navigation strategy performance and the mul-

timodal cognitive interaction (see Section 5.3.1 and 5.3.2). In both experiments, the user was asked to start the navigation in a point localized at the corridor center.



(a)



(b)

Figure 5.7: a) Ellipses distances design; b) Corridor distances, wide = 3 m, length = 28 m.

### 5.3.1 Navigating Through a Controlled Scenario

The first experiment aimed at validating our social navigation strategy in five controlled and practical situations that could happen when navigating in a corridor. Figure 5.8 illustrates these scenarios. In this experiment, besides the volunteer interacting with the SW, one person simulated the different situations proposed in each one of the experiment runs. At the first moment of the experiment, the SW user began the locomotion being accompanied by another person, as if they were engaged in a conversation, on approximately the first 4m (Situation 1, Fig. 5.8). The Situation 2 simulated a person walking in front of the SW in the same moving direction (Situation 2, Fig. 5.8).

This situation was simulated to show that the social navigation strategy ignores to the person

that moves in the same SW direction with a higher velocity as the SW, as it does not represent a collision risk. Then, in Situation 3, the person would stop moving to simulate a fixed obstacle (Situation 3, Fig. 5.8). This case shows the performance of the obstacle avoidance algorithm and the functionality of IPSz ellipse. Another scenario is represented in the Situation 4, which shows when a person crosses in front of the SW (Situation 4, Fig. 5.8). Here, the user perceives the quick reaction of the multimodal cognitive interaction, feeling haptically the presence of a mobile obstacle, and knows the way to avoid the collision.

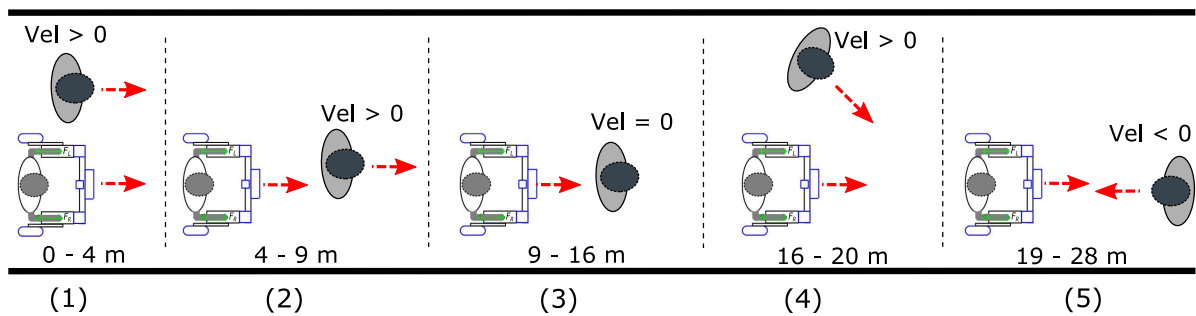


Figure 5.8: Situations within a corridor. Situation 1: navigation with accompanying person. Situation 2: person walking in front of the SW. Situation 3: person represents a fixed obstacle. Situation 4: person crosses in front of the SW. Situation 5: person walks in the opposite direction to the SW.

Finally, in Situation 5, the person started to walk in the opposite direction to the SW (Situation 5, Fig. 5.8). In this case, the functionality of the IPPz ellipse is shown to avoid the incoming person.

### 5.3.2 Navigating Through an Uncontrolled Scenario

The second experiment was conducted to validate the social navigation strategy in a real environment (see Fig. 5.9). Once the user was related to the SW maneuverability, he/she was asked to navigate through the corridor in the presence of several students. In this case, the students were not instructed in any way about the experiment or how to behave, in the hope for natural reaction while observing the SW navigation. This way, the social navigation strategy and the multimodal interaction channels were validated in a real situation within a confined space with fixed and mobile obstacles.

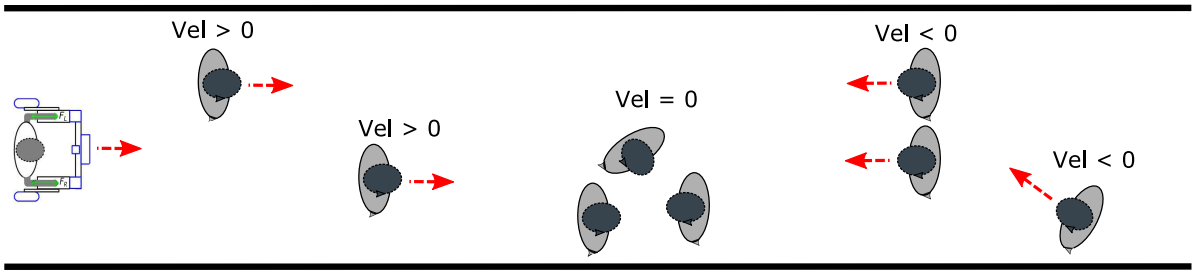


Figure 5.9: Natural situations within a corridor.

## 5.4 Results and Discussions

### 5.4.1 Navigating Through a Controlled Scenario

In the first experiment, users were asked to follow the navigation recommendations from the multimodal cognitive interaction in each of the different situations proposed in Section 5.3.1. Once the data was recorded, figure 5.10 shows the path navigation for one participant within the corridor. The two channels of the multimodal cognitive interaction could hint the direction that the user should follow in each of the five simulated situations.

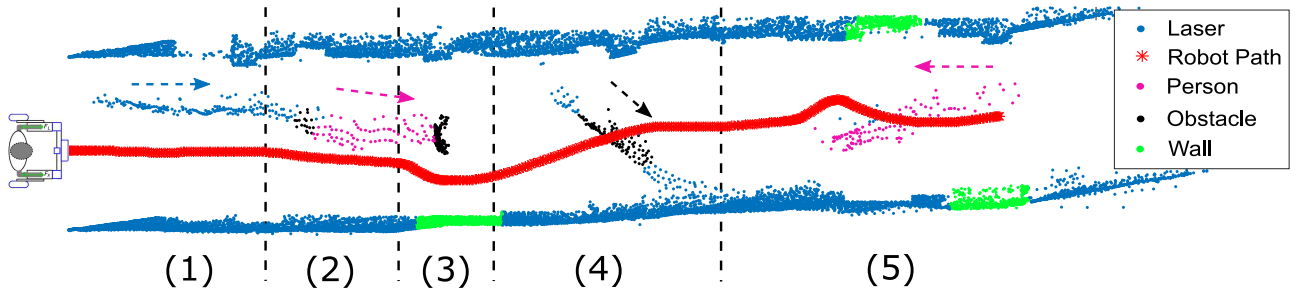


Figure 5.10: Controlled situations within a corridor. Corridor dimensions:  $w = 3\text{ m}$ ,  $l = 28\text{ m}$

Fig. 5.10 also shows the classifier behavior. During displacement in Section 1 (see Fig. 5.10), the RP-LIDAR detects an object near the SW, however, as this object lies side-by-side with the SW, it is not within the IPSz or IPPz ellipses, and the classifier ignores it. In this way, the social navigation strategy allows the companion of a person during the locomotion.

Then, the accompanying person starts walking in front of the SW (Section 2, Fig. 5.10), stopping after walking 5 m (Section 3, Fig. 5.10). While the person was walking in front of the SW, the classifier identified that the person had a positive relative velocity, which means that

the person is moving in the same direction of the SW and faster, thus not representing any risk of collision. Nevertheless, just when the person started to walk in front of the SW, he/she gets in the IPSz ellipse, and the classifier identifies him/her as an obstacle during a short time (black cluster on Section 2 in Fig. 5.10). The duration of this event was not enough to produce any haptic feedback on the user (see force and torque signals of Section 2 in Fig. 5.11 and 5.12, respectively).

Section 4 of Fig. 5.10 shows the situation in which the accompanying person crosses in front of the SW. The classifier identifies the person as an obstacle to avoid, and thus a haptic feedback is generated. Such reaction can be seen in the force and torque signals of Fig. 5.11 and Fig. 5.12, respectively.

Finally, the Section 5 of Fig. 5.10 presents the situation when a person is walking towards the SW. As the person approaches the SW, he/she is detected by the classifier within the IPPz zone. As this person is moving with a negative relative velocity, the  $\theta_d$  value is taken into account, producing an error  $\tilde{\theta}$ . The SW then deviates to the left as the person was coming by the right side of the SW (see Fig. 5.10, Section 5).

Regarding the haptic feedback strategy, Fig. 5.11 illustrates the forward forces detected by the force sensors and the control signals from the haptic strategy. When there is no value on  $\tilde{\theta}$  signal different to zero, the user is able to maneuver the SW, but imposing forward forces lower than 5 N (see Fig. 5.11). As a consequence of the  $\tilde{\theta}$  value,  $d_v$  assumes its minimum value ( $d_v = 10$ ), and the SW is allowed to move with higher linear velocities, which is limited to 0.38 m/s. The velocity limitation is set as people prefer to interact with mobile robots with velocities between 0.25 m/s and 0.38 m/s [83]. While the control strategy does not detect any obstacle within the social zones established, the SW follows the user motion intention (see Section 1,2 and 4 in Fig. 5.11).

Once the control strategy recommends a turn to avoid an obstacle, the haptic feedback changes the way that the user's force affects the SW, demanding a bit more effort to maintain the speed (see red asterisks in Fig. 5.11). When the admittance modulator acts, the linear damping increases, thus diminishing the SW's velocity. When there is no more obstacles detected, the

control parameters change to the initial state. The parameters values of the spatial modulator were chosen for the user to feel a quick change in the haptic feedback when an obstacle is detected. That is the reason for the abrupt changes in  $d_\nu$  signal (see Fig 5.11,  $d_\nu$  signal). In addition, the MSE of the linear velocity oscillates between  $0.1 \text{ m/s}$  and  $0.16 \text{ m/s}$ .

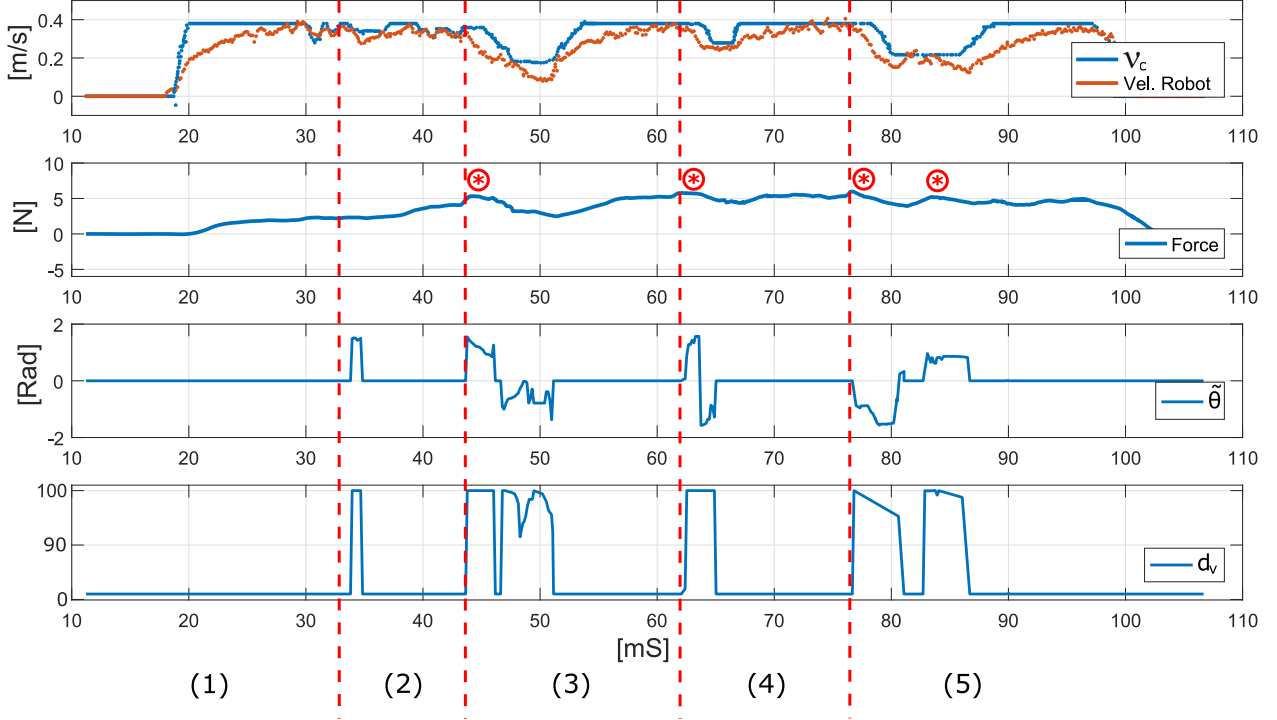


Figure 5.11: Spatial modulation curve of  $d_\nu$  and haptic force response of the social navigation. From top to bottom: a) Control and SW linear velocities; b) User's force signal; c)  $\tilde{\theta}$  signal; and d)  $d_\nu$  signal. All the corridor situations are described in Sections 1 to 5.

Figure 5.12 shows the control signals related to the torque. When an error in  $\tilde{\theta}$  is generated,  $d_\omega$  changes along (see Fig. 5.12,  $d_\omega$  signal). The haptic feedback is perceived (and increases) as the  $\tilde{\theta}$  error increases. While there are no detected obstacles within the IPSz and IPPz zones, the torque applied by the user is low (close to zero). As a consequence, the angular velocity of the SW is approximately zero (see Section 1 and 2 at Fig. 5.12). When an obstacle is detected, the user must rotate in the opposite direction of the angular position error (see the beginning of Section 3 in Fig. 5.12) [10]. Once the SW orientation is corrected or an obstacle is not detected anymore, the torque applied by the user decreases (see red asterisks in Fig. 5.12) and the user is able to maneuver freely again. In addition, the MSE of the angular velocity oscillates between  $0.055 \text{ rad/s}$  and  $0.066 \text{ rad/s}$ .

When an obstacle close to the SW is detected (Situation 4, Fig. 5.8), the user knows about

the obstacle presence through the haptic feedback channel of multimodal cognitive interaction, and not by the two LEDs channels, due to the user does not have time to review the visual cHRi indications. Therefore, the best channel to indicate the obstacles detection close to the SW in an intuitive way is the haptic feedback. However, when the obstacle is detected within the IPPz zone, the user has time enough to review the LEDs indications and follow the turn recommendation given by such visual channel.

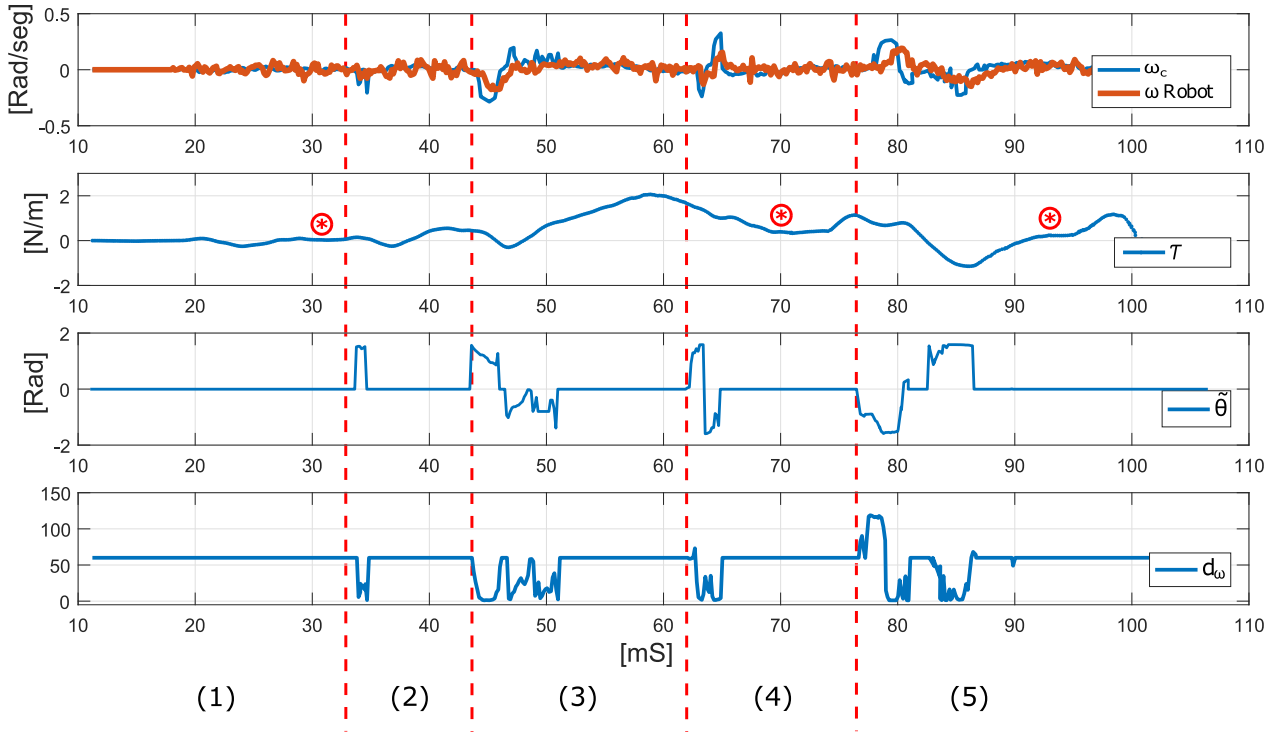


Figure 5.12: Spatial modulation curve of  $d_\omega$  and haptic force response of the social navigation. From top to bottom: a) Control and SW angular velocities; b) user's torque signal; c)  $\hat{\theta}$  signal; and d)  $d_\omega$  signal. All the corridor situations are described in sections 1 to 5.

Through the signals of Figs. 5.11 and 5.12, it can be seen the effect imposed by the haptic feedback on the user. Through such interaction channel, the user can perceive, in an intuitive way, the HREI and, consequently, have a safer navigation.

On the other hand, the average linear velocity of all participants was  $0.244 \text{ m/s} \pm 0.1196$ , which is within the limits recommended by [83]. Also, all participants were able to arrive at the end of the corridor, following, in a natural and intuitive way, the HREI strategy established for the SW.

The performance of the visual cognitive channel is shown Fig. 5.13. It can be seen that



the activation of the LEDs occurs every time the error  $\tilde{\theta}$  is higher than  $\pm 0.43 \text{ rad}$  or  $\pm 25^\circ$ , recommending the SW to turn direction to correct the angular position error (see Fig. 5.13). This adds another feedback channel to interact with the user, easing the user's interpretation and understanding of the HREI.

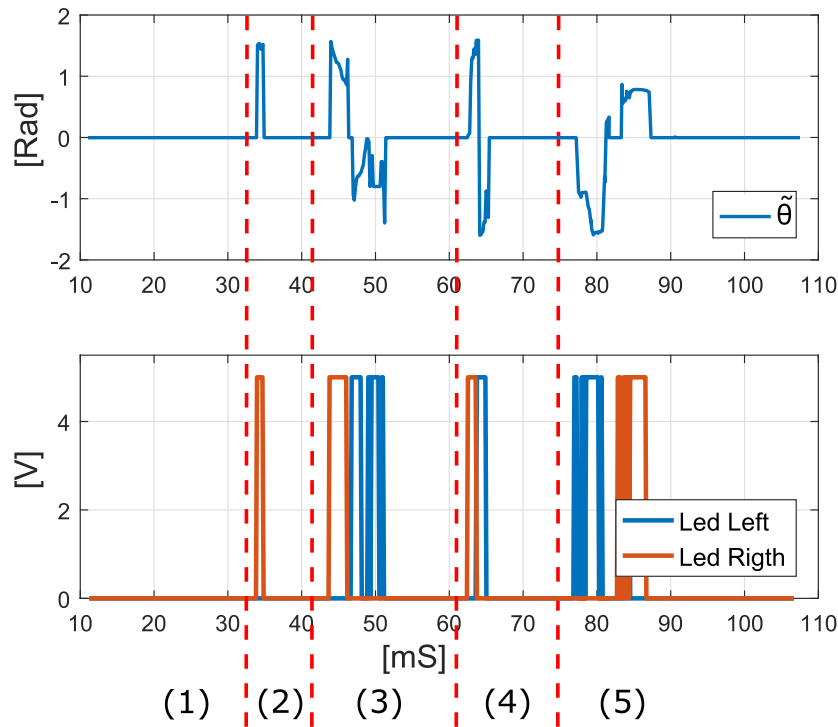


Figure 5.13: Recommendation of turn by the multimodal cognitive interface using the LEDs channel. All the proposed at the corridor situations are described in sections 1 to 5.

### 5.4.2 Navigating Through an Uncontrolled Scenario

During the second experiment, the SW's user was asked to navigate within the same corridor again in an uncontrolled scenario. The focus of this experiment was to observe the behavior of the SW's user and other people, therefore, none of the other individuals navigating in the corridor were informed about the role that they should have during the experiment (see Fig. 5.14) in order to emulate a very realistic situation.

Figure 5.15 shows a representative result of this experiment. It can be observed that the control strategy ignored individuals that were not tagged by the classifier. Also, at the beginning of this experiment run, one person passes near the SW in the same direction, and the user does

not need to change his/her direction. This is a clear example of the ellipse functionality within the social navigation strategy proposed here. During the experiment, some people naturally deviated from the SW (see black asterisk in Fig. 5.15), but, when people could not see the SW, the SW's user was able to avoid them using the navigation strategy recommendations (see red asterisk in Fig. 5.15). One of the situations presented in the Experiment 1 (Situation 5, Fig 5.8) occurs in this experiment (see green asterisk of Fig. 5.15). It can be seen that the user can correct his/her path travel when a person comes in the SW direction (Section 5, Fig. 5.15). In addition, it can be observed that the wall collisions are avoided too.



Figure 5.14: Real environment within the corridor.

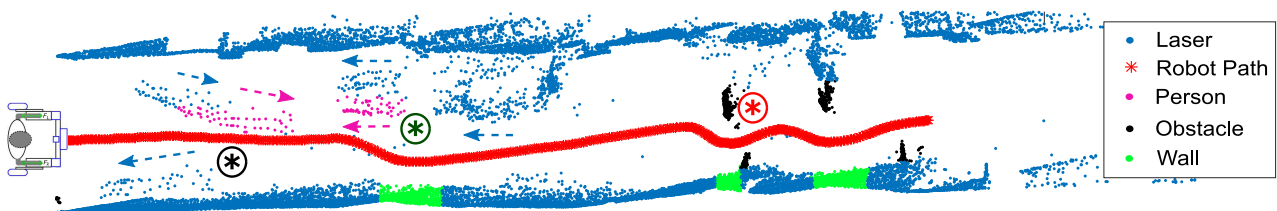


Figure 5.15: Real situations within a corridor. Corridor dimensions:  $w = 3\text{ m}$ ,  $l = 28\text{ m}$

The use of the two channels of the multimodal cognitive interaction allows enough freedom to maneuver the SW. Also, the shapes of the social interaction zones allow having more space to navigate in confined spaces, due to the strategy proposed here ignoring obstacles that do not affect the SW navigation. Moreover, during the experiments, the users evaluated the SW speed as a “good velocity for locomotion”. Other comments listened during the experiments are related to the safety perception during guidance and the intuitive interaction between user and robot.

In this chapter, the performance of safety rules of the supervisor was not verified as such evaluation was realized already in the Chapter 4.

As a conclusion, this Chapter presented a new strategy for HREI, which includes social zones within the SW's control to allow a social-aware navigation in confined spaces. In addition, the use of the social zones defined by proxemics may contribute to the social inclusion of the SW's user, as it allows a natural interaction with other people of the environment, following social conventions too. Here, it is necessary to take into account that the SW has a person within its activity area. For this reason, strengthen the social factors for the SW navigation may improve the quality of life and wellbeing of SW's users, in addition to improve the social acceptance of the SW.

Furthermore, the navigation strategy proposed here involves a classifier and ellipse shapes for the social zones, which allows a wide navigation area within the corridor, due to many of the detected obstacles (fixed and mobile) may be ignored. In this context, this strategy improves the HREI and allows that the user of the SW can navigate in a safe way with a comfortable velocity. This was verified through real experiments where the user, by means of the multimodal cognitive interaction, was able to navigate within the corridor using the SW's recommendations to overpass the different situations that were forced during the travel.

# Chapter 6

## Haptic Feedback to Guide Visually Impaired People Across Complex Environments

Many technological solutions to guide blind people have explored the HREI. For example, force sensors have been used in Smart Canes as physical interfaces to detect the user's motion intention [94]. Complementarily, ultrasonic [94, 95] and laser [9, 16] sensors have been used to detect obstacles and to provide navigational information. Wearable sensors and vibrators motors have also been used together with Smart Canes to assist navigation of blind people [96]. However, the use of these wearable sensors and actuators might be unnatural and uncomfortable for the user, due to the interpretation of the navigation commands requires a user's cognitive process, which may induce fatigue [58]. Also, when the user has a poor balance control, a Smart Cane may not provide enough physical assistance.

Passive SWs (see Chapter 2 - Section 2.3.1) have been used to offer physical and sensorial assistance to blind people [9, 97]. In contrast, although active SWs offer full motion control of the device and provide maximum assistance in navigation and guidance [6], there have been little literature that reports their use oriented to guide the visually impaired. Nevertheless, it is also necessary to pay more attention to the HREI and, especially, to the user experience, as

at the end, is he/she who evaluates the SW performance. Several HREI solutions require either the use of wearable sensors by the user [96] or the placement of landmarks [94] and sensors on the environment. Moreover, HREI should be natural and intuitive for the user in order to provide a good usability and user experience, allowing its continued use [10].

In this chapter, the USW uses an admittance controller to guide visual impaired people. Through the use of haptic feedback, the control strategy guides the mobility of the visually impaired through a desired path. This way, the user can impose not only the start and end of the locomotion with the SW, but also a comfortable gait speed. The SW's angular velocity control is implemented as a function of a virtual torque, which depends on the angular position error of the SW. The proposed controller relies upon cognitive interaction through haptic feedback, which results from the physical interaction between the user and the SW. This way, such controller informs the user about the direction to follow. In order to keep the user along the path, inputs interpreted as independent intention to turn do not affect the guidance, hence minimizing the tracking error and providing feedback over the correct direction to follow. Furthermore, this work attempts to identify important interaction parameters that must be taken into account during guidance to provide for a good user experience; such as the restraints on SW velocities, and design of the desired path.

This chapter is organized as follows. First, it describes the related works that use SWs as the assistance tool for people with blind and gait impairments. Then, it describes the proposed control strategy and the experimental setup. Additionally, it shows the experimental results and the discussion about them. Finally, conclusions are presented.

## 6.1 Related Works

Many research groups have worked over the last few decades on healthcare with focus on assisting mobility and visually impaired people [9, 95, 98]. Several assistive devices have been developed to improve user's quality of life, each better suited to different special needs [61]. As smart canes might not offer proper weight support or assistance for those with moderate

severe gait disorders [99], due to they are usually employed only to assist the displacement of people with some degree of blindness [99], most of the works that relate to ours are within smart walkers field [9, 99].

On a classic work, Lacey [100] presents PAM-AID, a passive smart walker aimed to guide the elderly blind. Aware of the environment, such walker takes as inputs the user's desires (e.g., move forward or turn left) to guide through corridors, providing warnings of nearby obstacles. In a later work [97], it was also able to steer the user around such obstacles. Some of the users who tested the system reported that a point-to-point guidance feature would be of interest, so the user would input a desired location to be guided to. This was later resolved on Guido [51], an evolution of the PAM-AID, which was able to guide the user to specific places by generating a path based on a simultaneous localization and mapping feature.

On a more recent work [9], authors attempt to navigate people with visual and walking impairments using an off-the-shelf passive walker modified with laser sensors. It relies on pHRi with two vibro-tactile interfaces, which could be used independently or combined, to provide navigational information. Such interfaces consisted of "vibrating handles" and a "vibration belt" with multiple motors worn around the waist. The walker presented one operation mode in which the user was only informed about surrounding obstacles, and another operation mode to guide the user to a specific location. This point-to-point guidance leveraged mapping features to conduct the user throughout a path, avoiding both static and dynamic obstacles. Experiments revealed that users preferred the haptic interface on the handles over the belt, which was considered a rather obtrusive interface.

Experiments with blindfolded subjects have been performed on works for passive smart walkers [101] and [102]. [102] used the walker's brakes as means of influencing the direction of motion for obstacle avoidance, whereas [101] leveraged the input of a specific destination to generate a path and used the brakes to assure that the user would remain over the desired path.

The aforementioned passive walkers either aimed to assist people with some degree of both visual and mobility impairments or were tested by blindfolded subjects. Other works explored point-to-point guidance on active smart walkers, though not mainly focused on the blind pop-

ulation. [103] presented Care-O-Bot II, a SW capable of guiding the user throughout an established path while respecting user's inputs. Both pHRi and cHRi based on force sensors were implemented to evaluate the interaction and control velocities, and the guidance feature allowed for obstacle detection and path deviations. A similar strategy had been previously presented by [52], which introduced an active walker able to weigh user's force inputs against the desired path in order to guide while maintaining some degree of freedom for deviations. A so-called "forced mode" was also implemented by [52], and user inputs were only considered for switching motion on and off, removing from the user any further control over the direction of the walker. Other similar shared-control strategies have been presented by [49] and [15].

Interaction methods that rely on haptic interfaces were more commonly employed when guiding the user. While vibration signals are used on passive walkers, strategies based on force sensors and dynamic motors to provide haptic feedback to guide and interact with the user are predominant on active devices. As HRI began to grow as an independent field, user evaluation of the interaction per se gained attention over the robotics aspects of the systems. [100] evaluated system's usability and safety through user rating. In [9], users rated the performance of the walker and also answered to a qualitative questionnaire over how they perceived the interaction. The active SWs researched on this work did not evaluate the HRI, though [6] states that full motion control provides maximum assistance in navigation and guidance, referencing both [52] and [103] studies. A range of information and control parameters impacts HREI. For instance, the design of the path to be followed, the obstacle avoidance strategies, and the design of the HRI itself are reflected in the user experience during guidance. Nevertheless, the SW should not only offer physical, sensorial and cognitive assistance, but also offer a natural and intuitive way of navigate through the environment.

## 6.2 Guidance Control Strategy

The control strategy uses the path follower control proposed by [75], which is leveraged to provide the desired orientation of the SW in relation to the path. An admittance controller is

used to detect user's motion intention to control the locomotion of the SW [10]. As there is a pre-established path to be followed, the path follower controller weights both the robot's current position and desired orientation to stay on or to get on the path. The admittance controller then sets velocities according to the physical interaction with the user and the desired orientation. In order for the interaction to be perceived as natural while still not allowing the user to deviate from the path, the robot's linear velocity is directly linked to user's interaction forces, whereas the steering velocities depend also the desired orientation. In other words, the user has no direct input in consciously changing the SW's orientation, which is mainly dictated by the device's relative position to the path, in order to guarantee that the user will not deviate from it.

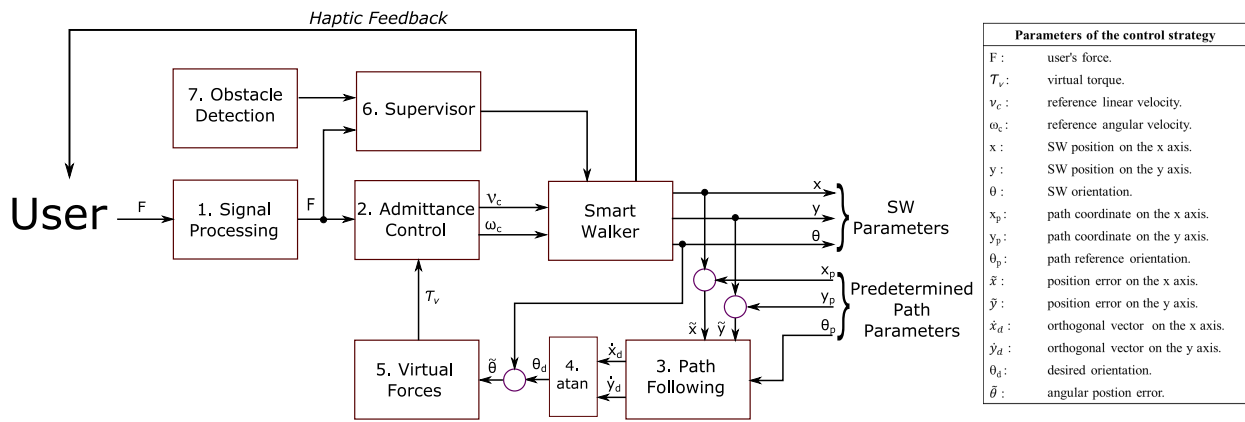


Figure 6.1: Block diagram of the controller strategy to guide visually impaired people.

The force sensors (see Fig. 3.1) are responsible for capturing the user's intention of movement, and data from each sensor are translated into a forward force, henceforth referred to merely as the force (box 1 Fig. 6.1). The human force  $F_H(t)$  and torque  $\tau_H(t)$  are obtained from the  $y$  axis signals of each force sensor, as shown in Equations 3.1 and 3.2, respectively (see Chapter 3).

To detect the user's motion intention, the method proposed in Chapter 3 is used here in offline mode, i.e., once the data were recorded. In addition to a FLC algorithm, inspired in [12], which is used to estimate and cancel cadence component of each input signal ( $F_{LY}(t)$  and  $F_{RY}(t)$ ), a Weighted-Frequency Fourier Linear Combiner (WFLC) algorithm is also used in order to perform the filtering of the force sensors signals. Thus, more stable signal of force  $F_H(t)$  and torque  $\tau_H(t)$  are obtained.



In the admittance controller, responsible to control the SW velocities,  $F_H(t)$  is related to the linear control velocity  $\nu_c(t)$  [10], as shown in Equation 3.3.

Here, it is necessary to recall that the mass  $m_\nu$  and damping  $d_\nu$  parameters are used to define the HREI dynamics. As the user intention to turn does not affect the guidance, the human torque ( $\tau_H(t)$ ) is measured only for evaluating the cognitive interaction through the haptic feedback obtained by the user's physical contact with the SW. The angular control velocity  $\omega_c(t)$  (i.e., the angular velocity output from the admittance controller) is used to point and conduct the user into the desired path and, further, maintain the user on the path.

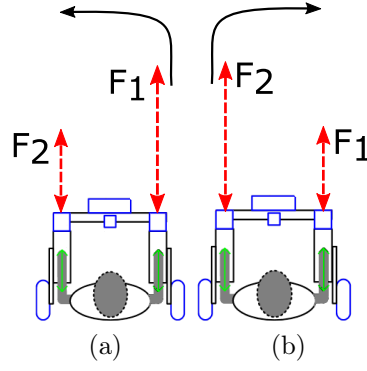


Figure 6.2: Virtual force modulation. a) Left turn. b) Right turn.

To guide the user through the desired path, the path following controller [75] described in Chapter 4 is used. The closed loop equation used by Andaluz et al. [75] (see Eq. 4.2) allows obtaining the desired orientation  $\theta_d$  to the SW (see Eq. 4.3).

Once, defined  $\theta_d$ , it is possible to calculate the orientation error  $\tilde{\theta}$  between the desired orientation  $\theta_d$  and the SW orientation  $\theta$ . Thus,  $\tilde{\theta}$  is calculated in the same way as shown in Eq. 4.6.

The orientation error is the spatial information used to set the virtual forces (see Fig. 6.2a and 6.2b), which are further used to define the virtual torque  $\tau_v(t)$  (see Eq. 6.1, 6.2, and 6.3). Hence, the equations are represented by:

$$F_1(t) = k(1 + \tanh(\tilde{\theta})), \quad (6.1)$$

$$F_2(t) = k(1 - \tanh(\tilde{\theta})), \quad (6.2)$$

$$\tau_v(t) = \frac{F_1(t) - F_2(t)}{2} \cdot d, \quad (6.3)$$

where  $k$  is gain constant used for properly setting forces, and  $d$  is the distance between sensors.

Then, the virtual torque (see Eq. 6.3) is used to calculate the angular control velocity  $\omega_c(t)$  (see Eq. 6.4) of the admittance controller [10], which is used to guide the user in a natural and intuitive way on the desired path.

$$\omega_c(t) = \frac{\tau_v - m_\omega \dot{\omega}(t)}{d_\omega}, \quad (6.4)$$

In Eq. 6.4, the mass  $m_\omega$  and damping  $d_\omega$  also participate in the HREI dynamics.

The end-result of this control strategy is that the user is able to control the movements of the SW during the interaction, and the human turn intention, which is not taken into account for  $\omega_c(t)$ , may not be perceived as a restriction. When the user desires to steer in a way that would lead to path deviation, the haptic feedback indicates the correct path to the user, and, as result, the correct direction to follow is presented to the user.

The SW has a safety supervisor, which is in charge of determining if the user can start the locomotion with the SW or not. The supervisor has two safety factors. The first one regards the user's partial body weight support on the SW platform, which has a threshold of 5  $N$  (empirically obtained) in the  $z$  axis of each force sensor. If a threshold is not surpassed, no motor/control command is sent to the drivers. Once the controller detects that the threshold has been reached in each sensor,  $\nu_c(t)$  and  $\omega_c(t)$  assume the values defined by the control strategy. In the second safety rule, a semicircle protection zone with 70  $cm$  of radio in front RP-LIDAR laser sensor is defined. Thus, if the laser sensor detects an obstacle within the interest zone,  $\nu_c(t)$  and  $\omega_c(t)$  become zero to avoid collisions. This simple solution was implemented to guarantee

user's safety when navigating with the robotic device.

### 6.3 Controller Simulation and Path Design

The control strategy was simulated in Matlab to verify the behaviors of the SW during straight paths and curves. In such simulation, the USW kinematic model and an approximation of its dynamic model were used. The admittance control strategy inserts inertia in the system by the mass  $m_\nu$  of the linear velocity equation (see Eq. 3.3). When the robot must steer along the path, the value of the linear velocity, inertia given by the admittance control, and the path attraction induced by the path following controller are combined to generate the steering movement. All those factors might affect the stability and balance of the user, as the maneuverability may be hardest. In order to understand how this might impact on the guidance and how it is related to the way the desired path is established, the simulations accounted for multiple path designs.

Figure 6.3 shows the simulation results of three different path designs. The linear velocity of the simulated SW was limited to  $0.58 \text{ m/s}$ , as this is the typical gait speed for an usual pace in elderly without any gait disorder [79]. The forward force  $F_H$  was constant and established in  $8 \text{ N}$ , which results in maximum linear velocity. The other parameters of the guidance control strategy were defined in such a way that the robot could follow the desired path.

Figures 6.3a and 6.3b show that the robot surpasses the desired path, due to the sharp shape of the curve and the inertia inherent to the controller. These result in intense additional angular movement to correct the orientation error and bring the robot back the desired path. .

Figure 6.3c presents a soft curve with radius of  $1.4 \text{ m}$ . Now, the robot follows the desired path and does not present any additional movement to keep on the path. Although the human factor is usually not considered for path generation in traditional robotics, soft curves along a path are natural to humans, and the absence of oscillatory movements may take an important role in the user's experience during physical interaction with robots.

In that sense, both the maximum allowed linear velocity and the curve form directly affect

the travel along the path. Thus, it is necessary to limit the maximum value of linear velocity and the minimum value of the curve radius. Furthermore, the inertia added by the admittance controller plays a positive role on guidance when these limits are included.

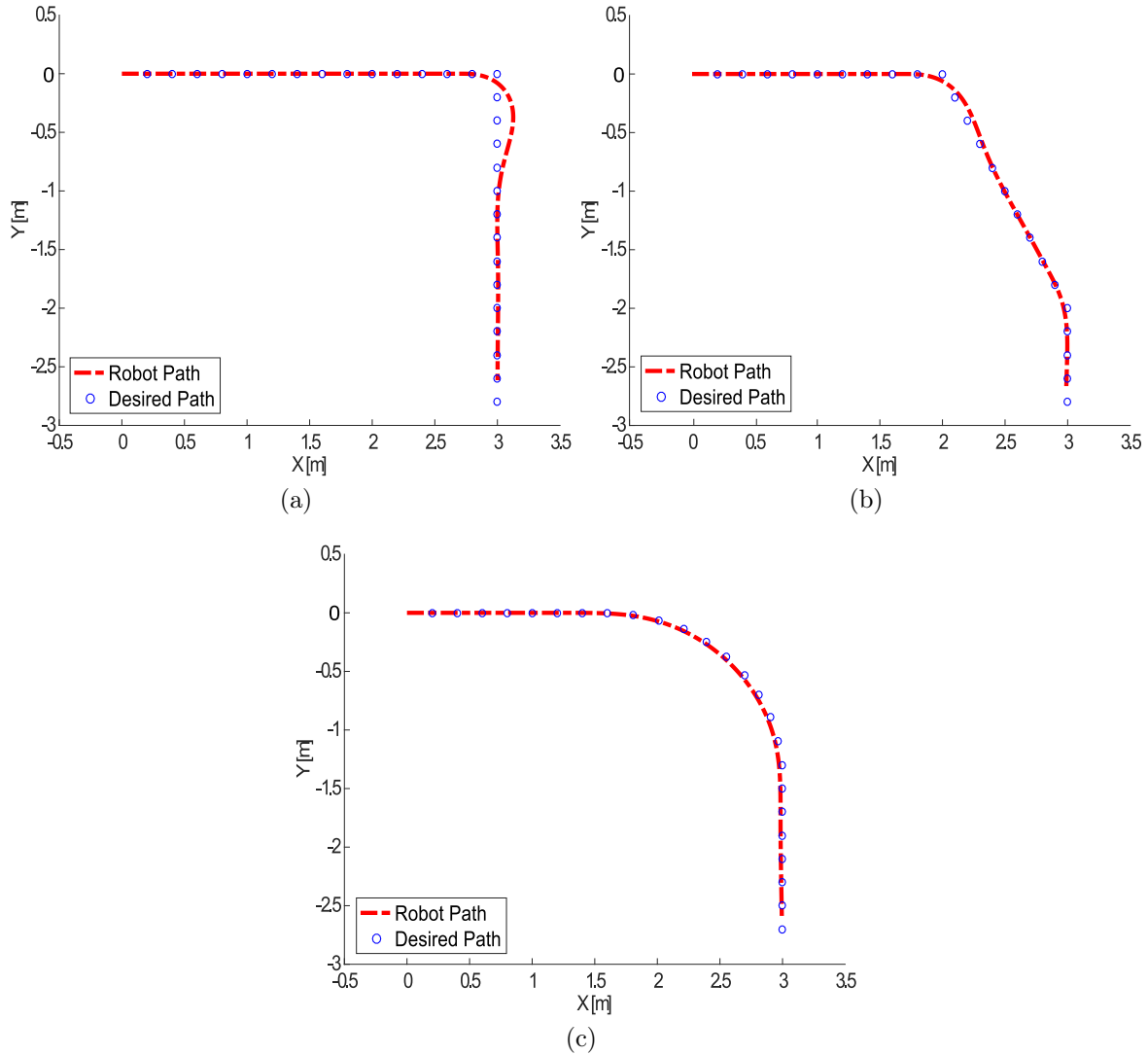


Figure 6.3: Control strategy simulated for different paths designs. a) Path with a curve of  $90^\circ$ ; b) Path with a curve of  $120^\circ$ ; c) Path with a soft curve (radius=  $1\text{ m}$ ).

## 6.4 Experimental Setup

Fifteen people (eight women) without previous training with the USW, and without any history of gait or visual impairments participated in the experiments. The height of participants ranged from  $1.53\text{ m}$  to  $1.72\text{ m}$ , and the body mass ranged from  $54\text{ kg}$  to  $73\text{ kg}$ . All participants were

healthy young individuals with no disabilities. Experiments took place in a real non-structured environment, and the path designed to guide the user from starting to ending point required the user and the SW to go over different surfaces (rug and corridor floor) and pass nearby tables and decoration objects. This path (see Fig. 6.4) consisted of three line segments linked by two soft curves and was previously unknown to the participants. The first line segment is 2.2 m long (see Figure 6.5, box 1) and is followed by a  $160^\circ$  curve with 1.6 m radius (see Figure 6.5, box 2). The third segment composing the path is a 5.6 m straight line (see Figure 6.5, box 3). A  $90^\circ$  curve with 1 m radius (see Figure 6.5, box 4) links the last segment, a 4.4 m straight line (see Figure 6.5, box 5).

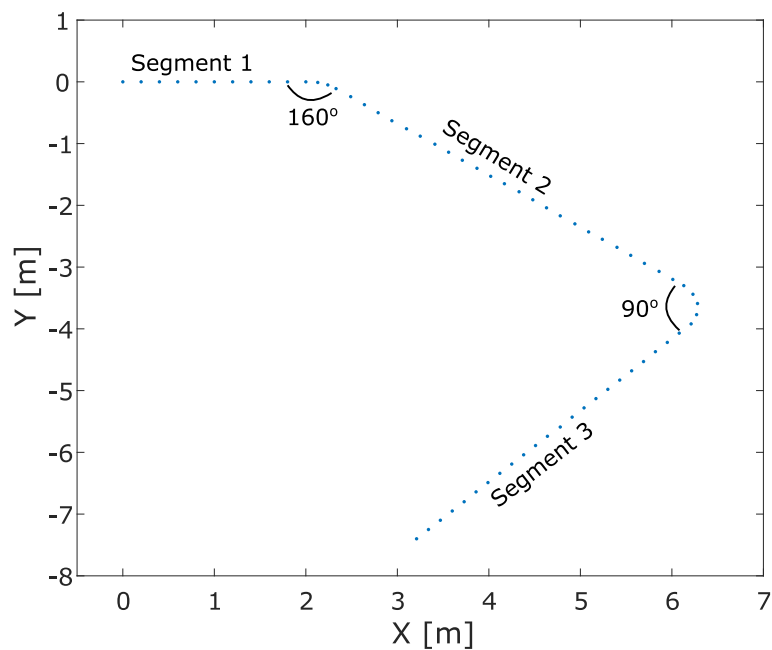


Figure 6.4: The pre-established path to be followed by participants.

The guidance was performed over the designed path to evaluate the proposed controller performance and the subsequent HREI. The parameters of the guidance control strategy were determined empirically from previous experiments, focusing on the comfort of user. The control parameters are described in Table 6.1.

The experiment consisted of two parts: on the first part, the user was unaware of the path and was required to use a blindfold during guidance. During the second part of the experiment, the guidance was performed without the blindfold. In both experiments, through force sensors localized under the forearm support of the SW, the user was able to interact and transmit the

movement intention to start or stop the locomotion, and also regulate the desired speed. During the first part of the experiment, the HREI and the controller behavior were observed to assess the proper functioning of the guidance strategy when there was no visual feedback to the user. Later, during the second part, special attention was paid to the haptic feedback behavior and the physical and cognitive interactions while maneuvering the SW along the path. The linear velocity was limited to  $0.25 \text{ m/s}$  in both parts of the experiment as a security factor. This limit in the linear velocity is enough to provide good and comfortable locomotion and guidance during the interaction with the USW.



Figure 6.5: Scenery of the experiment. The participant starts from the building entrance (box 1) and is guided to a room (box 5).

Table 6.1: Parameters values used in the control strategy.

<i>Path following</i>					
Constant	$k_x$	$k_y$	$l_x$	$l_y$	$\nu_r$
Value	0.7	0.7	3	3	0.3
<i>Admittance Control</i>					
Constant	$d_\nu$	$d_\omega$	$m_\nu$	$m_\omega$	$k$
Value	10	20	8	5	3

## 6.5 Results and Discussions

In the experiments, the participants interacted with the SW in the desired way. All experiments used the same initial pose (Figure 6.5, box 1) and path. Figures 6.6a and 6.6b show odometry data from two participants, one of them performing the first test, wearing the blindfold (Figure 6.6a), and the other one, the second test, without the blindfold (Figure 6.6b). It can be seen that in both cases the controller was able to guide and maintain the user along the desired path. Due to the absence of sharp curves and the fact that the user always starts in a point inside the desired path, there were no path deviations, as expected.

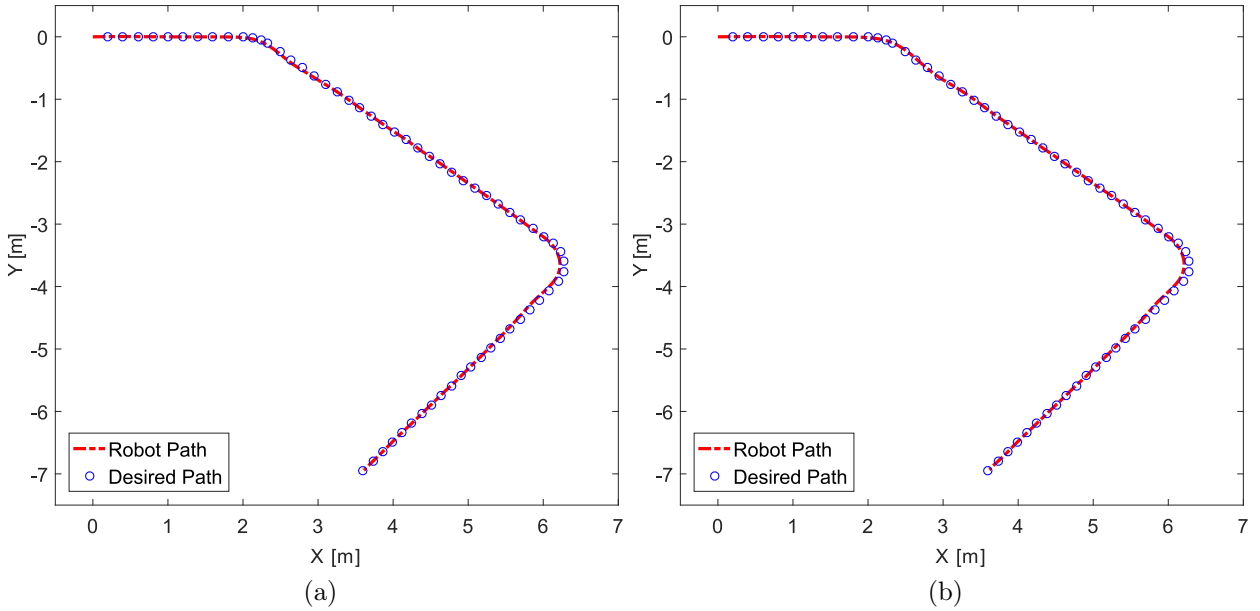


Figure 6.6: Following the desired path. a) User wearing the blindfold. b) User without the blindfold.

Figure 6.7 shows a representative result of the first part of the experiment, when the subject is wearing the blindfold. It can be observed the physical interaction forces between the user and the walker, and the control signals. Once the SW starts the movement, a small force signal (around 0.2 N) is demanded from the user to maintain the locomotion with the SW along the desired path. With the user wearing a blindfold, the controller haptically induces a torque on the he/she, due to the physical interaction between the user and the SW. In the straight segments of the desired path, the torque signal  $\tau_H(t)$  due to the HRI is around zero. However,

such torque can be clearly perceived during the curves, being particularly stronger in the second curve of the desired path. At the beginning of that curve, the torque  $\tau_H(t)$  detected is contrary to the curve direction (see red dotted line in second curve zone in Fig. 6.7), as the user was not able to perceive the beginning of the curve and attempted to keep going straight ahead. Once the user interprets the haptic feedback, the user follows the interaction and applies torque in the same direction of the curve. This interaction was perceived as natural and intuitive, and the controller strategy is able to indicate to the user the path to follow. The mean linear velocity is  $0.14 \text{ m/s}$ , and the angular velocity only appears on the SW in the curve zones (maximum absolute value of  $0.43 \text{ rad/s}$ ). The orientation position error is approximately zero, because the guidance controller strategy keeps the user on the desired path (see Figure 6.7).

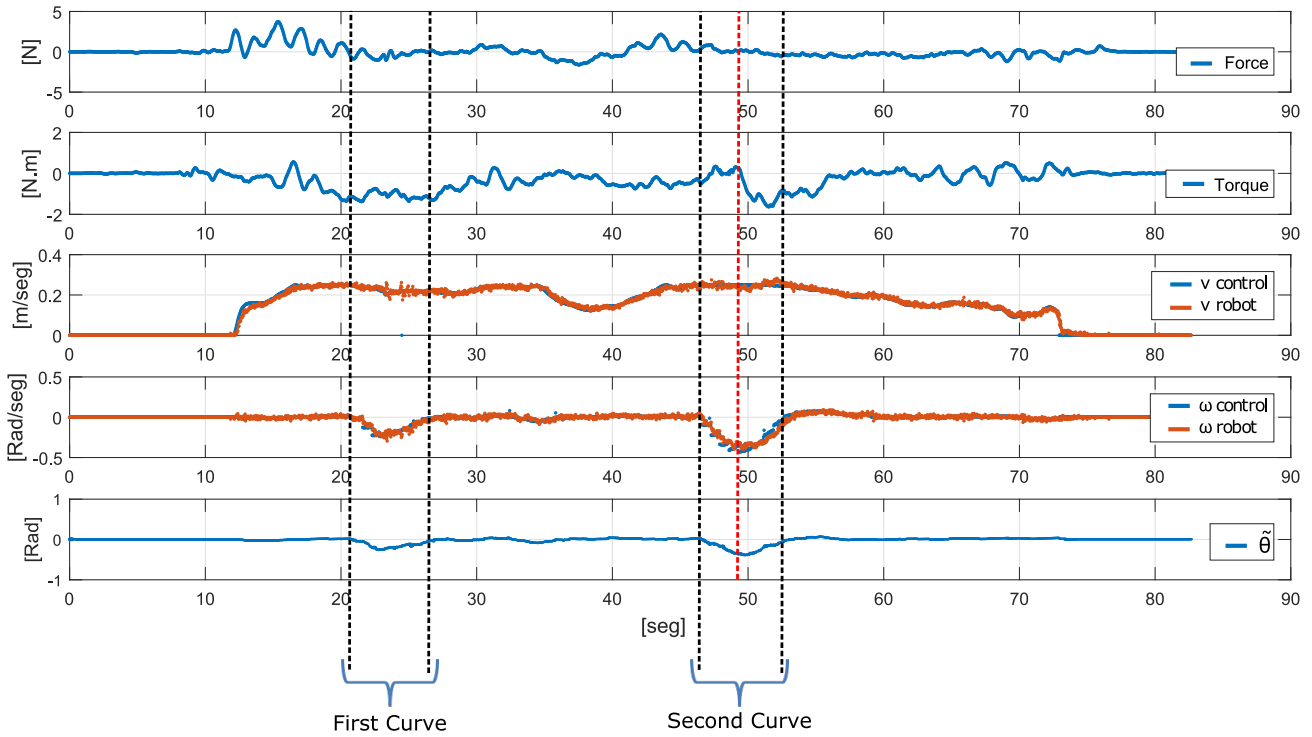


Figure 6.7: Following the desired path using the blindfold. Up to down: user's force signal  $F_H(t)$ , user's torque signal  $\tau_H(t)$ , Control and SW linear velocities, Control and SW angular velocities,  $\tilde{\theta}$  signal.

Figure 6.8 shows a representative result of the second part of the experiment, performed without the use of the blindfold. In this case, as the user felt more comfortable, he/she was able to use his/her own visual feedback, force and torque signals, which assumed larger values than when the user was wearing the blindfold, as the user was more confident and felt that he/she had the control over the SW maneuverability (see Fig. 6.9b). In the straight line, the mean force



value was of  $1.5 N$ , with a maximum value of  $5.4 N$ , and the human torque applied by the user was around  $0 N.m$ . It can be observed that the user applied torque signal before the beginning of the second curve (see the red dotted line in Figure 6.8), which happened because the user was able to see the environment by where he/she was moving without being fully aware of the desired path to follow. Even though the user applied  $\tau_H(t)$ , the SW only took the turn direction when the curve began on the desired path. The absolute maximum torque value applied by the user was  $12.6 N.m$ .

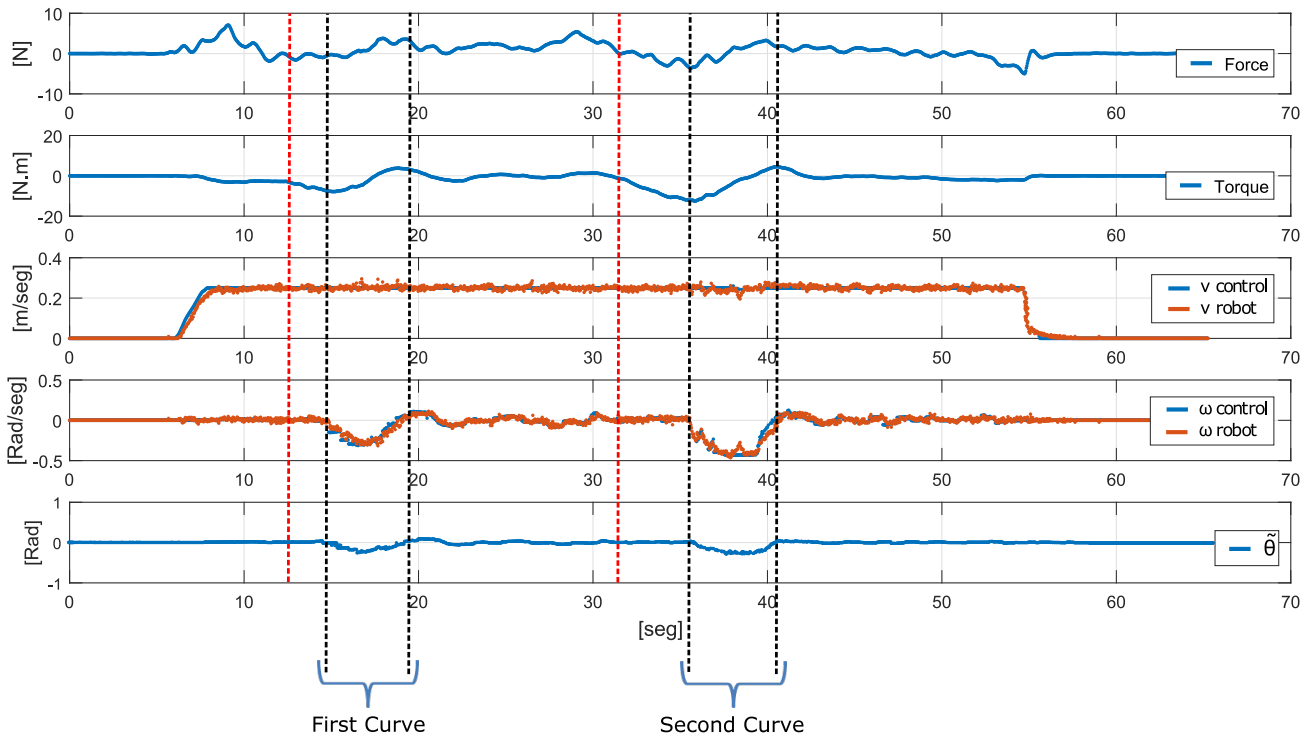


Figure 6.8: Following the desired path without use of blindfold. Up to down: user's force signal  $F_H(t)$ , user's torque signal  $\tau_H(t)$ , Control and SW linear velocities, Control and SW angular velocities,  $\tilde{\theta}$  signal.

As the user shown in Fig. 6.8 felt safer in this experiment (see Fig. 6.9a), the linear velocity was always the maximum limited value, which was  $0.25 m/s$ . This same behavior was observed on the signals obtained from 10 participants. In this case, the maximum absolute value of the angular velocity was  $0.48 rad/s$ , and the orientation position error was also approximately zero. In both parts of the experiment, all participants followed the desired path using the haptic feedback of the control strategy (see Fig. 6.9c), which, according to the perception of participants, allowed an intuitive interaction between the user and the SW (see Fig. 6.9d).

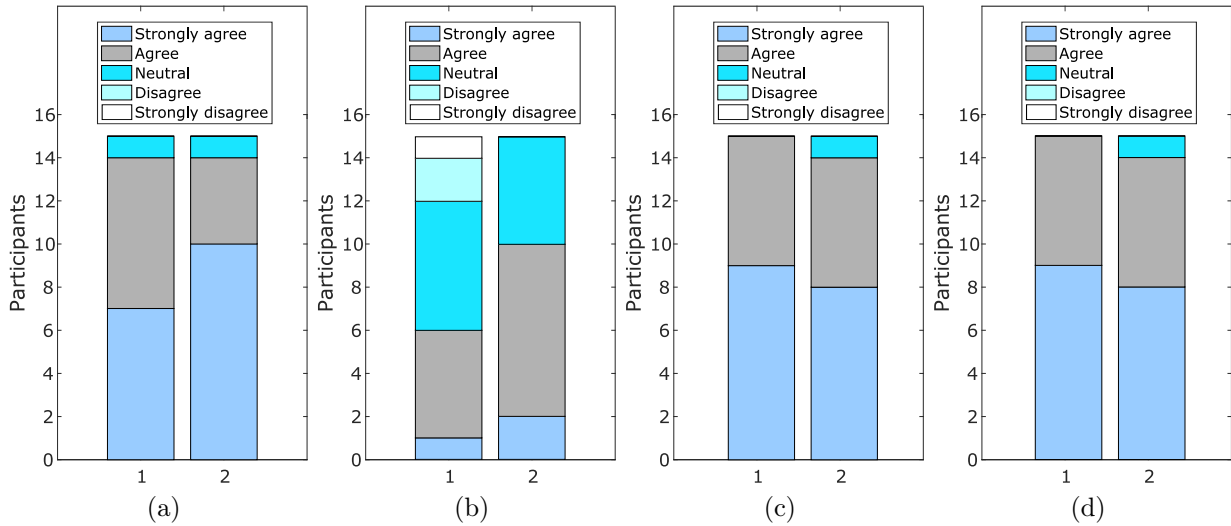


Figure 6.9: Qualitative evaluation for the guided experiments. Questions: a) “I felt safe handling the SW”. b) “I felt that I controlled the SW”. c) “I felt that the SW was guiding me”. d) “felt an intuitive interaction with the SW”. Group 1. Following the desired path using the blindfold. Group2. Following the desired path without use of blindfold.

Figure 6.10 shows the mean velocities obtained by the users in the experiments, and the respective errors. It can be seen that the mean velocities tend to increase when the users does not wear the blindfold. The mean linear velocity passes from  $0.1931 \pm 0.027 \text{ m/s}$  to  $0.2168 \pm 0.019 \text{ m/s}$ , and the mean angular velocity passes from  $0.1064 \pm 0.014 \text{ rad/s}$  to  $0.1164 \pm 0.009 \text{ rad/s}$ . We believe that this is due to the fact that the users, who present no visual impairment, feel more comfortable and confident when not wearing the blindfold, leading to an increase on their gait speed. The mean error in the linear velocity is similar for both cases. In the case of the mean error in the angular velocity, the error is higher in the second part of the experiment, due to the SW arrived at the curve with a higher linear velocity and, according to the controller strategy, the angular velocity is directly proportional to the linear velocity.

During the experiments, though many of the users reached the maximum linear velocity, no one commented on such limitation, which seems to be perceived as merely due the natural inertia of the SW. Users, in general, talked about the limiting speed value as a “good velocity for locomotion”. Moreover, they reported the perception of safety during guidance, and the interaction itself was considered intuitive along the desired path. In this sense, the control strategy does not require from the user a higher effort to maneuver the SW, allowing for guiding people through a desired path in a natural way.

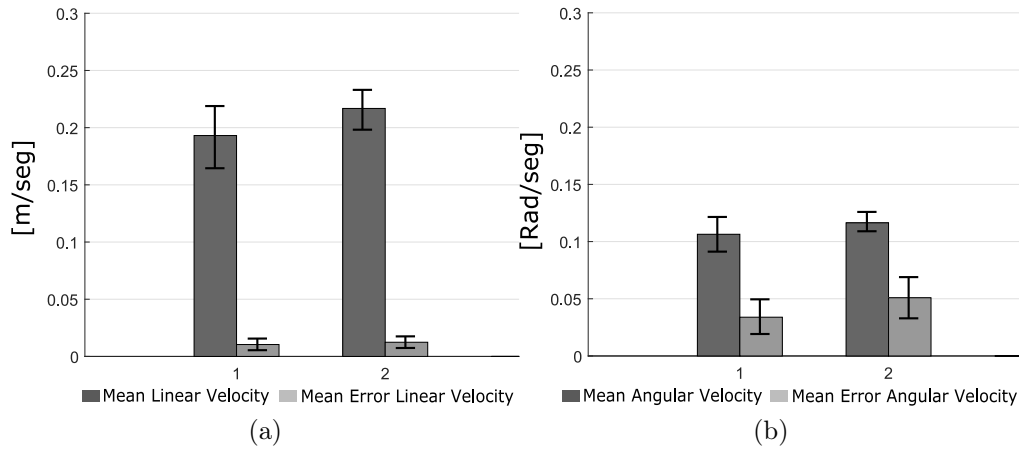


Figure 6.10: Group 1: Average data from all runs of the first part of the experiment. Group 2: Average data from all participants without the use of the blindfold. (a) Statistic of linear velocity. (b) Statistic of the angular velocity.

As a conclusion, this chapter presented a control strategy that allows the HREI to guide blind people with gait disorders. The haptic feedback given by the physical contact between the user and the SW allows guiding these people without the use of wearable devices or signals that require an additional cognitive process that may induce fatigue. With the haptic feedback, an intuitive information about the path to be followed is provided, and the user is easily able to manage the use of the SW.

The control strategy proposed here allowed a comfortable experience for the users when they were guided by the SW. The mass and damping parameters of the admittance controller did not demand a higher effort by the user, and hence, the SW was easily manipulated. By limiting the velocities of the SW and choosing a coherent path design, the control strategy had a good behavior and transmitted comfort and safety to the user.

# Chapter 7

## Conclusions and Future Works

Such as previously presented, there is a significant need to include the environment perception within the interaction layers when is navigating with an SW. This Ph.D. thesis used the environment information to propose and validate control strategies for a HREI (Human-Robot-Environment Interaction). Such strategies were implemented on a walker-assisted gait, which was used to assist people with mobility impairments. These control strategies demonstrated to demand less effort on the user to maneuvering the SW, as the control parameters can be adjusted to have an easy locomotion.

Two new control strategies for HREI were proposed and validated here. On the one hand, a proposal that contributes to a natural interaction among Human–Robot–Environment using a new criterion for admittance control strategy was presented. The spatial modulation concept allowed the guiding of the user in a natural and safe way through a path. Moreover, it gave the user enough sensation to understand that he/she had control over the device. Considering the second strategy, the user is able to impose the start and end of the locomotion with the SW, but not a turn intention. In this case, the control strategy generates the angular velocity to guide the user through a path in a comfortable and safe way. This strategy can be used to assist people with impaired postural control, (e.g.: post-stroke people who have one side with paralysis), as it only needs the user motion intention to keep forward with the SW.

One of the advantages of these control strategies is the use of sensors integrated into the SW

to detect the user motion intention, as it provides comfort and easy maneuverability of the walker. The lack of sensors placed on the user's body and the absence of landmarks or sensors installed on the environment make the presented solutions suitable for real-life applications.

This research also introduced a natural and intuitive HREI based on a haptic feedback as result from the physical interaction between the user and the SW. Such haptic signal was used to guide the SW's user across an environment in a safe and efficient way. In addition, the use of the haptic feedback allowed getting, in an intuitive way, the environment information. We believe that this can contribute, in a positive way, for the user's cognitive system, as it promotes the process of decision-making about the path to follow, which could be useful to enhance the design of assistive and rehabilitation devices.

Furthermore, the use of haptic feedback together the visual cHRi (cognitive Human-Robot interface) allowed obtaining a multimodal cognitive interaction between user and SW, which is used to give intuitive recommendations about the path that should be followed. This was verified through real experiments where the user, by means of the multimodal cognitive interaction, was able to follow the path. Also, through the pHRi (physical Human-Robot interface) and the cHRi (cognitive Human-Robot interface) used in this work, the user was able to establish, in a natural and intuitive way not only the start and the end of the locomotion, but also regulate the desired speed.

The multimodal cognitive interaction was also used in a navigation strategy, which included the social interaction within the SW by mean of spatial zones defined through elliptic shapes. In this case, the use of the haptic feedback and the LEDs allowed enough freedom to maneuver the SW, as they do not saturate any user vital sign during navigation. This was also verified through real experiments where the user was able to navigating in a safe way along a corridor.

Spatial zones defined by ellipses shapes, not only allowed having more space to navigate in confined spaces, but also offered the opportunity to interact with other people during navigation using social conventions. This kind of solutions is reflected in the user quality of life and wellbeing. In addition, it establishes a research field that, according to the literature, has not been fully explored for SWs.

As future work, a clinical protocol is being prepared to validate the control strategies and the multimodal cognitive interaction with patients, as clinical evaluation and the adaptation of the control strategies is an important future task for rehabilitation. Experiments will be conducted with people with motor disabilities (e.g.: post-stroke patients) to evaluate the interaction schemes developed and the communication channels used by the multimodal cognitive interaction.

New control strategies are also being developed to promote the haptic feedback for the user of SWs. Also, it is necessary implement a strategy to generate the value of the admittance controller parameters in real time, in order to improve the HREI.

With the RP-LIDAR sensor, the aim is to have more information about the environment to be used in probabilistic techniques, such as SLAM, to define, in real time, the path that the SW should follow to reach a specific location. Moreover, video cameras are being integrated on the SW to improve the social navigation strategy. This way, new algorithms can be implemented for detection and classification of other obstacles within the environment, which can empower the features of the SW during navigation. Therefore, new control strategies should be developed to include simple tasks, such as directing the SW to a specific object into the environment, and, for example, assist the user to pick up a glass on a table, or, improve the social factors addressed in this research. In this sense, safer navigation strategies for the user must also be implemented. In addition, it will be necessary to develop new HREI strategies, in which the user has an active role. Here, new interfaces between the user and the SW must be implemented on the SW to improve the interaction strategies.

SWs are assistive devices that provide benefits to the mobility of impaired people. However, these devices have been slightly explored in real scenarios. For this reason, the control strategies proposed in this Ph.D. thesis should be tested in real environments, such as hospitals, nursing homes, and clinical settings, observing also, the behavior of these devices when operating close to other people, which is an important information to improve the HREI.

## 7.1 Contributions

The work contributions of this Ph.D. thesis are the development of novel HREI control strategies and a multimodal cognitive interaction to guiding the SW's user during navigation. Objectively, the most important technical and scientific contributions of the research presented in this work are listed below.

1. Proposal and validation of an HRI strategy using force sensors to recognize the human motion intention.
2. Study of the influence of the admittance control parameters on the Human-Smart walker interaction.
3. Use of the physical contact between the user and the SW to generate haptic feedback to indicate the path that should be followed by the user.
4. Design and implementation of a multimodal cognitive interaction to indicate the right direction, and intuitively find the easy navigation with the SW. Such cognitive interaction is composed of the haptic feedback and visual interface.
5. Design and validation of a new control strategy for HREI based on an admittance controller with spatial modulation and a haptic feedback to guide the user through a predetermined path.
6. Proposal and validation of a social navigation strategy that uses social conventions inspired by proxemics.
7. Development of a control strategy to guide visually impaired people through a predetermined path using haptic feedback.

## 7.2 Acknowledgements

This research was supported by CAPES/Brazil (grant number 88887.095626/2015-01), FAPES/Brazil (grant number 80709036, 72982608) and CNPq/Brazil (grant number 304192/2016-3).

## 7.3 Publications

The research developed in this Ph.D. thesis allowed the publication of the following works:

1. (Journal Paper) Mario F. Jiménez, Matias Monllor, Anselmo Frizera, Teodiano Bastos, Flavio Roberti, and Ricardo Carelli. Admittance Controller with Spatial Modulation for Assisted Locomotion using a Smart Walker. *Journal of Intelligent and Robotic Systems: Theory and Applications*. April, 2018. DOI: 10.1007/s10846-018-0888-3.
2. (Conference Proceeding) Mario F. Jiménez, Anselmo Frizera and Teodiano Bastos. Recognition of Navigation Commands for a Smart Walk-er Through Force Sensors. XXVI Brazilian Congress on Biomedical Engineering (CBEB), Búzios-Brazil. October, 2018.
3. (Conference Proceeding) Mario F. Jiménez, Ricardo C. Mello, Anselmo Frizera and Teodiano Bastos. Assistive Device for Guiding Visually Impaired People With Mobility Disorders. HRI'18 Companion of the 2018 ACM/IEEE International Conference on Human-Robot Interaction, Chicago-USA. March, 2018.
4. (Conference) Mario F. Jiménez, Matias Monllor, Anselmo Frizera, Teodiano Bastos, Flavio Roberti, and Ricardo Carelli. Estrategia de Interacción Para la Movilidad Humano-Robot Usando el Control de Admitancia. IX Congreso Iberoamericano de Tecnologías de Apoyo a la Discapacidad. IBERDISCAP, Bogotá-Colombia. November, 2017.

Other works were also published as a consequence of the interaction with other researchers during the development of this Ph.D. thesis. The most important ones are listed below.



1. (Journal Paper) Arnaldo G. Leal-Junior, Camilo R. Díaz, Mario F. Jiménez, Cátia Leitão, Carlos Marques, Maria José Pontes, Anselmo Frizera. Polymer Optical Fiber Based Sensor System for Smart Walker Instrumentation and Health Assessment. *IEEE Sensors Journal*. October, 2018. DOI: 10.1109/JSEN.2018.2878735.
2. (Journal Paper, accepted) Ricardo C. Mello, Mario F. Jiménez, Moises R.N. Ribeiro, Rodrigo L. Guimares, Anselmo Frizera. On Human-in-the-Loop CPS in Healthcare: A Cloud-Enabled Mobility Assistance Service. *Robotica*, Submitted in July, 2018.
3. (Conference Proceeding) Ricardo C. Mello, Mario F. Jiménez, Franco Souza, Moises R.N. Ribeiro and Anselmo Frizera. Towards a New Generation of Smart Devices for Mobility Assistance: CloudWalker, a Cloud-Enabled Cyber-Physical System. 7th IEEE RAS & EMBS International Conference on Biomedical Robotics and Biomechatronics (BioRob). Enschede - The Netherlands. August, 2018.
4. (Conference Proceeding) Ricardo C. Mello, Mario F. Jimenez, Franco Souza, Moises R.N. Ribeiro and Anselmo Frizera-Neto. Impacto da Latência em Sistemas Cyber-Físicos em Nuvem: Métricas Subjetiva e Objetiva para Aandador Robótico. XIII Simpósio Brasileiro de Automação Inteligente (SBAI). Porto Alegre - Brazil. October, 2017.
5. (Conference Proceeding) Ana Cecilia Villa-Parra, Mario F. Jimenez, Jessica Lima, Thomaz Botelho, Anselmo Frizera-Neto and Teodiano Freire Bastos. Robotic System to Improve Volitional Control of Movement During Gait. II Congreso Internacional Tecnología y Turismo. Accesibilidad 4.0 para todas las personas. Málaga - Spain. September, 2017.
6. (Conference Proceeding) Matias Monllor, Flavio Roberti, Mario Jimenez, Anselmo Frizera and Ricardo Carelli. Path following control for assistance robots. XVII Workshop on Information Processing and Control (RPIC). Mar del Plata - Argentina. September, 2017.
7. (Conference Proceeding) Franco Souza, Anselmo Frizera-Neto, Mario F. Jimenez, Ricardo C. Mello. Desvio de obstáculos móveis em andador inteligente. IX Congreso Iberoamericano de Tecnologías de Apoyo a la Discapacidad. IBERDISCAP, Bogotá-Colombia.

November,2017.

In addition, the following works were recently submitted to journals:

1. (Journal Paper, under revision) Mario F. Jiménez, Ricardo C. Mello, Teodiano Bastos and Anselmo Frizera. Assistive locomotion device with haptic feedback for guiding visually impaired people. *Medical Engineering & Physics*. Submitted in November, 2018.
2. (Journal Paper, under revision) Mario F. Jiménez, Wanderleyson Scheidegger, Ricardo C. Mello, Teodiano Bastos and Anselmo Frizera. Bringing proxemics to walker-assisted gait: Using admittance control with spatial modulation to navigate in conned spaces. *Robotica*, Submitted in September, 2018.

# Bibliography

- [1] Jennifer C. Davis, Stirling Bryan, Linda C. Li, John R. Best, Chun Liang Hsu, Caitlin Gomez, Kelly A. Vertes, and Teresa Liu-Ambrose. Mobility and cognition are associated with wellbeing and health related quality of life among older adults: a cross-sectional analysis of the Vancouver Falls Prevention Cohort. *BMC geriatrics*, 15:75, 2015.
- [2] United Nations and Department of Economic and Social Affairs Population Division. *World Population Ageing 2017 - Highlights*. 2017.
- [3] Neil B Alexander and Allon Goldberg. Gait disorders : Search for multiple causes. *CLEVELAND CLINIC JOURNAL OF MEDICINE*, 72(7):586–600, 2005.
- [4] Roger Bemelmans, Gert Jan Gelderblom, Pieter Jonker, and Luc de Witte. Socially assistive robots in elderly care: A systematic review into effects and effectiveness. *Journal of the American Medical Directors Association*, 13(2):114–120, 2012.
- [5] Margot Shields. Use of wheelchairs and other mobility support devices. 15(3):37–41, 2014.
- [6] Christian Werner, Phoebe Ullrich, Milad Geravand, Angelika Peer, Jürgen M. Bauer, and Klaus Hauer. A systematic review of study results reported for the evaluation of robotic rollators from the perspective of users. *Disability and Rehabilitation: Assistive Technology*, 0(0):1–12, 2017.
- [7] Sara M. Bradley, Cameron R Hernandez, Mount Sinai, New York, and New York. Geriatric Assistive Devices. pages 405–411, 2011.

- [8] Maria M. Martins, Cristina P. Santos, Anselmo Frizera-Neto, and Ramn Ceres. Assistive mobility devices focusing on Smart Walkers: Classification and review. *Robotics and Autonomous Systems*, 60(4):548–562, 2011.
- [9] Andreas Wachaja, Pratik Agarwal, Mathias Zink, Miguel Reyes, Knut Möller, and Wolfram Burgard. Navigating blind people with walking impairments using a smart walker. *Autonomous Robots*, pages 1–19, 2016.
- [10] Mario F. Jiménez, Matias Monllor, Anselmo Frizera, Teodiano Bastos, Flavio Roberti, and Ricardo Carelli. Admittance Controller with Spatial Modulation for Assisted Locomotion using a Smart Walker. *Journal of Intelligent and Robotic Systems: Theory and Applications*, pages 1–17, 2018.
- [11] Maria Martins, Cristina Santos, Anselmo Frizera, and Ramón Ceres. A review of the functionalities of smart walkers. *Medical Engineering and Physics*, 37(10):917–928, 2015.
- [12] Carlos A Cifuentes and Anselmo Frizera. *Human-Robot Interaction Strategies for Locomotion*. Springer International Publishing Switzerland 2016, 2016.
- [13] Carlos Valadão, Eliete Caldeira, Teodiano Bastos-Filho, Anselmo Frizera-Neto, and Ricardo Carelli. A new controller for a smart walker based on human-robot formation. *Sensors (Switzerland)*, 16(7):1–26, 2016.
- [14] Hayley Robinson, Bruce MacDonald, and Elizabeth Broadbent. The Role of Healthcare Robots for Older People at Home: A Review. *International Journal of Social Robotics*, 6(4):575–591, 2014.
- [15] Haoyong Yu, Matthew Spenko, and Steven Dubowsky. An Adaptive Shared Control System for an Intelligent Mobility Aid for the Elderly. *Autonomous Robots*, 15:53–66, 2003.
- [16] Milad Geravand, Christian Werner, Klaus Hauer, and Angelika Peer. An Integrated Decision Making Approach for Adaptive Shared Control of Mobility Assistance Robots. *International Journal of Social Robotics*, 8(5):631–648, 2016.

- [17] Joao Paulo, Paulo Peixoto, and Urbano J. Nunes. ISR-AIWALKER: Robotic Walker for Intuitive and Safe Mobility Assistance and Gait Analysis. *IEEE Transactions on Human-Machine Systems*, pages 1–13, 2017.
- [18] Giovanni Morone, Roberta Annicchiarico, Marco Iosa, Alessia Federici, Stefano Paolucci, Ulises Cortés, and Carlo Caltagirone. Overground walking training with the i-Walker, a robotic servo-assistive device, enhances balance in patients with subacute stroke: a randomized controlled trial. *Journal of NeuroEngineering and Rehabilitation*, 13:1–10, 2016.
- [19] Andreas Wachaja, Pratik Agarwal, Mathias Zink, Miguel Reyes Adame, Knut Muller, and Wolfram Burgard. Navigating blind people with walking impairments using a smart walker. *Autonomous Robots*, 41(3):555–573, 2016.
- [20] M. Reyes Adame, J. Yu, and K. Moeller. Mobility Support System for Elderly Blind People with a Smart Walker and a Tactile Map. In *XIV Mediterranean Conference on Medical and Biological Engineering and Computing*, volume 57, pages 602–607. Springer, Cham, 2016.
- [21] Mf. Chang, Wh. Mou, CK. Liao, and LC. Fu. Design and implementation of an active robotic walker for Parkinson’s patients. *SICE Annual Conference*, pages 2068–2073, 2012.
- [22] M. Aggravi, A. Colombo, D. Fontanelli, A. Giannitrapani, D. Macii, F. Moro, P. Nazemzadeh, L. Palopoli, R. Passerone, D. Prattichizzo, T. Rizano, L. Rizzon, and S. Scheggi. A smart walking assistant for safe navigation in complex indoor environments. *Biosystems and Biorobotics*, 11:487–497, 2015.
- [23] Luigi Palopoli, Antonis Argyros, Josef Birchbauer, Alessio Colombo, Daniele Fontanelli, Axel Legay, Andrea Garulli, Antonello Giannitrapani, David Macii, Federico Moro, Payam Nazemzadeh, Pashalis Padelaris, Roberto Passerone, Georg Poier, Domenico Prattichizzo, Tizar Rizano, Luca Rizzon, Stefano Scheggi, and Sean Sedwards. Navigation assistance and guidance of older adults across complex public spaces: the DALi approach. *Intelligent Service Robotics*, 8(2):77–92, 2015.

- [24] J. Paulo, L. Garrote, C. Premebida, A. Asvadi, D. Almeida, A. Lopes, and P. Peixoto. An innovative robotic walker for mobility assistance and lower limbs rehabilitation. *ENBENG 2017 - 5th Portuguese Meeting on Bioengineering, Proceedings*, 2017.
- [25] Vitor Faria, Jorge Silva, Maria Martins, and Cristina Santos. Dynamical system approach for obstacle avoidance in a Smart Walker device. *2014 IEEE International Conference on Autonomous Robot Systems and Competitions, ICARSC 2014*, pages 261–266, 2014.
- [26] Walter Pirker and Regina Katzenschlager. Gait disorders in adults and the elderly: A clinical guide. *Wiener Klinische Wochenschrift*, 129(3-4):81–95, 2017.
- [27] Hamid Bateni and Brian E. Maki. Assistive Devices for Balance and Mobility : Benefits , Demands , and Adverse Consequences. *Archives of physical medicine and rehabilitation*, 86(January):134–145, 2005.
- [28] Sara M. Bradley and Cameron R. Hernandez. Geriatric assistive devices. *American Family Physician*, 84(4):405–411, 2011.
- [29] Jordan Carver, Ashley Ganus, Jon Mark Ivey, Teresa Plummer, and Ann Eubank. The impact of mobility assistive technology devices on participation for individuals with disabilities. *Disability and Rehabilitation: Assistive Technology*, 11(6):468–477, 2016.
- [30] Aron S. Buchman, Patricia A. Boyle, Sue E. Leurgans, Lisa L. Barnes, and David A. Bennett. Cognitive function is associated with the development of mobility impairments in community-dwelling elders. *American Journal of Geriatric Psychiatry*, 19(6):571–580, 2011.
- [31] WHO. World report on ageing and health. Technical report, 2015.
- [32] WHO. World Health Organization, 2016.
- [33] Klaske Van Kammen, Anne M. Boonstra, Lucas HV. Van Der Woude, Heleen A. Reinders-Messelink, and Rob Den Otter. Differences in muscle activity and temporal step parameters between Lokomat guided walking and treadmill walking in post-stroke hemiparetic patients and healthy walkers. *Journal of NeuroEngineering and Rehabilitation*, 2017.

- [34] Carmen E. Capó-Lugo, Christopher H. Mullens, and David Brown. Maximum walking speeds obtained using treadmill and overground robot system in persons with post-stroke hemiplegia. *Journal of neuroengineering and rehabilitation*, 9:80, jan 2012.
- [35] Lauren S. Talman, Esther R. Bisker, David J. Sackel, David A. Long, Kristin M. Galetta, John N. Ratchford, Deacon J. Lile, Sheena K. Farrell, Michael J. Loguidice, Gina Remington, Amy Conger, Teresa C. Frohman, Dina A. Jacobs, Clyde E. Markowitz, Gary R. Cutter, Gui Shuang Ying, Yang Dai, Maureen G. Maguire, Steven L. Galetta, Elliot M. Frohman, Peter A. Calabresi, and Laura J. Balcer. Longitudinal study of vision and retinal nerve fiber layer thickness in multiple sclerosis. *Annals of Neurology*, 67(6):749–760, 2010.
- [36] Marilyn Poole, Doug Simkiss, Alice Rose, and François-Xavier Li. Anterior or posterior walkers for children with cerebral palsy? A systematic review. *Disability and Rehabilitation: Assistive Technology*, 0(0):1–12, 2017.
- [37] Eline A.M. Bolster, Astrid C.J. Balemans, Merel Anne Brehm, Annemieke Buizer, and Annet J. Dallmeijer. Energy cost during walking in association with age and body height in children and young adults with cerebral palsy. *Gait and Posture*, 54:119–126, 2017.
- [38] KE. Musselman, C. Arnold, C. Pujol, K. Lynd, and S. Oosman. Falls, mobility, and physical activity after spinal cord injury: an exploratory study using photo-elicitation interviewing. *Spinal Cord Ser Cases*, 4:39, 2018.
- [39] Giorgio Scivoletto, Federica Tamburella, Letizia Laurenza, Monica Torre, and Marco Molinari. Who is going to walk? A review of the factors influencing walking recovery after spinal cord injury. *Frontiers in Human Neuroscience*, 8(March):1–11, 2014.
- [40] Lisette H.J. Kikkert, Nicolas Vuillerme, Jos P. van Campen, Bregje A. Appels, Tibor Hortobágyi, and Claudine J.C. Lamothe. The relationship between gait dynamics and future cognitive decline: a prospective pilot study in geriatric patients. *International Psychogeriatrics*, pages 1–9, 2017.

- [41] World Health Organization. WHO global disability action plan 2014–2021: better health for all people with disability. Technical report, 2014.
- [42] T. Bardsley, G., Blocka, D., Borg, J., Brintnell, S., Constantine, D., Dillu, A., . . . Verhoeff. Joint position paper on the provision of mobility devices in less-resourced settings. Technical Report 2, 2011.
- [43] Benjamin K. Kocher, Robyn L. Chalupa, Donna M. Lopez, and Kevin L. Kirk. Comparative Study of Assisted Ambulation and Perceived Exertion with the Wheeled Knee Walker and Axillary Crutches in Healthy Subjects. *Foot and Ankle International*, 37(11):1232–1237, 2016.
- [44] Jeanine Beasley, Lisa Kenyon, Amber Midena, Jaimie Chartier, Karrie Meyers, Blake Ashby, and Kirk Anderson. Cane Handle Designs—Pressure and Preference. *Journal of Acute Care Physical Therapy*, 8(2):58–64, 2017.
- [45] Lucas R. Nascimento, Louise Ada, and Luci F. Teixeira-Salmela. The provision of a cane provides greater benefit to community-dwelling people after stroke with a baseline walking speed between 0.4 and 0.8 metres/second: an experimental study. *Physiotherapy (United Kingdom)*, 102(4):351–356, 2016.
- [46] Anselmo Frizera Neto, Arlindo Elias, Carlos Cifuentes, Camilo Rodriguez, Teodiano Bastos, and Ricardo Carelli. Comparative Study of Assisted Ambulation and Perceived Exertion with the Wheeled Knee Walker and Axillary Crutches in Healthy Subjects. In Benjamin K. Kocher, Robyn L. Chalupa, Donna M. Lopez, and Kevin L. Kirk, editors, *Foot and Ankle International*, volume 37, pages 1232–1237. 2015.
- [47] Jonathon R. Priebe and Rodger Kram. Why is walker-assisted gait metabolically expensive? *Gait and Posture*, 34(2):265–269, 2011.
- [48] Margaret P. O’Hare, Shona J. Pryde, and Jacqueline H. Gracey. A systematic review of the evidence for the provision of walking frames for older people. *Physical Therapy Reviews*, 18(1):11–23, 2013.



- [49] Cunjun Huang, Glenn Wasson, Majd Alwan, and Pradip Sheth. Shared navigational control and user intent detection in an intelligent walker. *AAAI Fall 2005*, 2005.
- [50] G. Wasson, J. Gunderson, and S. Graves. Effective Shared Control in Cooperative Mobility Aids. *Proceedings of the Fourteenth International Florida Artificial Intelligence Research Society Conference*, 1:1–5, 2001.
- [51] Gerard J. Lacey and Diego Rodriguez-losada. The Evolution of Guido. *IEEE Robotics & Automation Magazine*, 15(December):75–83, 2008.
- [52] Aaron Morris, Raghavendra Donamukkalat, K Anuj, Aaron Steinfeldt, T M Judith, Jacqueline Dunbar-jacob, and Sebastian Thrunti. A Robotic Walker That Provides Guidance. In *IEEE International Conference on Robotics & Automation*, pages 25–30, 2003.
- [53] J. Alves, E. Seabra, I. Caetano, and C. P. Santos. Overview of the ASBGo++ Smart Walker. *2017 IEEE 5th Portuguese Meeting on Bioengineering (ENBENG)*, pages 1–4, 2017.
- [54] Geunho Lee, Takanori Ohnuma, and Nak Young. Design and control of JAIST active robotic walker. *Intelligent Service Robotics*, 3:125–135, 2010.
- [55] Maria M. Martins, Anselmo Frizera-Neto, Eloy Urendes, Cristina dos Santos, Ramon Ceres, and Teodiano Bastos-Filho. A novel human-machine interface for guiding: The NeoASAS smart walker. In *2012 ISSNIP Biosignals and Biorobotics Conference: Biosignals and Robotics for Better and Safer Living, BRC 2012*, 2012.
- [56] Angelika Peer. (2018-08-30). Intelligent Active MObility Assistance RoBOT integrating Multimodal Sensory Processing, Proactive Autonomy and Adaptive Interaction. [Online]. Available: <http://www.mobot-project.eu/?Contact>, 2018.
- [57] M. Aggravi, A. Colombo, D. Fontanelli, A. Giannitrapani, D. Macii, F. Moro, P. Nazemzadeh, L. Palopoli, R. Passerone, D. Prattichizzo, T. Rizano, L. Rizzon, and S. Scheggi. DALi: A smart walking assistant for safe navigation in complex indoor environments. *Biosystems and Biorobotics*, 11:487–497, 2015.

- [58] José L. Pons (CSIC). *Wearable Robots: Biomechatronic Exoskeletons*. John Wiley & Sons Ltd, Madrid, 2008.
- [59] Wolfgang Rampeltshammer and Angelika Peer. Control of Mobility Assistive Robot for Human Fall Prevention. In *2015 IEEE International Conference on Rehabilitation Robotics (ICORR)*, pages 882–887. IEEE Xplore, 2015.
- [60] Chun Hsu Ko, Kuu Young Young, Yi Che Huang, and Sunil Kumar Agrawal. Active and passive control of walk-assist robot for outdoor guidance. *IEEE/ASME Transactions on Mechatronics*, 18(3):1211–1220, 2013.
- [61] Yacine Amirat, David Daney, Samer Mohammed, Anne Spalanzani, Abdelghani Chibani, and Olivier Simonin. Assistance and Service Robotics in a Human Environment. *Robotics and Autonomous Systems*, 75:1–3, 2016.
- [62] Edward Twitchell Hall. *The hidden dimension*. Garden City, NY, 1966.
- [63] Christian Werner, George P. Moustiris, Costas S. Tzafestas, and Klaus Hauer. User-Oriented Evaluation of a Robotic Rollator That Provides Navigation Assistance in Frail Older Adults with and without Cognitive Impairment. *Gerontology*, 64(3):278–290, 2018.
- [64] Naemeh Nejatbakhsh and Kazuhiro Kosuge. User-environment based navigation algorithm for an omnidirectional passive walking aid system. *Proceedings of the 2005 IEEE 9th International Conference on Rehabilitation Robotics*, 2005:178–181, 2005.
- [65] Federico Moro, Antonella de Angeli, Daniele Fontanelli, Roberto Passerone, Domenico Prattichizzo, Luca Rizzon, Stefano Scheggi, Stefano Targher, and Luigi Palopoli. Sensory stimulation for human guidance in robot walkers: A comparison between haptic and acoustic solutions. BT - IEEE International Smart Cities Conference, ISC2 2016, Trento, Italy, September 12-15, 2016. pages 1–6, 2016.
- [66] François Pasteau, Vishnu K. Narayanan, Marie Babel, and François Chaumette. A visual servoing approach for autonomous corridor following and doorway passing in a wheelchair. *Robotics and Autonomous Systems*, 75:28–40, 2016.

- [67] Vishnu K. Narayanan, François Pasteau, Maud Marchal, Alexandre Krupa, and Marie Babel. Vision-based adaptive assistance and haptic guidance for safe wheelchair corridor following. *Computer Vision and Image Understanding*, 149:171–185, 2016.
- [68] Ricardo Carelli and Eduardo Oliveira Freire. Corridor navigation and wall-following stable control for sonar-based mobile robots. *Robotics and Autonomous Systems*, 45(3-4):235–247, 2003.
- [69] Philipp Beckerle, Gionata Salvietti, Ramazan Unal, Domenico Prattichizzo, Simone Rossi, Claudio Castellini, Sandra Hirche, Satoshi Endo, Heni Ben Amor, Matei Ciocarlie, Fulvio Mastrogiovanni, Brenna D. Argall, and Matteo Bianchi. A human-robot interaction perspective on assistive and rehabilitation robotics. *Frontiers in Neurorobotics*, 11(MAY):1–6, 2017.
- [70] Dirk Helbing and Péter Molnár. Social force model for pedestrian dynamics. *Physical Review E*, 51(5):4282–4286, 1995.
- [71] Abir Bellarbi, Souhila Kahlouche, Nouara Achour, and Nouredine Ouadah. A social planning and navigation for tour-guide robot in human environment. *Proceedings of 2016 8th International Conference on Modelling, Identification and Control, ICMIC 2016*, pages 622–627, 2017.
- [72] Wenxia Xu, Jian Huang, and Qingyang Yan. Multi-sensor based human motion intention recognition algorithm for walking-aid robot. *2015 IEEE International Conference on Robotics and Biomimetics, IEEE-ROBIO 2015*, pages 2041–2046, 2015.
- [73] Cheng-kai Lu, Yi-che Huang, and Cheng-jung Lee. Adaptive guidance system design for the assistive robotic walker. *Neurocomputing*, 170:152–160, 2015.
- [74] Ulises Cortés, Antonio Martínez-velasco, Cristian Barrué, Toni Benedico, Carlo Caltagirone, and Roberta Annicchiarico. A SHARE-it service to elders ’ mobility using the i-Walker . *Gerontechnology*, 7:95–100, 2008.
- [75] Victor H. Andaluz, Flavio Roberti, Juan Marcos Toibero, Ricardo Carelli, and Bernardo Wagner. Adaptive Dynamic Path Following Control of an Unicycle Like Mobile Robot.

- In *Intelligent Robotics and Applications*, chapter 56, pages 563–574. Springer Berlin Heidelberg, 2011.
- [76] Anselmo Frizera Neto, Juan A Gallego, Eduardo Rocon, José L Pons, and Ramón Ceres. Extraction of user 's navigation commands from upper body force interaction in walker assisted gait. *Biomedical engineering online*, 9(1):1–17, 2010.
- [77] Carlos A. Cifuentes, Anselmo Frizera, Ricardo Carelli, and Teodiano Bastos. Human – robot interaction based on wearable IMU sensor and laser range finder. *Robotics and Autonomous Systems*, 62(10):1425–1439, 2015.
- [78] Cameron N. Riviere, Stephen G. Reich, and Nitish V. Thakor. Adaptive Fourier modeling for quantification of tremor. *Journal of Neuroscience Methods*, 74(1):77–87, 1997.
- [79] Nancye M. Peel, Suzanne S. Kuys, and Kerenaftali Klein. Gait Speed as a Measure in Geriatric Assessment in Clinical Settings: A Systematic Review. *The Journals of Gerontology: Series A*, 68(1):39–46, 2012.
- [80] D M Egelman, C Person, and P R Montague. A computational role for dopamine delivery in human decision-making. *Journal of cognitive neuroscience*, 10:623–630, 1998.
- [81] Celso de la Cruz and Ricardo Carelli. Dynamic Modeling and Centralized Formation Control of Mobile Robots. *IEEE Industrial Electronics, IECON 2006 - 32nd Annual Conference on*, pages 3880–3885, 2006.
- [82] Chiara Piezzo and Kenji Suzuki. Feasibility study of a socially assistive humanoid robot for Guiding elderly individuals during walking. *Future Internet*, 9(3), 2017.
- [83] J. Rios-Martinez, A. Spalanzani, and C. Laugier. From Proxemics Theory to Socially-Aware Navigation: A Survey. *International Journal of Social Robotics*, 7(2):137–153, 2015.
- [84] Irwin Altman and Joachim F Wohlwill. *Human Behavior and Environment : Advances in Theory and Research*. 1977.

- [85] Yoichi Morales, Takahiro Miyashita, and Norihiro Hagita. Social robotic wheelchair centered on passenger and pedestrian comfort. *Robotics and Autonomous Systems*, 87:355–362, 2017.
- [86] Daniel Herrera, Javier Gimenez, Flavio Roberti, and Ricardo Carelli. Pedestrian collision avoidance and motion control with mobile robots based on cognitive social zones. *IEEE Robotics and Automation Letters*, pages 1–6, 2018.
- [87] Ross Mead and Maja J. Matarić. Autonomous human–robot proxemics: socially aware navigation based on interaction potential. *Autonomous Robots*, 41(5):1189–1201, 2017.
- [88] Birgit Graf. Reactive Navigation of an Intelligent Robotic Walking Aid. *Robot and Human Interactive Communication, 2001. Proceedings. 10th IEEE International Workshop on*, (March):353–358, 2001.
- [89] Elena Pacchierotti, Henrik Christensen, and Patric Jensfelt. Design of an Office Guide Robot for Social Interaction Studies. *IEEE/RSJ International Conference on Intelligent Robots and Systems*, pages 4965–4970, 2006.
- [90] Peng Wang. Understanding Social-Force Model in Psychological Principles of Collective Behavior. (May 2016), 2016.
- [91] Paulo Leica, Flavio Roberti, Matías Monllor, Juan M. Toibero, and Ricardo Carelli. Control of bidirectional physical human–robot interaction based on the human intention. *Intelligent Service Robotics*, 10:31–40, 2017.
- [92] M. Daszykowski and B. Walczak. Density-Based Clustering Methods. *KDD-96 Proceedings*, 96(34):226–231, 1996.
- [93] Richard A Becker, Sallie Keller-mcnulty, Richard A Becker, and Sallie Keller-mcnulty. Model Comparisons and R 2. 48(2):113–117, 1994.
- [94] Matthew Spenko, Haoyong Yu, and Steven Dubowsky. Robotic Personal Aids for Mobility and Monitoring for the Elderly. *IEEE Transaction on Neural Systems and Rehabilitation Engineering*, 14(3):344–351, 2006.

- [95] Mounir Bousbia-Salah, Maamar Bettayeb, and Allal Larbi. A navigation aid for blind people. *Journal of Intelligent and Robotic Systems: Theory and Applications*, 64(3-4):387–400, 2011.
- [96] Bruno Andò and Salvatore Graziani. Multisensor strategies to assist blind people: A clear-path indicator. *IEEE Transactions on Instrumentation and Measurement*, 58(8):2488–2494, 2009.
- [97] Shane Macnamara and Gerard Lacey. A Smart Walker for the Frail Visually Impaired. pages 1354–1359, 2000.
- [98] Qing Lin and Youngjoon Han. A context-aware-based audio guidance system for blind people using a multimodal profile model. *Sensors (Switzerland)*, 14(10):18670–18700, 2014.
- [99] Kabalan Chaccour, Jean Eid, Rony Darazi, Amir Hajjam El Hassani, and Emmanuel Andres. Multisensor guided walker for visually impaired elderly people. *2015 International Conference on Advances in Biomedical Engineering, ICABME 2015*, pages 158–161, 2015.
- [100] G Lacey. Context-Aware Shared Control of a Robot Mobility Aid for the Elderly Blind. *The International Journal of Robotics Research*, 19(11):1054–1065, 2000.
- [101] Yi-hung Hsieh, Yi-che Huang, Kuu-young Young, Chun-hsu Ko, and Sunil K Agrawal. Motion Guidance for a Passive Robot Walking Helper via User’s Applied Hand Forces. *IEEE Transactions on Human-Machine Systems*, 46(6):869–881, 2016.
- [102] Thomas Hellström, Olof Lindahl, Tomas Bäcklund, Marcus Karlsson, Peter Hohnloser, Anna Brändal, Xiaolei Hu, and Per Wester. An intelligent rollator for mobility impaired persons, especially stroke patients. *Journal of medical engineering & technology*, pages 1–10, 2016.
- [103] Birgit Graf. An Adaptive Guidance System for Robotic Walking Aids. *Journal of Computing and Information Technology*, 17(1):109, 2009.